Technische Universität München - Lehrstuhl für Verkehrstechnik
Univ.-Prof. Dr.-Ing. Fritz Busch
Arcisstraße 21 80333 München, www.vt.bgu.tum.de

MASTER'S THESIS

Analysis of Imperfections of Vehicular Communication on Cooperative Intelligent Transportation Systems

Author:

Meng XIE

Mentoring:

Dr.-Ing. David Eckhoff (TUMCREATE)

M.Sc Xiaodong Liu (TUMCREATE)

Dipl.-Ing. Jakob Kaths (TUM)

M.Sc Eftychios Papapanagiotou (TUM)

Date of Submission: 2018-01-15

Technische Universität München - Lehrstuhl für Verkehrstechnik
Univ.-Prof. Dr.-Ing. Fritz Busch
Arcisstraße 21 80333 München, www.vt.bgu.tum.de

MASTER'S THESIS

of Meng Xie

Date of Issue: 2017-10-01

Date of Submission: 2018-03-31

Topic: **Analysis of imperfections of vehicular communication on cooperative intelligent transportation systems**

In recent years, vehicular communication systems have received increasing attention in the field of traffic engineering. The wireless information exchange between vehicles and infrastructure enables an advancement from current Intelligent Transportation Systems (ITS) to Cooperative Intelligent Transportation Systems (C-ITS). On a large scale, vehicular information such as speed, acceleration and heading is communicated, while infrastructure provides information about current or predicted control actions, for example signal phase and timing information. The comprehensiveness and the level of precision of the shared data outperforms the data collected with stationary detections by far. Therefore, existing ITS systems can be improved or new ITS functionalities can be established to increase the safety and efficiency of the transportation network and lower the negative impacts of traffic.

In order to enable the information exchange between vehicles and traffic infrastructure, the dedicated communication standard IEEE 802.11p has been developed alongside with message formats such as the Cooperative Awareness Message (CAM). However, the performance of field tests of C-ITS systems is often impossible or restricted to small-scale tests due to the lack of equipped vehicles. Therefore, microscopic traffic flow simulation is often used to evaluate the effects of C-ITS functionalities. To increase the reliability of the evaluation results, vehicular communication can be used to represent the imperfections of vehicular communication. A number of well-established communication models exist and can be distinguished into physical and probabilistic models. Models of the first category can reproduce detailed physical behaviour such as reflections and interference of signals, while models of the second category are limited to less detail. However, the lower level of detail also reduces the computational effort of the communication simulation.

The purpose of the thesis is to analyse the imperfections of vehicular communication in an urban scenario based on microscopic traffic simulation. With this intention, communication models and a traffic signal control algorithm for cooperative public transport priority will be coupled with a microscopic traffic simulation tool in order to evaluate the direct effects of packet losses on the performance of the signal priority. This shall be done for both a physical communication model as well as a probabilistic communication model to allow for a comparison of the different approaches.

The objectives can be outlined more specifically as follows:

i. Implementation of a cooperative public transport priority control scheme for a single intersection to generate the scenario for the use-case.

ii. Comparison of the implications of imperfect communication on the effectiveness of the public transport prioritization. Loss-free communication, physically modelled communication and probabilistically modelled communication shall be compared, also regarding their computational effort.

iii. Different influencing factors on the system, such as density of obstructing buildings, distance of the priority request point to the intersection, penetration rate of vehicles and packet generation rate shall be evaluated in order to facilitate transferability to other use-cases. Especially the last two influencing factors require a strong focus on the probabilistic modelling of interference and collisions to generate meaningful results.

The student will present intermediate results to the mentors (Dipl.-Ing. Jakob Kaths, Eftychios Papapanagiotou, M.Sc., Dr.-Ing. David Eckhoff (TUMCREATE), Xiaodong Liu, M.Sc. (TUMCREATE)) in the fifth, tenth, 15th and 20th week.

The student must hold a 20-minute presentation with a subsequent discussion at the most two months after the submission of the thesis. The presentation will be considered in the final grade in cases where the thesis itself cannot be clearly evaluated.

Univ.-Prof. Dr.-Ing. Fritz Busch

Abstract

The present Master's thesis seeks to develop a better understanding of how to evaluate the performance of vehicular communication networks with realistic vehicle mobility impacts. As a starting point, vehicular communication network technologies and different performance assessment methodologies as the fundamentals were carefully studied. In particular, this thesis argued that from the perspectives of efficiency and scalability it is possible to exploit more potentials and opportunities from analytical approaches in analysing the performance of vehicular communication networks. Despite the extensive body of research on statistical models in vehicular communication networks, unrealistic assumptions, oversimplifications and ignorance of realistic vehicle mobility impacts lead to their limited usage. Thus, on the basis of both a study of the literature and improvements of an existing analytical model, this thesis established an interlink between vehicle mobility and wireless communication network with a focus on the performance analysis. Extending upon Hassan and Vu's (2011) model, a new integrative analytical module was developed, which merges realistic vehicle mobility impacts and wireless channel characteristics. As a result, an integrative module was tested, compared and validated on urban scenarios with a widely used hybrid simulator, in order to prove its effectiveness of providing rich insights in the performance assessment of vehicular communication networks.

Table of Contents

1 Introduction

In recent decades, the vehicular communication networks have become one of the key research areas in the Intelligent Transportation Systems (ITS). The vehicular communication networks are integrated networks for supporting intelligent traffic management and intelligent dynamic information service. It is a large-scale distributed system for wireless communication and information exchange between vehicles and infrastructures according to agreed communication protocols (Chen, Xu, Liu, Hu, & Wang, 2014). With the help of Vehicle-to-Everything (V2X) technologies, vehicular communication networks aim to improve the traffic flow by assisting drivers and infrastructures with useful and real-time information. The main driving force of vehicular communication networks is to improve traffic safety and efficiency. According to Global Status Report on Road Safety 2015 (World Health Organization, 2015), 1.25 million road traffic deaths occur per year. The information sharing of vehicles with other vehicles and infrastructure, provides more precise and comprehensive knowledge of the traffic situation across the entire road network, thus helping cut accident numbers and improve traffic efficiency (Edwards, Hankey, Kiefer, Grimm, & Leask, 2011). The vehicular communication networks are also beneficial to alleviate emission problems (Suthaputchakun, Sun, & Dianati, 2012).

Vehicular communication networks outperform traditional traffic-data acquisition technologies in terms of accessing diverse data types (including position, speed, acceleration etc.), enhancing detection rate, lowering error rate, and continuous tracking. Traditional local detectors usually suffer from limited lifetime, while there is no such concern for wireless vehicular communication since the data exchange takes place “in the air”. In addition, wireless communication networks are able to overcome adverse weathers with a difficult visual safety check (TSUGAWA, 2005), by extending the vehicles’ ability to detect surroundings and supporting drivers with situational awareness. From the perspective of traffic management, vehicular communication networks interlinks centralized and decentralized decision makings, further providing strategies for efficient control, e.g. by applying real-time dependent signal plans to incorporate the actual traffic situations (Görmer, Jana, et al., 2011). From the viewpoint of drivers and other road users, vehicular communication networks can inform them of the current situation without considerable delay and location limitation (Schmidt-Eisenlohr, 2010).

Due to the characteristics of fast-moving vehicles, high vehicle densities, and data synchronization requirement, the primary building block of vehicular communication is the periodic transmission of status information by individual vehicles and other components (Schmidt-Eisenlohr, 2010). This information is often called beacon message, which has specific and unusual communication properties. First, every connected vehicle transmits the beacon message. Second, beacon messages are transmitted in a periodic manner, i.e. several times per second. Third, the beacon messages are transmitted in a broadcast way, and there is no specific recipient. Numerous articles have made efforts in simulating and investigating the

performance and challenges of the vehicular communication networks for further deployment in reality. There are two major challenges in this field: how to integrate the vehicle mobility and how to exactly estimate the characteristics of the wireless channel (Dressler, Sommer, Eckhoff, & Tonguz, 2011). Although Field Operational Tests (FOT) are able to show the realistic performance and are helpful to explore new and unexpected aspects, they are too time and cost-intensive for evaluation (Eckhoff, 2016). The widely used solution is to integrate a simulator that models the vehicular communication network and some vehicle mobility models. However, there is the need to have mobility models that are more realistic in incorporating microscopic vehicle behaviour and macroscopic traffic flow behaviour (Dressler et al., 2011), because of the significant impacts of vehicle mobility on communication network. From the side of traffic engineering, an efficient performance assessment approach of vehicular communication networks is more attractive, in case of conducting road-traffic impact analysis of vehicular communication networks applications in urban area. When coupled with road-traffic simulators, the existing communication network simulators consume too much computational effort especially under scenarios with complicated urban environments, due to the high road traffic density and the presence of many obstacles (buildings, foliage, overpasses etc.). Another possible solution is to use analytical approaches to show fundamental dependencies of the communication network, and further evaluate the systems and implement with realistic road-traffic simulators. Compared to communication network simulators, analytical approaches are more flexible, scalable. To the best of the author's knowledge, a well-developed analytical approach that describes the vehicular communication network under realistic conditions has not yet existed, as the majority are under idealized or limited conditions with some unrealistic assumptions and simplifications.

In such a situation, an analytical approach is developed and coupled with a microscopic simulation tool in this study. The key objective of this study is to offer new opportunities for evaluating the performance of vehicular communication networks. This study also establishes analyses of the influencing factors and their impacts on some performance metrics. For the concern of reliability, the analytical approach is compared with a widely used communication network simulator. The comparison shows a promising result, which indicates that the analytical approach can be an alternative to the communication network simulators with an appropriate level of details. The analytical approach is also implemented with a microscopic road-traffic simulator with the intention of considering the realistic vehicle mobility. Aside from inter-vehicular communication, the analytical approach is capable of modelling Vehicle-to-Infrastructure (V2I) communication as well.

The remainder of this study is organized as follows. *Chapter 2* gives some fundamental information of vehicular communication networks. *Chapter 3* presents the method and procedures of the analytical approach. *Chapter 4* provides an example of how to couple the analytical approach with microscopic vehicle mobility simulators and demonstrates the sensitivity analysis of the selected performance metrics. The case study of cooperative intelligent transportation systems is depicted in *Chapter 5*. *Chapter 6* outlines the capabilities, potentials and limitations of the analytical approach, including a comparison with a simulator and

loss-free scenario. Finally, the outcome of this study and several future research directions are concluded in *Chapter 7*.

2 Fundamentals

In general, vehicular communication systems are networks in which vehicles, infrastructures and other road users are the communicating nodes, dynamic exchanging each other with real-time information, such as safety warnings, road traffic information etc. The vision for vehicular communication systems is that such rich set of data and communications will support a new generation of active safety applications and comprehensive traffic management strategies. As the basis of vehicular communication systems and interlink between different users, the wireless communication network requires particular attention. Except the wireless communication network, there are also necessary devices at the user ends for deploying vehicular communication systems. The components of vehicular communication networks are listed as follows.

- Wireless communication network:

  Vehicular Ad-hoc Networks (VANETs)

  Infrastructure-based cellular network

- Devices:

  On Board Unit (OBU) in vehicles

  Road Side Unit (RSU) at infrastructure side

This chapter will first describe basic concepts of the wireless communication networks in vehicular environment, and then introduce the devices in the systems.

2.1 Wireless communication network in vehicular environment

The existence of multiple radio access technologies brings opportunities towards meeting the requirements of vehicular communication networks applications. However, communication technologies initially developed for other purposes cannot meet the demanding requirements of applications with vehicular communication networks (Sepulcre & Gozalvez, 2011), such as mobility support, communication area coverage and low latency. Therefore, the development of the Dedicated Short-Range Communication (DSRC) technology is motivated, which enables primarily Vehicle-to-Vehicle (V2V) but also V2I communication. While long-range infrastructure-based cellular communication technology can be used for V2I purposes.

Feature	Wi-Fi	802.11p/DSRC	UMTS[1]	LTE[2]	LTE-A[3]
Channel width	20 MHz	10 MHz	5 MHz	1.4, 3, 5, 10, 15, 20 MHz	Up to 100 MHz
Frequency band(s)	2.4 GHz, 5.2 GHz	5.86 – 5.92 GHz	700 - 2600 MHz	700 - 2690 MHz	450 MHz-4.99 GHz
Bit rate	6 – 54 Mb/s	3 – 27 Mb/s	2 Mb/s	Up to 300 Mb/s	Up to 1 Gb/s
Range	Up to 100 m	Up to 1 km	Up to 10 km	Up to 30 km	Up to 30 km
Capacity	Medium	Medium	Low	High	Very High
Mobility support	Low	Medium	High	Very High (up to 350 km/h)	Very High (up to 350 km/h)
QoS[4] support	EDCA	EDCA	QoS and bearer selection	QCI[5] and bearer selection	QCI and bearer selection
Broadcast/multicast support	Native broadcast	Native broad-cast	Through MBMS[6]	Through eMBMS[7]	Through eMBMS
V2I support	Yes	Yes	Yes	Yes	Yes
V2V support	Native (ad hoc)	Native (ad hoc)	No	No	Potentially, D2D[8]
Market penetration	High	Low	High	Potentially high	Potentially high

Tab. 2.1 Main candidate wireless technologies for vehicular communications (Araniti et al., 2013)

[1] Universal Mobile Telecommunications System
[2] Long Term Evolution
[3] Advanced LTE
[4] Quality of Service
[5] QoS Class Identifier
[6] Multimedia Broadcast/Multicast Service
[7] Evolved Multimedia Broadcast/Multicast Service
[8] Device to Device communication

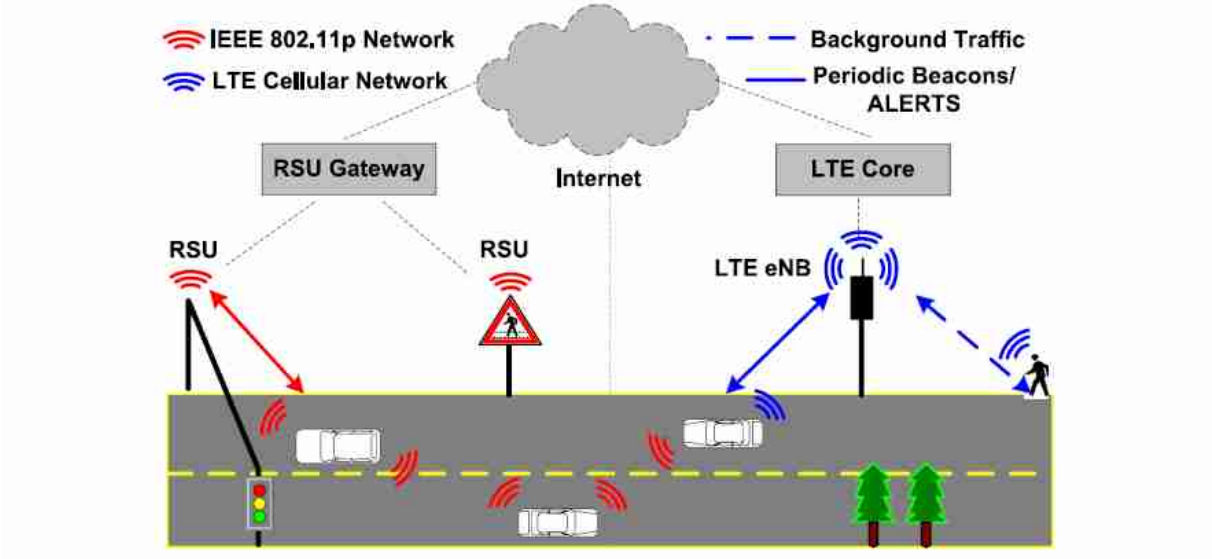

Fig. 2.1 Vehicular networking scenario using IEEE 802.11p and LTE (Mir & Filali, 2014)

Some candidates of wireless technologies for the vehicular communication networks are given in Tab. 2.1. Additionally, the option of integrating both communication technologies also exists (Papadimitratos, La Fortelle, Evenssen, Brignolo, & Cosenza, 2009). An example of vehicular networking scenarios with an integration of IEEE 802.11p and LTE is demonstrated in Fig. 2.1. In the following parts of this section, detailed descriptions of DSRC technology and infrastructure-based cellular technologies are demonstrated.

2.1.1 Vehicular Ad hoc NETworks (VANETs)

In VANETs system, vehicles are able to communicate with each other using DSRC technology without the infrastructure assisted channel access mechanism. In North America, the IEEE 802.11p is an amendment standard based on IEEE 802.11, published by Institute of Electrical and Electronics Engineers (IEEE) body for supporting vehicular data exchange by means of implementing WLAN communication in the 5.9 GHz DSRC spectrum bands. In Europe, the spectrum allocated by European Telecommunications Standards Institute (ETSI) has a range of 5.875-5.925 GHz. There are two types of channels in DSRC: the Control Channel (CCH) and the Service Channel (SCH), with a width of ten MHz for each channel. Fig. 2.2 shows the 75 MHz of spectrum at 5.850-5.925 GHz that used exclusively for VANETs, allocated by IEEE 802.11p. The CCH is used to broadcast status beacons and emergency messages etc., while the SCHs are used for infotainment or commercial applications (Eckhoff, 2016). Safety-related messages cannot be missed or lost as the vehicles synchronize the switching between the CCH and the SCHs (Hafeez, Zhao, Ma, & Mark, 2013).

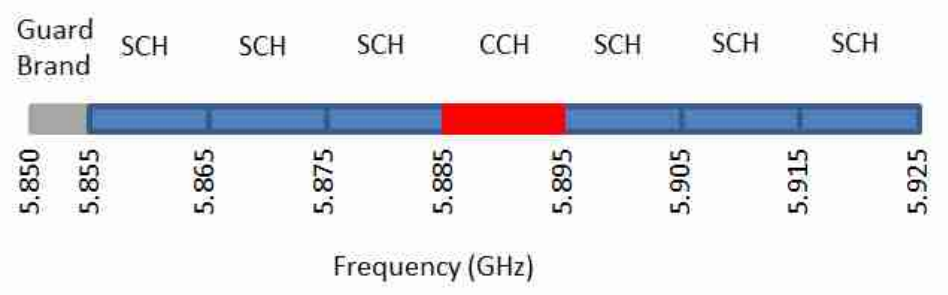

Fig. 2.2 DSRC frequency band and channels in IEEE 802.11p

Aside from IEEE 802.11p, there are other standards concerned with vehicular communication networks that are included in IEEE Wireless Access in Vehicular Environment (WAVE) family, as displayed in Fig. 2.3. For instance, IEEE 1609.4, which is an extension to the WAVE Medium Access Control (MAC) that defines Quality-of-Service (QoS) strategies and multi-channel operations such as alternating access (Eckhoff, 2016).

The major concern of VANETs is that the specified wireless channel has to be shared by all users, including every individual vehicle, which causes unbounded delays before channel access and collisions on the channel. The following paragraphs in this section introduce the medium access schemes in VANETs and further explain the reasons of collisions and channel access delays.

The two layers: MAC layer and Physical (PHY) layer are the main application fields of IEEE 802.11p standard, as shown in Fig. 2.3. In principle, the MAC layer is for accessing the medium in a coordinated way, and PHY layer deals with the details of medium transmission and reception (Schmidt-Eisenlohr, 2010). The IEEE 802.11p PHY layer adopts an Orthogonal Frequency-Division Multiplexing (OFDM) transmission technique that is similar to 802.11a, but the bandwidth of a single channel is half as 802.11a (Han, Dianati, Tafazolli, Kernchen, & Shen, 2012). As mentioned earlier, the key problem of the ad-hoc mode is that all the users share the same frequency band to communicate. IEEE 802.11p uses Carrier Sense Multiple Access/Collision Avoidance (CSMA/CA) as a solution: through carrier (i.e. the medium) sensing, the channel is only accessed if the PHY layer does not observe any ongoing activity, thus the transmission only take place when the channel is sensed to be idle before (Schmidt-Eisenlohr, 2010). If the medium is sensed as busy, the transmission will be postponed for a certain time and then another trial for the same packet transmission starts.

Though CSMA/CA requires each individual vehicle to listen to the channel before transmitting any packets for avoiding collisions, there are still possibilities of packets collisions. For instance, collisions occur when two or more packets are transmitted concurrently. In addition, because of the limitation of the communication range and carrier sensitivity, it is impossible that all vehicles are able to hear from each other. This leads to packets collisions from remote vehicles, as they may transmit packets to a common vehicle that within their communication ranges, without the awareness of the transmitting status of the other remote transmitting vehicles.

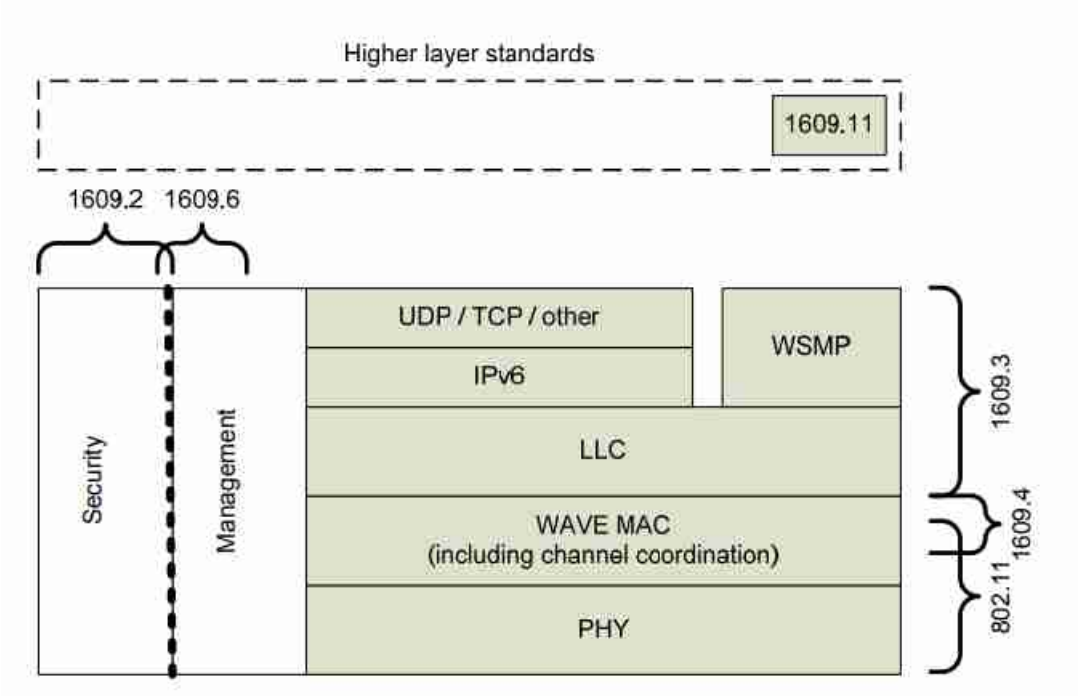

Fig. 2.3 The IEEE WAVE architecture (IEEE Standards Association. (2013))

The channel access mechanism within individual vehicles is handled by Enhanced Distributed Channel Access (EDCA) with contention-based prioritized QoS support, and the logical function EDCAF determines when a packet that is in the transmit queue with the associated Access Category (AC) is permitted to be transmitted (IEEE standards, 2016). The EDCAF originates from Distributed Coordination Function (DCF), as shown in Fig. 2.4. The medium is indicated busy if the carrier sensing power level is higher than a certain threshold, thus observing a valid packet transmission. The Inter Frame Space (IFS) is the time duration that the medium has to be indicated as idle before the access. A shorter inter frame space (SIFS) is required as the waiting packet has a higher priority. A regular data packet needs to wait longer than SIFS after the medium is sensed to be idle, for the duration of a Distributed Inter Frame Space (DIFS).

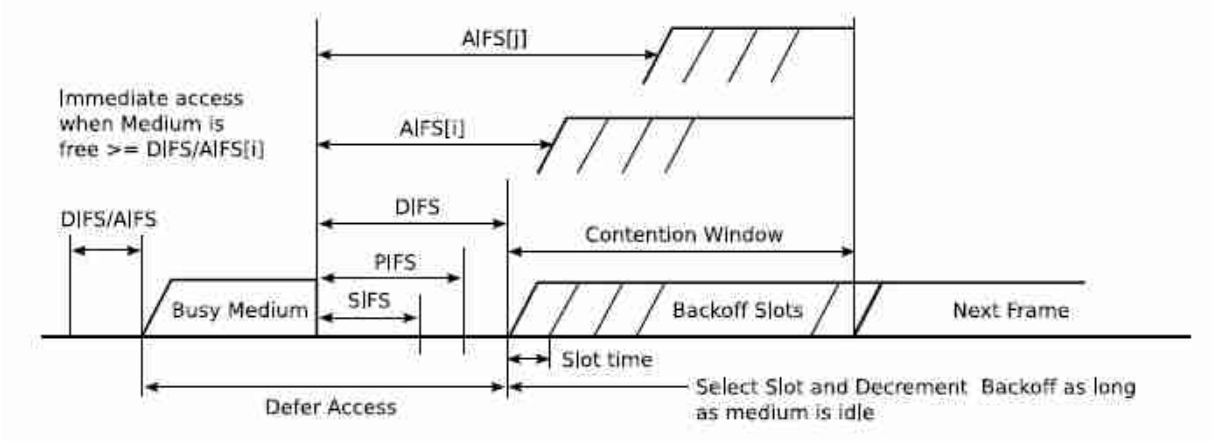

Fig. 2.4 IEEE 802.11 DCF (Schmidt-Eisenlohr, 2010)

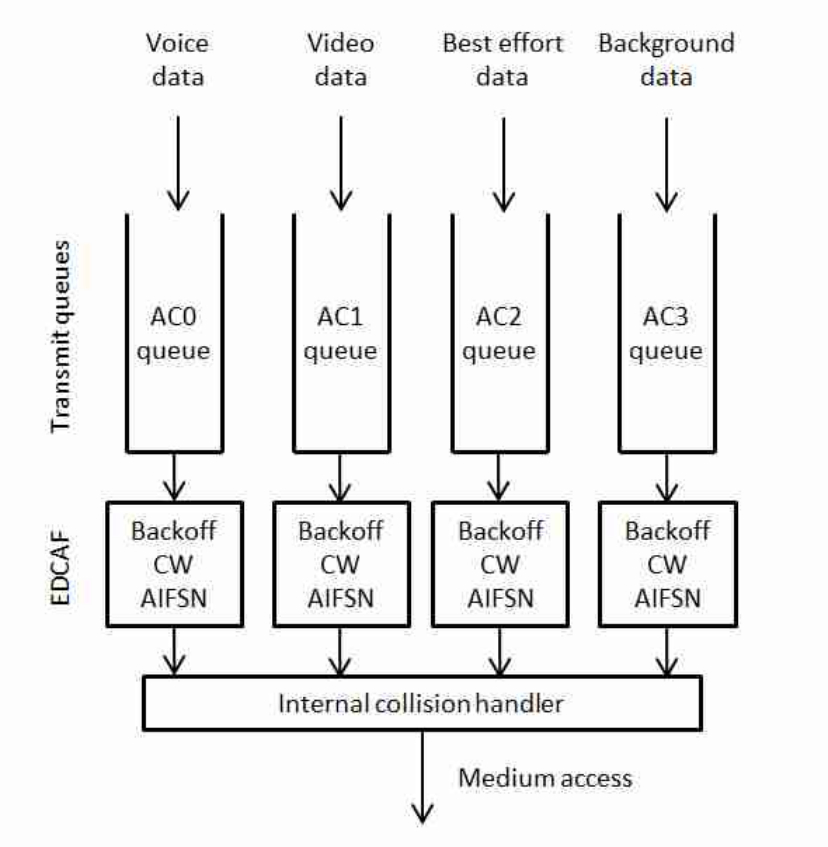

Fig. 2.5 EDCA mechanism of IEEE 802.11p

As shown in Fig. 2.5, EDCA mechanism defines four ACs with different priorities of data transmission support. For each AC, there is one transmit queue and one function EDCAF. The EDCAF maintains a back off counter and determines the AC's own Arbitration Inter Frame Space Numbers (AIFSNs) and Contention Window (CW) size. The relevant parameters are shown in Tab. 2.2. The AC with a smaller AIFS has a higher priority to access the channel. The duration of AIFS[AC] is a duration derived from the value AIFSN [AC] by the relation,

$$AIFS[AC] = AIFSN[AC] \times aSlotTime + aSIFSTime \text{ (Han et al., 2012)} \quad (2.1)$$

where

$AIFSN[AC]$ is the value set by MAC protocol in Tab. 2.2;

$aSlotTime$ is the duration of a slot time, as shown in Tab. 2.3;

$aSIFSTime$ is the length of SIFS, as shown in Tab. 2.3.

AC No.	Access class	CW min	CW max	AIFSN
0	Background Traffic (BK)	aCWmin	aCWmax	9
1	Best Effort (BE)	aCWmin	aCWmax	6
2	Video (VI)	(aCWmin +1)/2-1	aCWmin	3
3	Voice (VO)	(aCWmin+1)/4-1	(aCWmin +1)/2-1	2

Tab. 2.2 Default EDCA parameter set on the CCH in IEEE 802.11p from (IEEE standards, 2016)

Slot time	SIFS
13µs	32µs

Tab. 2.3 Standard settings for IEEE WAVE protocols (IEEE standards, 2016)

When the medium is sensed busy, a random back-off period for an additional deferral time before transmitting is generated, unless the back-off counter already contains a non-zero value, in which case the selection of a random number is not needed (IEEE standards, 2016). This process minimizes collisions during contention among multiple users that have been deferring to the same event. After the channel is sensed being idle for a period equal to DIFS or SIFS without interruption, the back-off counter is counted down and it will be suspended whenever the medium is determined busy, that is, the back-off timer shall not decrement for that slot (IEEE standards, 2016). When the back-off counter reaches zero, the packet will be transmitted in the following slot (IEEE standards, 2016; Schmidt-Eisenlohr, 2010).

$$\text{Backoff Time} = \text{Random}() * aSlotTime \tag{2.2}$$

where

$\text{Random}()$ is a pseudorandom integer drawn from a uniform distribution over the interval [0, CW], where CW is an integer within the range of values of the PHY characteristics as a CWmin and aCWmax, aCWmin ≤ CW ≤ aCWmax (IEEE standards, 2016).

The CW shall be initialized to the value of the parameter CWmin[AC], for the EDCAF's AC. The CW shall be reset to aCWmin after every successful attempt to transmit a packet or reaching the retry counter limit. If a packet is requested to be transmitted, when the back-off counter for that queue was zero and the medium was busy, the CW remained to be the same. Otherwise, the CW shall take the next value in the series every time an unsuccessful attempt to transmission and once it reaches aCWmax, the CW shall remain the value of aCWmax until the CW is reset:

- If CW[AC] is less than CWmax[AC], CW[AC] shall be set to the value

$$(CW[AC] + 1) \times 2 - 1 \quad (2.3)$$

- If CW[AC] is equal to CWmax[AC], CW[AC] shall be left unchanged.

2.1.2 Infrastructure-based cellular networks

VANETs solutions fit well in safety services that require fast transmission, but they suffer from routing problems in long distance transmissions where multi-hop techniques might be used (Santa, J. and Gómez-Skarmeta, A.F., 2008). DSRC/WAVE established the foundation for V2X communications, though the performance of ad-hoc medium access mechanism tends to degrade as the vehicle density increases. Severe communication congestion comes forth with higher beaconing frequency and higher vehicle mobility (Mir & Filali, 2014). Besides, effective communication range depends heavily on the nearby vehicle density and the radio propagation environment. V2X applications have kept evolving since the inception stage of DSRC/WAVE. Yet, currently, there is no significant effort to evolve the DSRC technology to keep up with the more advanced use cases. In such a situation, cellular network steps in and become a promising foundation for V2X going forward. More researchers and developers argue that network technologies such as UMTS/LTE/LTE-A offer new capabilities than VANETs.

For instance, the LTE is a wireless broadband technology that provides high data rate and low latency to mobile users. Like all cellular systems, it benefits from covering a large area, high market penetration rate, and high-speed terminal support (Araniti, Campolo, Condoluci, Iera, & Molinaro, 2013). Recently, there is a warming discussion on extending its usage to support vehicular communication networks. The high-bandwidth demands and QoS strategies – sensitive requirements of vehicular information and entertainment applications (known as infotainment) -can be reached by LTE and fifth-Generation (5G) technology, but for traffic safety and efficiency is still an open issue (Araniti et al., 2013).

The main concern of centralized cellular architecture is that communications have to traverse the entire core network, even with localized V2V data exchange, which increases latency on beacon transmission (Araniti et al., 2013). Besides, the latency increases as the network load increases (Mir and Filali, 2014). Yet, (Liu, Xu, Li, & Wang, 2014) introduced the Device to Device (D2D) communication in LTE-A cellular networks that allows User Equipment (UE) in proximity to directly communicate with each other without the relay of cellular evolved nodeB (eNB), thus improving the overall system performance, such as throughput and power consumption.

LTE has the potential of addressing the V2X use cases with low-latency and high-reliability requirements in a complementary manner to DSRC. Compared to DSRC, the cellular vehicular communication network has a larger area coverage and higher stability. Additionally, the existing LTE infrastructure can be used to support Cellular-V2X applications either through an LTE-A enabled OBU or using smartphones with LTE connectivity. However, in the presence of higher cellular network load, current Cellular-V2X is tough to meet the stringent latency requirements (Mir & Filali, 2014). According to (5G americas, 2016), maximum latency

of a message transfer by LTE technology between two UEs is 100ms, and for messages sent via a network server is 1000ms. 5G-based V2V systems are expected to shorten end-to-end latency between vehicles to 5ms or less and provide over 99% packet delivery reliability within a short to medium range (80-200m).

The study of 5G-based V2X has already begun in 3GPP[9]. Cooperating with 5GAA (5G Automotive Association) partners including Audi, BMW, China Mobile, Daimler, Vodafone, Huawei, Qualcomm, etc., 3GPP is actively driving the Cellular V2X (C-V2X) standardization efforts to pioneer C-V2X technologies. There are two kinds of modes in LTE C-V2X technology: LTE Direct D2D and LTE Broadcast (via the network). The following two paragraphs are the description of the two modes from (5G americas, 2016):

- Direct communication uses the LTE PC5 interface, which is based on Release 12's proximity services (ProSe) communications feature, with enhancements to the adaption of high speeds/Doppler Effect, high vehicle density, improved synchronization and decreased latency. This mode is suitable for proximal direct communications (hundreds of meters) and for V2V safety applications that require low latency (e.g., ADAS-advanced driver assistance system, situational awareness). This mode can work both in and out of network coverage.
- Network-based communication uses the LTE-Uu interface from the UE located in the vehicle and the evolved Node B/base Station (eNB). UEs send unicast messages via the eNB to an application server, which in turn rebroadcasts them via evolved Multimedia Broadcast Multicast Service (eMBMS) for all UEs in the relevant geographical area to receive. This mode uses the existing LTE Wide Area Network (WAN) and is suitable for more latency-tolerant use.

2.2 OBU and RSU devices

The wireless communication network provides the connection bond within the vehicular communication networks, while OBUs and RSUs are the devices on the vehicle and infrastructure side respectively, as displayed in Fig. 2.6. The OBUs are used to describe the functions performed within the vehicle in addition to the radio transmission element. An OBU is logically composed of a radio transceiver, a GPS system, an application processor and interface systems to vehicle/human. The OBUs transmit status/safety messages to other vehicles and infrastructures (P. Gaspar, Z. Szalay, et.al., 2014). From the infrastructure domain, RSUs comprise the subsystems relevant to the infrastructure services. RSUs can be mounted at interchanges, intersections and other locations, providing the service to vehicles within communication range. An RSU is composed of a radio transceiver, an application processor, a GPS receiver and interface to the V2I/ Infrastructure-to-Vehicle (I2V) communication network (P. Gaspar, Z. Szalay, et.al., 2014).

[9] 3rd Generation Partnership Project

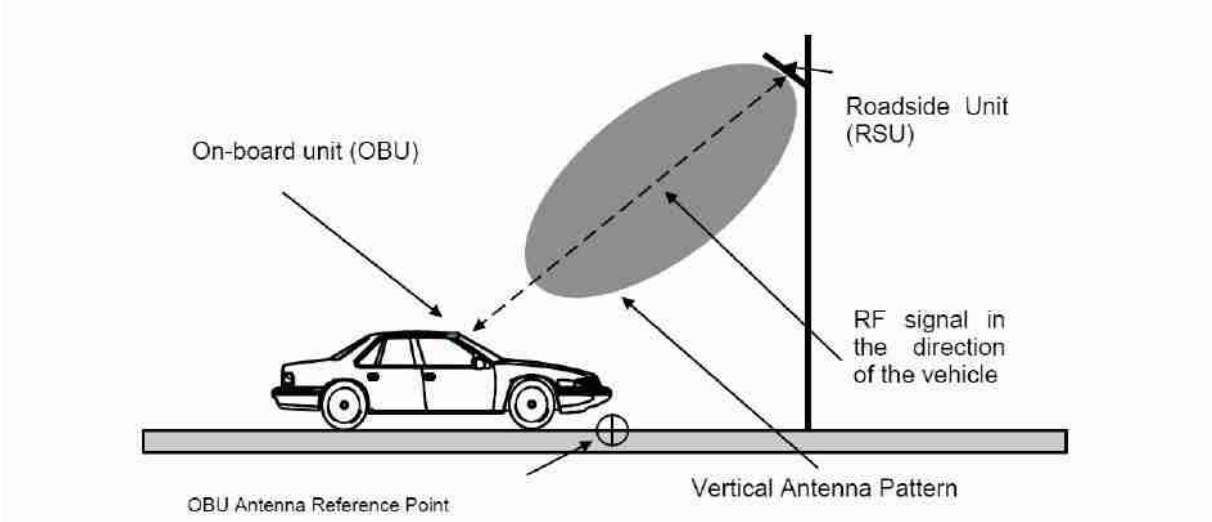

Fig. 2.6 OBU and RSU (Uzcategui & Acosta-Marum, 2009)

2.3 Vehicular communication networks simulation

Generally, there are three main kinds of methodologies to perform assessments of vehicular networks: FOT, simulation and analytical model. Due to a limited number of equipped vehicles and the expensive cost, FOT have not been widely used for evaluating the performance of vehicular communication networks. In view of long-term run and scalability, simulations and analytical models prevail over FOT. Though analytical models are easy to implement and require less computational effort than simulations, some researchers consider the analytical models as unqualified, because the analytical models are based on many assumptions. In the last decade, simulation has become the most popular tool for the performance evaluation of vehicular network applications, technology, and protocols (Eckhoff & Sommer, 2015). A large number of studies focused on IEEE 802.11p protocol simulation and some of them (Boban, 2013; Schmidt-Eisenlohr, 2010) included performance validation of the wireless network with FOT. However, most of the existing communication network simulators and FOTs are manipulated with small-scale highway scenarios while lacking appropriate consideration in vehicle mobility impacts. Urban scenarios are easily ignored to some degree due to the complicated environment. In this section, an overview of the vehicular communication network simulators is presented. The simulators of vehicular communication networks are commonly classified into 3 categories: vehicle mobility simulators, communication network simulators, and hybrid simulators (Martinez, Toh, Cano, Calafate, & Manzoni, 2011).

2.3.1 Vehicle mobility simulator

High mobility is one of the most representative characteristics of vehicular communication networks, and it heavily influences the communication network topology. Therefore a reliable mobility model is the basis of scientifically sound performance evaluation of vehicular networks (Eckhoff & Sommer, 2015). Vehicle mobility simulators are usually classified into submicroscopic, microscopic, mesoscopic and macroscopic, depending on the details of the

simulation, thus based on the smallest entity that the simulator considers. Exemplary, macroscopic traffic simulation considers the traffic flow as an entity, while microscopic traffic simulation is based on each individual vehicle composing the traffic stream (Barceló, 2010). Using microscopic traffic simulation is an adequate approach for vehicle mobility in vehicular network simulation because every individual vehicle is taken as a node and the simulation of the components of vehicles and the status of the components are not relevant.

One of the most well-known microscopic traffic simulators is Simulation for Urban MObility (SUMO) (Krajzewicz, Daniel, et al., 2002). It tightly connects modified version of space-continuous and time-discrete car-following model by (Krauß, 1998) and lane-changing model by (Krajzewicz, 2009) that capture decisions on whether and when a vehicle changes lane. It also includes a graphical application that provides 2D graphical visualization of traffic simulation and procedures for dynamic traffic assignment. It is available as “open source”, both as source code and in compiled, executable form for multiple Windows and Linux platforms (Barceló, 2010).

Another popular microscopic traffic flow simulation model is VISSIM (Lownes, N. E., & Machemehl, R. B., 2006). It includes a rule-based lane-changing model and the Wiedemann psychophysical driver behaviour model (Wiedemann & Reiter, 1992) that considers the influence of driver’s perception of velocity control. Besides, VISSIM uses a structure of one-way links connected with connectors, leading to a more flexible and precise way to construct road structures. VISSIM also offers many functionality options for modelling traffic signal controllers. Dynamic traffic assignment and various vehicle types (e.g. two-wheeled vehicles, trams) are allowed in VISSIM. In addition, it can cooperate with external hardware controllers which provides possibilities for adjustments of vehicle properties (Maciejewski, 2010).

There are other microscopic simulations as well, such as Dynameq (Florian, Mahut, & Tremblay, 2006), Aimsun (Barcelo, Ferrer, & Montero, 1989), Paramics (Cameron & Duncan, 1996), etc.

2.3.2 Communication network simulator

Communication network simulators are used to simulate and analyse the effects of various parameters on communication network performance (Sluijsmans, 2011). It not only saves the time and cost in setting up an entire communication network for testing new communication network protocols but also enables to implement in a controllable and reproducible way (Martinez et al., 2011). Communication network simulators are based on discrete event simulation, in which events are the cores of the simulation as only the impacts of the events are important, thereby saving simulation time. The existing and popular network simulators such as NS-2/NS-3 (Font, Juan Luis, et al., 2010), JiST (Barr, Haas, & van Renesse, 2005)/SWANS (Barr, 2004), OMNeT++ (Varga, 2001), and OPNET (Modeler, 2009) use simplified stochastic radio models for highly dynamic networks. These models rely on the statistical properties of the chosen environment, with limited consideration of obstacles and mobility influences. The reason for using simplified stochastic radio models is that reasona-

ble approximations can be achieved with low computational cost. For example, NS-3[5] is based on simple statistical models (e.g., free space, long-distance path loss) that are used indiscriminately for all environments where the communication occurs. Obviously, these models cannot capture the characteristics of vehicular communication channels, changes in delay and Doppler Effects that caused by high vehicle mobility and complicated environment. On the other hand, topography-specific, highly realistic channel models that are in accordance with the reality require much more computational power and are bound to a specific location (Boban, Vinhoza, Ferreira, Barros, & Tonguz, 2011). It can be said that the main shortcoming of the network simulators is the lack of consideration of vehicle mobility, due to the fact that vehicle mobility models are not included in network simulators (Paikari, 2014).

2.3.3 Hybrid simulator

A hybrid simulator is known as the software or an integrated framework that allows changing the behaviour of vehicles and influencing travel patterns, based on the additional situational awareness from data sharing. The current hybrid simulators usually implement vehicle mobility and communication network in two separated simulation tools (Sluijsmans, 2011). Both simulators are running the same simulation and are continuously exchanging state information. As the microscopic vehicle mobility simulator provides vehicles movement to communication network simulator as topology dynamics; in return, the communication network simulator feeds back control and sensor data to the vehicle mobility simulator (Eckhoff & Sommer, 2015).

Several examples of hybrid simulators are iTETRIS (Rondinone et al., 2013), Veins (Eckhoff, D., & Sommer, C., 2012) and VSimRTI (Schünemann, 2011). iTETRIS was funded by the European Commission, which is a platform that integrates NS-3 and SUMO, with the aim of evaluating solutions based on ETSI ITS G5. Veins is an open source framework for running vehicular network simulations, integrating simulators of communication networks and road traffic, thus OMNeT++ and SUMO respectively. VSimRTI couples different simulators and enables the simulation of the various aspects of ITS.

3 Method and Procedures

For performance assessments of vehicular communication networks in urban scenarios, it is highly recommended to investigate the wireless channel characteristics with influences of vehicle mobility. In the field of performance assessment for vehicular communication networks, communication network simulators and analytical models are commonly used rather than large-scale FOT, due to the lack of equipped vehicles. The communication network simulators are able to evaluate the performance assessment with an appropriate level of details, because of a suite of inner models that are specific to vehicular network simulation. However, when it comes to coupling with vehicle mobility simulators for generating realistic road-traffic impact analysis, the required computational resources for using communication network simulators are significantly high. This restricts communication network simulators to be used on specific small-scale communication network scenarios (Sommer, German, & Dressler, 2011). Compared with communication network simulators, analytical models take much less computational effort yet still provide valuable analysis results. From the viewpoint of traffic engineers, analytical models can be the most efficient tool for evaluating the impacts of vehicular communication networks. However, the reliability is the main demerit of analytical models, because of its oversimplification and unrealistic hypothesis.

(Bianchi, 2000) analysed the performance of a saturated communication network using a Markov chain model. (Malone, Duffy, & Leith, 2007) extended the model to the unsaturated case. The Markov chain model is a memoryless model, which is not suitable for depicting the back off process when deferring packet transmission. Additionally, they only considered unicast communications and ignored the hidden terminal problem by assuming a fully connected scenario, i.e. there are no hidden terminals. However, (Hassan, Vu, & Sakurai, 2011) pointed out that the hidden terminal problem is the principal reason for the low packet delivery rate, and they also developed an analytical model for unsaturated broadcast networks with consideration of the hidden terminal problem. Recently, more researchers study in hidden terminal problems, for instance (Yao, Rao, Liu, & Zhou, 2013) proposed a 2D Markov chain model for MAC access delay distribution of broadcast communication. (Hafeez et al., 2013) also used Markov chain to analyse the communication network performance for a highway scenario with the integration of self-developed mobility model. To the best of my knowledge, an analytical model that suits both saturated and unsaturated cases for realistic urban traffic scenarios has not yet existed. To fill this gap, a reliable and efficient module for evaluating the performance of VANETs is developed in this study, with sufficient considerations of both saturated and unsaturated cases in urban traffic scenario.

Generally, different applications of VANETs have different particular performance metrics requirements, for instance, end-to-end delay for traffic safety applications, total collision probability for traffic efficiency applications, and throughput for infotainment applications. With the intention of evaluating VANETs performance in traffic efficiency applications, the proposed module is designed with a focus on the total collision probability. Besides, this

module is able to provide analyses of some other performance metrics, such as channel busy time and delay.

Before deriving the total collision probability, the causes of collisions should be analysed. Collisions happen when packets arrive at the same receiver (the receiving vehicle) within certain time overlap. Both nearby and remote vehicles of the transmitter (the transmitting vehicle) can trigger collisions. For nearby vehicles, IEEE 802.11p uses CSMA/CA to try to avoid collisions, however, concurrent transmissions can still occur, resulting in direct collisions at the same receiver. Recall that CSMA/CA highly depends on the carrier sensing sensitivity, which means for vehicles that are out of each other's sensing range, it is unable to avoid collisions among them. Hence, for remote vehicles those are unable to hear from the transmitter, they can trigger hidden terminal collisions. In summary, to ensure successful reception of the transmitting packets, there are three conditions to be fulfilled:

i. The receiving signal power level of the packet is higher than the receiving power level threshold, which is denoted as P_{th}.
ii. No other vehicles within the communication range of the transmitter send packets at the same time slot as the transmitter does. Thus, there is no other transmission from nearby vehicles while the transmitter is sending a packet.
iii. For remote vehicles that are within the interfering range of the transmitter, they should not start transmission during the vulnerable period of the transmitting packet since CSMA/CA requires this period to be quiet for the successful reception at the receiver. The interfering range refers to the area that is out of the transmitter's communication range while within the receiver's communication range. The remote vehicles within the interfering range of the transmitter are called hidden terminals.

Based on above requirements, the total collision probability for each packet can be calculated. The following parts of this chapter show the complete procedures and inner channel models of the proposed module. *Section 3.1* provides a general view of the structure of the proposed module with a flowchart as shown in Fig. 3.1. *Section 3.2* and *Section 3.3* describe the receiving power model and collision probabilistic model respectively.

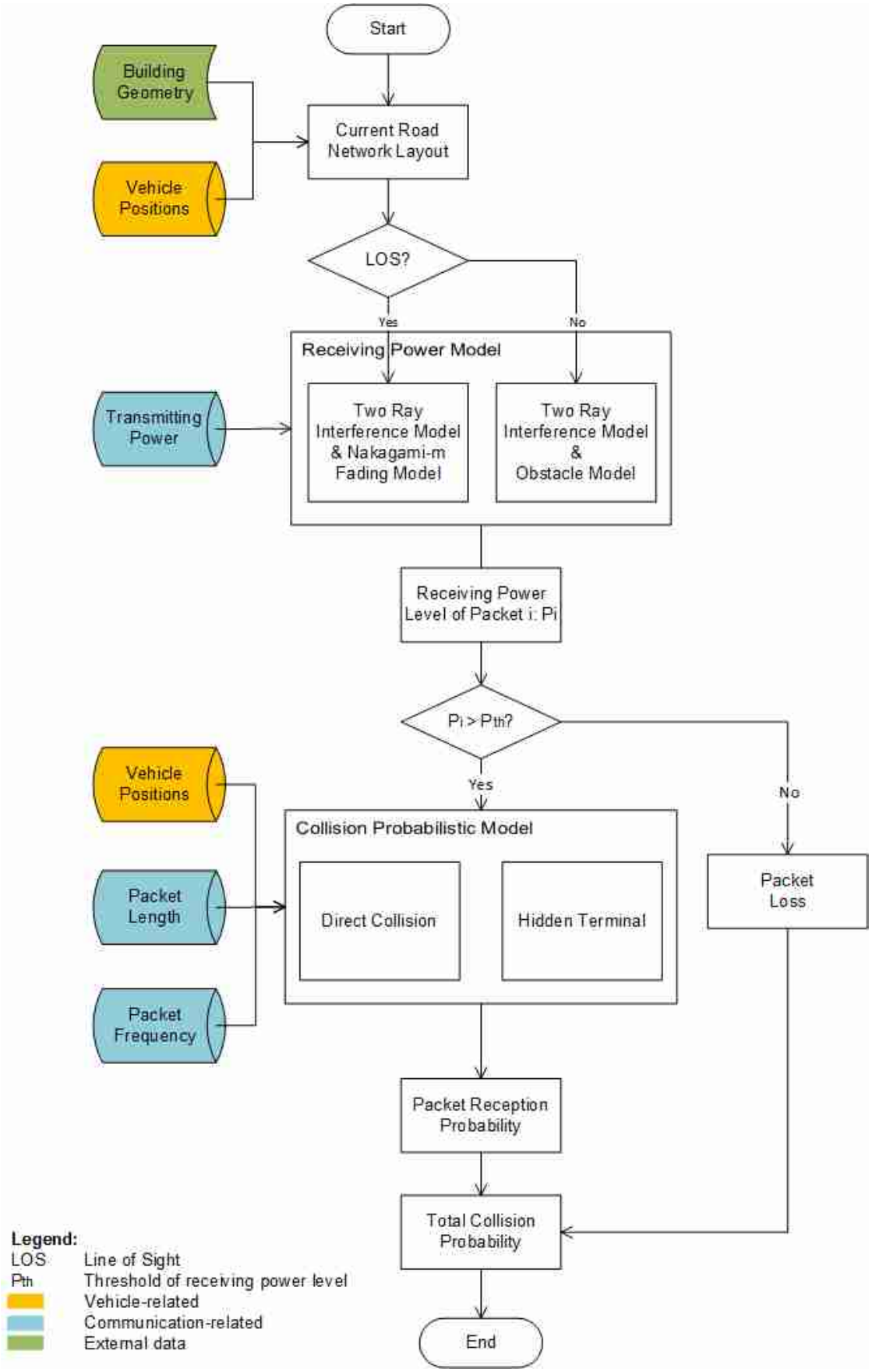

Fig. 3.1 Module structure

3.1 Module structure

The proposed module has five inputs, which can further be classified into three categories: vehicle-related, communication-related and external data. Vehicle-related data is the *Vehicle Positions*, which can be extracted from the microscopic vehicle mobility simulator. *Transmitting Power*, *Packet Length* and *Packet Frequency* are in the second category, as they are related to the communication network's side. *Building Geometry* is from the external source data, such as OpenStreetMap. By combining *Building Geometry* with *Vehicle Positions* data, the *Current Road Network Layout* is created.

Based on the network layout, every potential communicating pair is checked whether there are buildings obstructing the transmission. If there is no building between the transmitter and the receiver, the radio ray is transmitted via Line of Sight (LOS), or else it is a Non-Line of Sight (NLOS) transmission, as shown in Fig. 3.2. The white rectangles represent vehicles and grey rectangles represent buildings. The link type of transmission affects the applied receiving power level model. The receiving power level of a packet is first calculated by *Two Ray Interference Model* (Rappaport, 2002) as long-distance path loss model. This module also provides Nakagami-m fading model (NAKAGAMI, 1960) as the small-scale fading model, with the concern of multi-path environment. For NLOS transmission, Obstacle Model (Sommer, Eckhoff, German, & Dressler, 2011) is used as an additional attenuation model for shadowing effects. *Section 3.2.1* gives an explicit description of the receiving power model. The inputs for *Receiving Power Model* are the transmitting power of the packet i, the positions of the transmitter and receiver, and the building geometry. After the calculation of the radio propagation models, the receiving power level of the packet i, P_i is obtained.

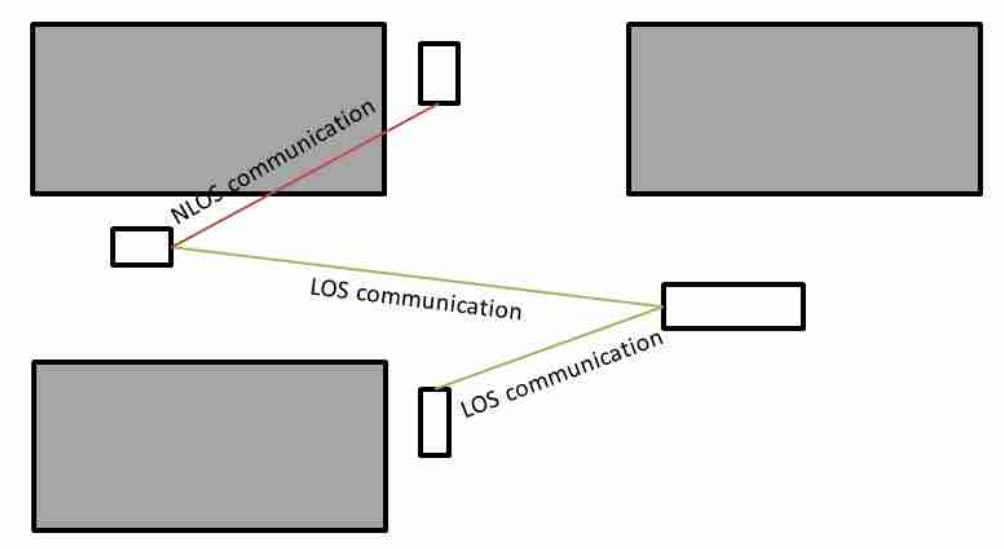

Fig. 3.2 Transmission link types of V2V communication

The next step is to compare the receiving power level P_i with the receiving power level threshold - P_{th}. If P_i is smaller than P_{th}, which means the receiving power level is too low for decoding, the packet is considered as lost. For packets with higher receiving power levels, they will be processed with the *Collision Probabilistic Model*, which takes the *Vehicle Posi-*

tions, *Packet Length* and *Packet Frequency* as inputs. The *Vehicle Positions* are used for getting the number of neighbours and the number of hidden terminals. Recall that the neighbours are nearby vehicles of the tagged transmitter, whose distances from the tagged transmitter are within the communication range. Recall that hidden terminals are the remote vehicles that cannot communicate with the transmitter, yet still able to communicate with the receiver. Therefore, the number of hidden terminals is calculated by filtering the common members in two respective neighbour groups of the transmitter and the receiver. Except interference from the vehicles, the *Collision Probabilistic Model* also considers the influences of packet length and packet sending frequency. The detailed deduction of *Collision Probabilistic Model* is in *Section 3.2.2*. After this, the *Packet Reception Probability of Packet* i, PRP is obtained. The total collision probability is calculated using the following formula:

$$total\ collision\ probability = 1 - PRP \tag{3.1}$$

Note that in the case that the receiving power level is lower than the threshold, PRP is determined as zero, thus the total collision probability is one.

3.2 Receiving power model

This section presents models to describe and characterize radio wave propagation. Radio wave propagation forms the basis for wireless communication and follows the underlying physical principles. First, the basic concepts of wireless channels are given, which can be characterized from the view of physical phenomena occurring to electromagnetic waves. The channel represents a resource that is used to establish a connection between a transmitter of information and a receiver of this information (Schmidt-Eisenlohr, 2010). (Matolak, Sen, & Xiong, 2006) stated that “one can define the channel as the complete set of parameters for all paths that transmitted electromagnetic waves in the frequency band of interest take from transmitter to receiver over the spatial region of interest”. The signals in vehicular communication environments will face many challenges like absorption, reflection, refraction, diffraction and scattering, due to obstacles on the road such as heavy trucks, buildings, foliage, and overpasses. Absorption is one of the most common reactions of wireless signals facing other materials when a material converts the signal’s energy into heat. Reflection is the phenomenon in which after striking the reflecting surface the radio waves return to the same medium. The reflecting surface can be buildings, ground etc. Refraction involves a change in the direction of waves as they pass from one medium to another, and it is accompanied by a change in speed and wavelength of the waves. Diffraction occurs when waves encounter an obstacle and travel around it, in which case both the wave’s direction and intensity change. Scattering occurs when signals scatter with the presence of dust, humidity, unevenness and other qualities in a material.

To describe the effects of the environment on the signals, three types of channel models are used in this module: long-distance path loss, shadowing or large-scale fading, and small-scale fading. Long-distance path loss relates to the physical phenomenon of wave radiation

in the far field. Shadowing or large-scale fading occurs whenever the radio waves have to pass solid material, e.g. walls that absorb some of the energy. Due to the dynamic mobility of VANETs, shadowing conditions may quickly vary over time and it is difficult to precisely reflecting the individual situation and corresponding shadowing effects. Small-scale fading describes the fast changing and variations of reception conditions due to surrounding changes. A usual way to calculate the receiving power level of a signal lies in subsequently applying mathematical description of these phenomena to the transmitted signal: first, the signal attenuation due to the long-distance path loss is calculated, then, shadowing effects are additionally considered, and finally, the effects of fading are applied (Schmidt-Eisenlohr, 2010). In addition, antenna gains at the transmitter and the receiver should be considered. Generally, the calculation of the receiving power level is calculated as follows.

$$P_r[dBm] = P_t[dBm] + G_t[dB] + G_r[dB] - \sum L_i[dB] \quad (3.2)$$

where

P_r is the receiving power level;

P_t is the transmitting power level;

G_t, G_r are antenna gains of the transmitter and the receiver;

L_i is the attenuation component, which includes deterministic and probabilistic attenuation effects.

Two Ray Interference Model is selected as the path loss model, which captures the effect of constructive/destructive self-interference effects caused by reflection of the signal from the ground and effect of lowering signal strength over distance (Eckhoff & Sommer, 2015), as shown in Fig. 3.3. According to experiments conducted by (Sommer, C., & Dressler, F., 2011), the proposed two-ray interference model predicts a more accurate result than the simplified two-ray ground model and free-space path loss model. This is the main reason of choosing this model in the proposed module. Additionally, buildings as obstacles that attenuate the signal also influence radio propagation. Buildings that block the LOS transmission between the transmitter and the receiver degrade the received power level. This shadowing effect is captured by an *Obstacle Model* developed by (Sommer et al., 2011). For small-scale fading effects, *Nakagami-m Fading Model* is available to apply as the small-scale fading model. It takes the receiving power level determined by deterministic propagation models (two-ray interference model and obstacle model) as input, and it models multi-path fading effects based on Gamma distribution.

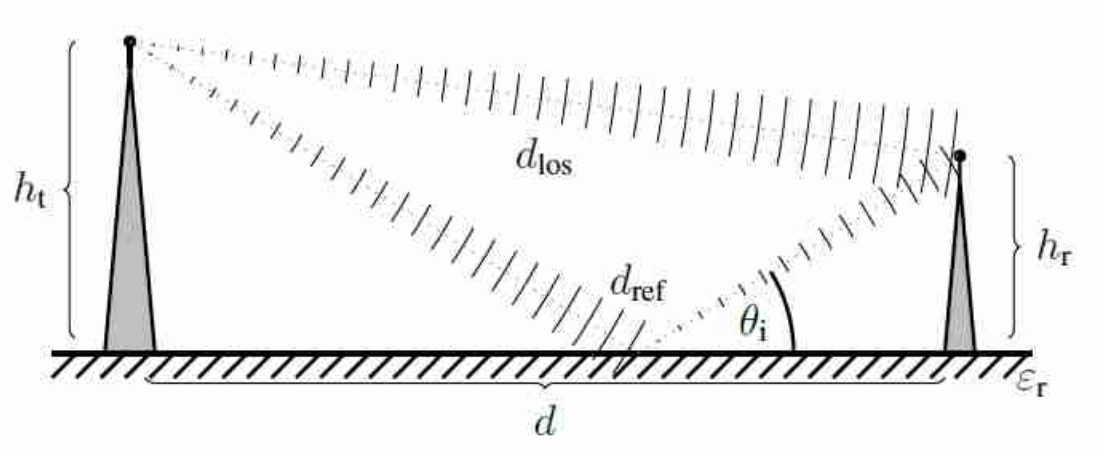

Fig. 3.3 Conceptual model of two-ray interference model (Sommer, Joerer, & Dressler, 2012)

$$P_r[dBm] = P_t[dBm] + G_t[dB] + G_r[dB] - L_{tri}[dB] - L_{nkg}[dB] - L_{obs}[dB] \quad (3.3)$$

$$L_{tri}[dB] = 10log_{10}\left(4\pi\frac{d}{\lambda'}\left|1 + \Gamma_{\perp}e^{i\varphi}\right|^{-1}\right)^2 \quad (3.4)$$

$$L_{nkg}[dB] \sim Nakagami\left(m, \frac{P_r{}'}{m}\right) \quad (3.5)$$

$$L_{obs}[dB] = \beta n + \gamma d_m \quad (3.6)$$

where

L_{tri} , L_{nkg}, L_{obs}, are attenuation components from *Two-Ray Interference Model*, *Nakagami-m Fading Model*, and *Obstacle Model* respectively;

d is the distance between the transmitter and the receiver;

λ' is the radio wave length;

$\Gamma_{\perp}$ is the reflection coefficient, which depends on fixed permittivity of the ground and the incidence angle θ_i;

φ is the phase difference between the LOS and the reflection component (ground), depending on the length of the two rays and the wave length;

$Nakagami(m, \frac{P_r{}'}{m})$ is the Nakagami-m distribution function, with shape of m (multi-path) and scale of $\frac{P_r{}'}{m}$;

$P_r{}'$ is the receiving power level after deterministic model calculation;

β represents the attenuation that a transmission experiences due to the exterior wall of a building, which is given in dB per wall;

n is the number of times that the border of obstacle is intersected by the LOS;

γ serves as a rough approximation of the internal structure of a building, which is given in dB per meter;

d_m is the total length of the obstacle's intersection with LOS.

When the receiving power level P_r of a packet has been obtained, the next step is to determine whether the packet is decodable, which is done usually by evaluating the Signal-to-Interference-plus-Noise Ratio (SINR) in channel modelling part of communication network simulators.

$$SINR(i) = 10log_{10}\left(\frac{P_r}{Noise+\sum_{i\neq j}P_j}\right), \quad (3.7)$$

where

$Noise$ is the background noise, unit in mW;

$\sum_{i\neq j}P_j$ is the sum of the power levels of all packets other than the tagged packet on the channel, thus, the interference from other vehicles, unit in mW.

The probability of failing to decode one bit (bit error rate) is computed with SINR, and it depends on the used modulation scheme (QPSK, BSK …). In the case of QPSK and under the assumption of an Additive White Gaussian noise channel, the Bit Error Rate (BER) is calculated as:

$$BER = \frac{1}{2}erfc\sqrt{SINR} \text{ (Eckhoff \& Sommer, 2015)} \quad (3.8)$$

where

$erfc$ represents the complementary error function.

The probability of a packet can be decoded successfully is computed by:

$$P_{succ} = (1 - BER)^{packet\ length[bits]} \quad (3.9)$$

In communication network simulations, the reception of a packet is decided by drawing a random number $RNG \in [0, 1)$ and then comparing it with the P_{succ}. The packet is handed over to the MAC layer if $RNG < P_{succ}$ (Eckhoff & Sommer, 2015). This is the main reason of high computational resource demand for communication network simulations. While in the proposed module, an analytical model is presented to calculate the interference from other vehicles, i.e. the *Collision Probabilistic Model*. The following section explains the analytical model explicitly.

3.3 Collision Probabilistic Model

The analytical models that attempt to characterize the performance of vehicular communication networks are usually not as competent as simulators, because of the oversimplifications and impractical assumptions. The challenge of the analytical models lies in describing the complicate MAC mechanism of the protocol in a probabilistic manner. The majority of analytical models are only able to focus on conditioned performance evaluation, for instance, only on unsaturated or saturated situations. Here, saturated and unsaturated situations describe the density level of connected vehicles. However, some existing analytical models offer the possibility of developing a further comprehensive statistical solution to performance assessment of vehicular communication networks. This *Collision Probabilistic Model* takes (Hassan et al., 2011) model as the basis. One thing should be mentioned is that the original model from (Hassan et al., 2011) is claimed to be used only for unsaturated situations. With some extension and modification, the *Collision Probabilistic Model* for both saturated and unsaturated situation is developed. The rest of this section demonstrates it in detail.

The *Collision Probabilistic Model* is developed based on several necessary assumptions, listed as follows:

i. Vehicles on the road are represented as a collection of random and statistically identical nodes in a mobile ad-hoc network. Vehicles are stationary during the communication interval, as the interval is so small that the distance the vehicle has driven can be ignored (Hassan et al., 2011).
ii. The transmitting and interfering range for each vehicle are not equal or deterministic. Instead, they are based on the vehicle locations and the surrounding environment. For each individual vehicle, its potential receivers are determined based on the packet receiving power levels at them.
iii. Data packets are generated at each vehicle according to a Poisson process with rate λ [in packets per second] (Hassan et al., 2011). The IEEE 802.11p recommends that the packets transmitted in the CCH shall be sent with a frequency of ten Hz, i.e. ten packets per second.
iv. With aforementioned assumptions, each vehicle is modelled as an M/G/1 queue with an infinite transmitting buffer size, thus no packet loss due to buffer overflow. Recall that for each AC, there is a queue of packets that are waiting to be transmitted. The ρ is defined as the queue utilization, expressed as

$$\rho = \lambda * E[S] \text{ (Hassan et al., 2011)} \quad (3.10)$$

where
ρ represents the queue utilization;
λ is the number of packets each vehicle generated per second;
$E[S]$ is the average service time per packet.

As mentioned earlier, there are two kinds of collisions that cannot be avoided by CSMA/CA. One is defined as direct collisions, which occur when two or more vehicles that are close to

each other coincidentally transmit their packets at the same time. *Section 3.3.1* depicts the deduction process of the direct collision probability. The other is called hidden terminal collisions, caused by the fact that not all vehicles are able to hear from each other. *Section 3.3.2* presents the hidden terminal collisions in details.

3.3.1 Direct collision probability

Because of the CSMA/CA that requires every vehicle to listen to the channel before transmitting packets, a considerable number of collisions are avoidable. However, there are still concurrent transmissions that lead to direct collisions within nearby vehicles. In this section, the direct collision probability without consideration of hidden terminals is deducted. Before deducting the direct collision probability, the scenarios when a new packet is generated from a vehicle are listed as follows (Hassan et al., 2011):

i. A packet is generated at an empty buffer and the channel is sensed as idle for a DIFS period.
ii. A packet is generated at an empty buffer and the channel is sensed as busy.
iii. A packet is generated at a non-empty buffer.

An empty buffer means that there are no packets waiting in the queue, thus the newly generated packet can be transmitted once it is allowed to. Otherwise, except a potential back-off process, this packet shall wait until it reaches the first place of the queue.

For the first case, a collision occurs only when there are other packets generated at other vehicles within the propagation delay. As the propagation delay time within the transmitting range is negligible (Wang, Z., & Hassan, M., 2009), this type of collisions can be ignored. From the standard M/G/1/∞ queuing theory, the probability that the buffer is empty is expressed as $1-\rho$. The probability that the channel is sensed as busy when a new packet generates at the tagged transmitter is denoted as p_b. Assuming independence between an empty buffer and a busy channel, the probability of finding an empty buffer and sensing the channel idle is $(1-\rho)*(1-p_b)$. In the second case, the joint probability of a packet is generated at an empty buffer and the channel being busy due to transmission by other vehicles is $(1-\rho)*p_b$. For the last case, the probability of a packet is generated at a non-empty buffer is ρ. Recall that the queue utilization is expressed as ρ, which depends on the average service time of the packet and the packet generation rate. For the last two cases, the packet must undergo a back off process before its transmission. After the back off counter reaches zero, the transmitter sends the packet in the following slot, and if another nearby vehicle sends a packet simultaneously, a direct collision occurs. Given there is only one packet in the queue, the probability that a vehicle attempts to transmit a packet in an arbitrary slot is denoted as τ, which is assumed to be the same for every slot and relates to the reciprocal of mean time of back off period, as shown in (3.11).

$\tau = \frac{1}{W_m+1}$ (Hassan et al., 2011) (3.11)

where

τ is the probability that a vehicle attempts to transmit the packet in an arbitrary slot, given that there is one packet in the queue;

W_m is denoted as the average number of back off slots preceding a transmission.

For any vehicle other than the transmitter, the probability of transmitting a packet in an arbitrary slot is $\rho * \tau$. Let N be the number of vehicles within the transmission range of the tagged transmitter. The probability of the event that no nearby vehicle transmits a packet in an arbitrary slot is $(1 - \rho * \tau)^{N-1}$. The complementary event of this is that one or more nearby vehicles transmit a packet in an arbitrary slot, which is denoted as $1 - (1 - \rho * \tau)^{N-1}$. As stated earlier, a direct collision occurs when any of the nearby vehicles transmit in the same slot as the tagged transmitter, given that the tagged transmitter is in either of the last two cases. Recall that the first case has a probability of $(1 - \rho) * (1 - p_b)$, thus the combined probability of the last two cases is $1 - (1 - \rho) * (1 - p_b)$. Therefore, the direct collision probability is expressed as:

$$p_{dc} = \left(1 - (1 - \rho) * (1 - p_b)\right) * (1 - (1 - \rho * \tau)^{N-1}) \text{ (Hassan et al., 2011)} \quad (3.12)$$

where

p_{dc} is the direct collision probability;

p_b is the sensed channel busy probability when a new packet is generated at the tagged transmitter;

N is the number of vehicles within the transmission range of the tagged transmitter, including the tagged transmitter.

Next, p_b is deducted in a way that: first assuming there is no collision, all the packet transmissions from nearby vehicles other than the tagged transmitter should take $(N - 1) * \lambda * T$ time per second; however, with the direct collision probability p_{dc}, a number of $(N - 1) * \lambda * p_{dc}$ packets will be involved in collisions. When only considering collisions between two packets, the transmission time for sending the packets involved in collisions would be $(N - 1) * \lambda * T * p_{dc}/2$. Therefore, the sensed channel busy probability when a new packet generated at the tagged transmitter can be calculated as follows.

$$p_b = (N - 1) * \lambda * T * (1 - p_{dc}/2) \text{ (Hassan et al., 2011)} \quad (3.13)$$

where

T is the complete transmission time of a packet, including one DIFS period.

In (3.13), p_b is calculated based on quantifying the communication traffic load on the channel, thus under unsaturated situations, the collision would only occur between two packets. How-

ever, in reality, there could be more than two packets involved in one collision under more saturated situations. Though the original model claims that it only considers unsaturated situations, this study finds that there is a potential in extending the model to apply in saturated situations. The extension is done by means of giving a general formula to express the average number of packets involved in one collision, denoted as K. In terms of timing, here one collision refers to the time that the concurrent transmission occupies for one packet length time. First, assuming that there is no direct collision, all the packets from the neighbouring vehicles transmissions would take $(N-1) * \lambda * T$ per second. Recall that the total number of packets involved in direct collisions is$(N-1) * \lambda * p_{dc}$, with a direct collision probability p_{dc}. With the assumption that on average there are K packets involved in one collision, the number of direct collisions should be $(N-1) * \lambda * p_{dc}/K$. Based on the definition of one collision in terms of timing, each direct collision actually only occupies one packet length time T so that all direct collisions take $(N-1) * \lambda * p_{dc}/K * T$ time per second. Thus, when considering collisions with an average number of involved packets K, the extra-calculated transmission time for sending the packets involved in collisions would be $(N-1) * \lambda * p_{dc}/K * (K-1) * T$. Therefore, the extended version of sensed channel busy probability formula for both unsaturated and saturated situations is expressed as follows:

$$\mathrm{P_b} = (N-1) * \lambda * T * (1 - p_{dc}/K * (K-1)) \tag{3.14}$$

The rest of this section deducts the average number of packets involved in one collision K. Based on the assumptions that packets generations at each vehicle's buffer follow a Poisson process and the arbitrary slots are homogeneous, the combined packets generations at all vehicles also follow Poisson process with rate $\lambda * N$ [in packets per second]. In such a way, the probability P_A of the event that n packets are generated from all the vehicles during T period is expressed as

$$P_A = P(N(T) = \mathrm{n}) = \frac{(\lambda NT)^n * e^{-\lambda NT}}{n!} \tag{3.15}$$

Thus, the expectation of number of packets generated during T period is expressed as:

$$K_g = \sum_0^N \frac{(\lambda * N * T)^n * e^{-\lambda NT}}{n!} * n = \lambda * N * T \tag{3.16}$$

It is assumed that the packet transmission by each vehicle occurs continuously and independently at a constant average rate. Based on this, the time intervals between combined packets transmissions from all the vehicles follow an exponential distribution, with rate $\lambda * N$[in packets per second]. Thus, given that there are K_g generated packets from all vehicles, the probability P_B that there is no packet transmission during T period is expressed as:

$$P_B = P(X > T) = P(N(T) = 0) = \frac{(\lambda NT)^0 * e^{-\lambda NT}}{0!} = e^{-\lambda NT} \tag{3.17}$$

Given there are K_g generated packets from all vehicles, the probability $\overline{P_B}$ that there is at least one packet transmitted during T period is denoted as:

$$\overline{P_B} = P(X \leq T) = 1 - P(N(T) = 0) = 1 - e^{-\lambda NT} \quad (3.18)$$

Therefore, the number of packets transmitted during T period can be written as:

$$K_{tr} = K_g * \overline{P_B} = (\lambda * N * T) * (1 - e^{-\lambda NT}) \quad (3.19)$$

However, it needs at least two packets to form one collision, which means the formula (3.19) needs a bit modification:

$$K = 2 + (\lambda * (N - 2) * T) * (1 - e^{-\lambda (N-2)T}) \quad (3.20)$$

3.3.2 Hidden terminal collision probability

In VANETs, all vehicles listen to the shared channel. No new packet transmission is initiated when the channel is sensed busy. This requires that all vehicles can hear from each other's signals. However, due to radio propagation factors like fading and path loss, a vehicle may not be able to sense a transmission by another remote vehicle. As illustrated in Fig. 3.4, vehicle B is the common receiver of vehicle A and vehicle C, as B is in the far edge of both transmitters' communication range. C and A cannot communicate with each other due to the limitation of their transmission ranges. In such a case, the hidden terminal collision happens at vehicle B when A and C transmit their own packets with a time overlap. This kind of collision is unavoidable with current technologies, and an increasing number of studies (Cassidy et al., 2012; Hafeez et al., 2013, 2013; Ma, Yin, Wilson, & Trivedi, 2013) have stated that it has a strong impact on the total collision probability.

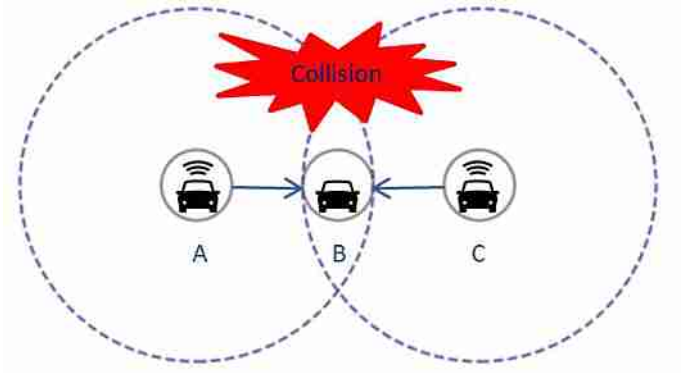

Fig. 3.4 Hidden terminal collision concept

There are two necessary conditions must be satisfied to avoid hidden terminal collisions (Hassan et al., 2011):

i. When the tagged transmitter starts its packet transmission, none of the hidden terminals should be in the transmitting state. This event is denoted by H_1.
ii. After the tagged transmitter starts its transmission, none of the hidden terminals should start transmitting until the tagged vehicle is finished. This event is denoted by H_2.

The event $\overline{H_1}$ is the complement of event H_1, thus finding at least one hidden terminal in the transmitting state at the same slot that the tagged transmitter starts transmission. The num-

ber of hidden terminals is denoted as N_h. First, it is assumed that within these hidden terminals, there is no direct collision. With this assumption, all the packets transmissions within hidden terminals would take $N_h * \lambda * T$ time per second. However, due to direct collisions within hidden terminals, some packets transmissions would have time overlaps. By using the direct collision probability p_{dc}, the number of overlapping packets is denoted as $N_h * p_{dc} * \lambda$ per second. Similar to the deduction of sensed channel busy probability at the direct collision part, an average number of packets involved in one collision K_{hid} within hidden terminals is used in the expression at (3.21). Thus, the probability of event H_1 is expressed as follows.

$$P(H_1) = 1 - P(\overline{H_1}) = 1 - (N_h - 1) * \lambda * T * (1 - p_{dc}/K_{hid} * (K_{hid} - 1)) \quad (3.21)$$

where

$P(H_1)$ denotes as the probability of event H_1;

N_h represents the number of vehicles within the interfering range of the tagged transmitter, including the tagged transmitter;

K_{hid} is the number of packets involved in one collision within the hidden terminals, expressed as follows.

$$K_{hid} = 2 + (\lambda * (N_h - 2) * T) * (1 - e^{-\lambda(N-2)T}) \quad (3.22)$$

For event H_2, it should be noted that the packets that are generated in the last time portion of a DIFS period by hidden terminals would not collide with the tagged transmitter's packet because they still need to defer for one DIFS period when the tagged transmitter finishes its transmission. Therefore, condition H_2 is fulfilled if no packet is generated at any of the hidden terminals during $t_{data} - t_{DIFS}$ period. With the assumption that the combined packets transmissions from all the hidden terminals also follow Poisson process with rate $\lambda * N_h$ [in packets per second], the probability of event H_2 is expressed as

$$P(H_2) = P(N(t_{data} - t_{DIFS}) = 0) = e^{-\lambda * N_h * (t_{data} - t_{DIFS})} \text{ (Hassan et al., 2011)} \quad (3.23)$$

where

$P(H_2)$ denotes as the probability of event H_2;

t_{data} is the data transmission time of a packet;

t_{DIFS} is the duration of a DIFS period.

The total collision probability of a packet that includes both direct collisions and hidden terminal collisions is expressed as

$$p_c = 1 - (1 - p_{dc}) * P(H_1) * P(H_2) \text{ (Hassan et al., 2011)} \quad (3.24)$$

3.3.3 Expressions for the delay

This section explains the expression for the packet delay with probabilistic arguments, basing on the work from (Hassan et al., 2011). The total delay experienced by a packet of the tagged transmitter includes the waiting time of the packet in the queue, the channel access delay, and the complete packet transmission time. The channel access delay is the time interval between the instant that the packet reaches the head of the queue and the instant when the packet transmission starts. The total delay of a packet is denoted as

$D = Q + S = Q + A + T$ (Hassan et al., 2011) (3.25)

where

D is the total delay time;

Q represents the queuing delay;

S is the service time, which is defined as the sum of channel access delay and complete transmission time of a packet;

A represents the channel access delay;

T is the sum of the one deferred DIFS period and the total data transmission time.

The channel access delay A is determined basing on the three scenarios determined in the direct collision part:

i. A packet is generated at an empty buffer and finds the channel being idle for a DIFS period with probability $(1-\rho) * (1-p_b)$. The access delay in this case is zero as the packet is transmitted without a back off stage.
ii. A packet is generated at an empty buffer and finds the channel being busy, with probability $(1-\rho) * p_b$. The packet must wait until the ongoing transmission is finished and then perform a back off process before transmission.
iii. A packet is generated at a nonempty buffer, with probability ρ. The packet must wait until it reaches the head of the queue and then perform a back-off process before transmission.

So the channel access delay according to the aforementioned three cases is expressed as

$$A = \begin{cases} 0, & w.p.\ (1-\rho) * (1-p_b) \\ B + T_{res}, & w.p.\ (1-\rho) * p_b \\ B, & w.p.\ \rho \end{cases}$$ (Hassan et al., 2011) (3.26)

where

B denotes the total back off duration, including periods when the back off process is suspended;

T_{res} is the residual lifetime of an ongoing packet transmission.

It is assumed that every back off slot can be interrupted at most once. This assumption needs more consideration in the future work, as under extremely saturated situation, the back off slot may have multiple interruptions. For current stage, this assumption is used. The total back off duration B is expressed as a random sum

$B = \sum_{n=1}^{U}(\sigma + Y)$ (Hassan et al., 2011) (3.27)

where

σ represents the duration of a back off slot;

Y is the interruption period per slot;

U is the back off counter value, which is uniformly distributed in the range [0, CW].

In case of no other vehicles transmit packets in a given slot, Y is equal to zero, thus, there is no interruption. When there are other packets transmissions in a given slot, the tagged transmitter will suspend its back off process for a period of the complete packet transmission time, i.e. T.

$Y = \begin{cases} 0, & w.p.\ (1-\rho*\tau)^{N-1} \\ T, & w.p.\ 1-(1-\rho*\tau)^{N-1} \end{cases}$ (Hassan et al., 2011) (3.28)

where

$1-(1-\rho*\tau)^{N-1}$ is the probability that a slot is sensed busy due to transmissions by other vehicles.

As the channel access delay A and the transmission time delay T are independent, the average service time of the packet is denoted as

$E[s] = E[A] + E[T]$ (Hassan et al., 2011) (3.29)

With the assumption that all packets have the same packet length, the transmission time delay is expressed as

$E[T] = T$ (Hassan et al., 2011) (3.30)

From (3.26), the mean of A can be written as

$E[A] = (1-\rho) * p_b * (E[B] + E[T_{res}]) + \rho * E[B]$ (Hassan et al., 2011) (3.31)

To calculate $E[T_{res}]$, the mean of the residual lifetime of an ongoing transmission T_{res}, the probability distribution function of T_{res} should be first determined. Based on the assumption that the packets generation at each vehicle follows a Poisson process, the interval time of packets generated at each vehicle follows a memoryless exponential distribution. Thus, the

time interval of packets transmissions also follows an exponential distribution with the same rate. Therefore, the interval between the starting time of an ongoing transmission and the generation of a new packet at the tagged transmitter can be seen as the difference between two exponential distributions with the same rate λ, and it is defined as $X \sim 1 - \frac{1}{2}e^{-\lambda t}$.

However, the original model made a math mistake during derivation of the probability distribution functions of Y. They implemented a wrong expression of the difference between two exponential distributions: $X \sim 1 - e^{-\lambda t}$. The following expressions are implemented with the correction of this part.

The probability distribution of T_{res} is represented as the remaining transmission time $Y = T - X$, which is conditioned on $X \leq T$. The probability distribution function of Y can be expressed as

$$F_{Y|X\leq T}(y) = \frac{P(Y\leq y|X\leq T)}{P(X\leq T)} = \frac{P(T-y\leq X\leq T)}{P(X\leq T)} = 1 - F_{X|X\leq T}(T-y) = \frac{\frac{1}{2}\left(e^{-\lambda(T-y)} - e^{-\lambda T}\right)}{1-\frac{1}{2}e^{-\lambda T}} \quad (3.32)$$

Differentiating (3.32), the probability density function is expressed as

$$f_{Y|X\leq T}(y) = \frac{\frac{1}{2}\lambda e^{-\lambda(T-y)}}{1-\frac{1}{2}e^{-\lambda T}} \quad (3.33)$$

Then the mean of T_{res} can be expressed as

$$E[T_{res}] = E[Y|X \leq T] = \int_0^T y f_{Y|X\leq T}(y)dy = \frac{\frac{1}{2}(\lambda T - 1) + \frac{1}{2}e^{-\lambda T}}{\left(1-\frac{1}{2}e^{-\lambda T}\right) * \lambda} \quad (3.34)$$

The mean of a total back-off duration B, it follows from (3.27)

$$E[B] = (\sigma + E[Y]) * E[U] \text{ (Hassan et al., 2011)} \quad (3.35)$$

As U is a random variable that is uniformly distributed in the range [0, CW],

$$E[U] = \overline{W} = \frac{W}{2} = \frac{CW}{2} \quad (3.36)$$

For interruption time Y, the mean can be calculated from (3.28)

$$E[Y] = (1 - (1 - \rho * \tau)^{N-1}) * T \text{ (Hassan et al., 2011)} \quad (3.37)$$

Thus, (3.10), (3.12), (3.14), and (3.29) constitute a nonlinear system of equations that can be iteratively solved to calculate ρ, p_{dc}, P_b and $E[S]$.

3.3.4 Summarization and validation

Based on the work from (Hassan et al., 2011), the *Collision Probabilistic Model* is developed. The *Collision Probabilistic Model* extends the applied situation of the original model, by

providing a general formula of the average number of packets involved in one collision. This change contains the consideration of both saturated and unsaturated situations. It should be stated that this factor not only influences the calculation of direct collision probability but also has impacts on the hidden terminal case, as direct collisions occur within hidden terminals as well. Moreover, the modification described in *Section 3.3.3* increases the level of plausibility. The *Collision Probabilistic Model* corrects the math mistake in calculating the residual lifetime of an ongoing transmission. In this section, for the concern of validation, the *Collision Probabilistic Model* is compared with the original model and a communication network simulator. Veins is selected as the communication network simulator and the benchmark of the validation work. The main reasons for choosing Veins include the wide usage in many researches, a bunch of inner available models that are able to capture the performance of vehicular communication channel, and it is under continuous development. Furthermore, it also combines the communication network simulation with a microscopic vehicle mobility simulator. This means it takes into account the impact of realistic vehicle mobility and provides the opportunity for future validation and comparison of the proposed module when coupling with realistic road traffic scenario.

For validating *Collision Probabilistic Model*, a static communication network is created in Veins. Here, the effects of vehicle mobility are excluded. The communication network part of Veins is operated in OMNeT++ simulator, with an implementation of IEEE 802.11p for the PHY and MAC layers and radio-propagation channel models. At this step, no vehicle mobility simulations or radio-propagation channel models are involved, because the collision probability is the focus. The validation work is divided into two parts, with the first part focusing on the direct collision probability and the second part on the total collision probability. For the direct collision probability part, all vehicles are static and located in a dense area so that all vehicles can hear from each other, thus, there is no hidden terminal collision problem in this network. The simulation time is 0.1 second. For reducing the randomness effects of the simulations, each simulation repeats for 50 times. The influence of vehicle density on communication network performance is the pivot of this validation work. Thus, each simulation is based on the number of vehicles in the road network, starting from 20 to 1000, with incremental steps of 20 vehicles. The other influencing factors are fixed, as shown in Tab. 3.1.

Packet Length	Transmitting Power	Sending Frequency
2000bits	20mW	10 packets per second

Tab. 3.1 Fixed influencing factors in Veins simulation

Fig. 3.5 shows a boxplot of the direct collision probability from Veins' results. The x-axis is the number of vehicles in the network, starting from 20 to 1000. The y-axis shows the direct collision probability, in range of [0, 1]. On each box, the central mark is the median of the set of data, and the edges of the box are the lower hinge (25^{th} percentile) and the upper hinge (75^{th} percentile). The circles are the outliers. With a lower number of vehicles, the spread of

direct collision probability distribution is more dispersed, compared to that with a higher number of vehicles. This is because of the randomness effect with fewer vehicles. With increasing number of vehicles, the direct collision probability gradually approaches 1.0. This makes sense because more vehicles in the network imply that more vehicles are competing for the channel access opportunity, which results in higher direct collision probability.

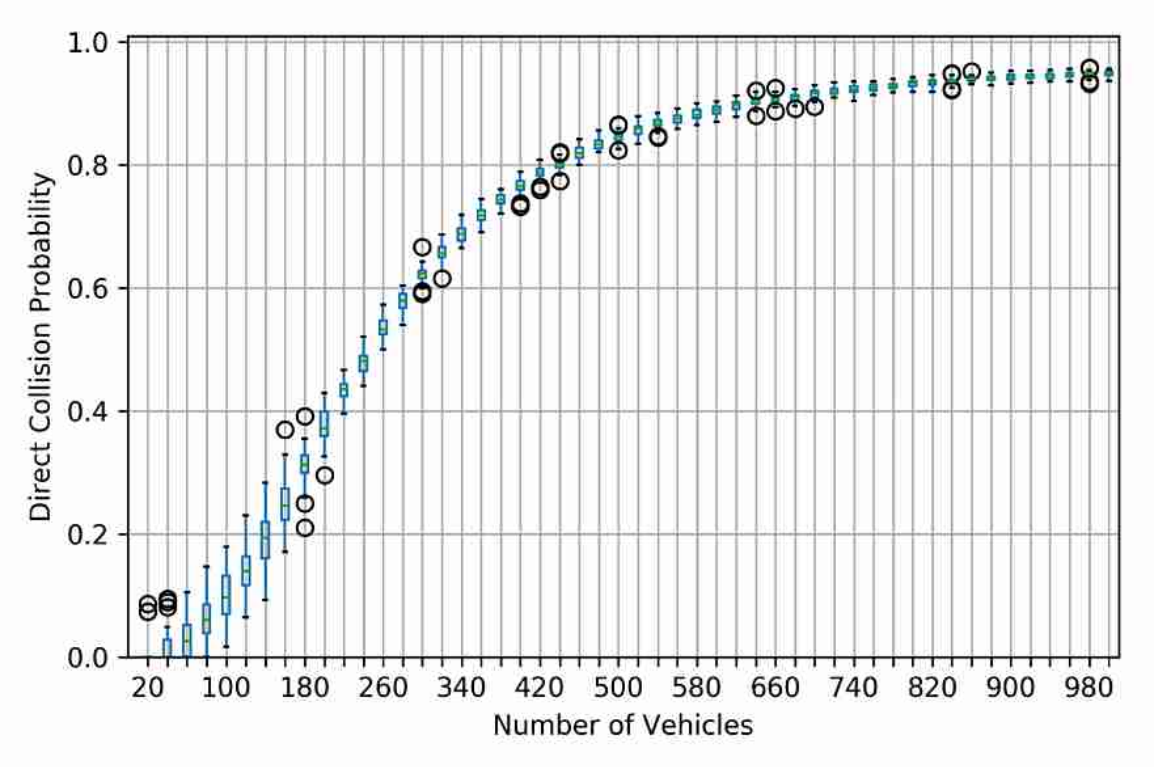

Fig. 3.5 Boxplot of the direct collision probability in Veins' result

Fig. 3.6 is the comparison graph between Veins' result and the original model, with the same values of packet length, transmitting power and packet sending frequency, as listed in Tab. 3.1. Hassan's formulas are coded in python and the result p_{dc} is plotted with green colour. Here, the x-axis again is the number of vehicles, from 20 to 1000. The y-axis is the direct collision probability, in range of [0, 1.4]. The blue boxplot is again the Veins' result. From Fig. 3.6, it can be said that under unsaturated situations, Hassan's model matches Veins' result to a certain degree, for instance when the vehicle number is less than 100. However, when it comes to more saturated situations, the green curve starts to shift away from Veins' result. After the vehicle number reaches 400, the direct collision probability of Hassan's model even exceeds one (denoted with a red horizontal line), which should not happen. This also verifies that the reliability of Hassan's model is limited to unsaturated conditions.

Using same fixed inputs, the direct collision probability p_{dc} of the *Collision Probabilistic Model* in the proposed module is shown in Fig. 3.7. The magenta curve in this figure is the proposed model's result, and the boxplot represents the Veins' result. For comparison purpose, the same x and y-axis as in Fig. 3.6 are used. It shows clearly that the magenta curve fits the boxplot of Veins' result quite well, not only for unsaturated situations but also for saturated

situations. It is observed that in some parts of the plot, the magenta curve even matches the median value of Veins' result.

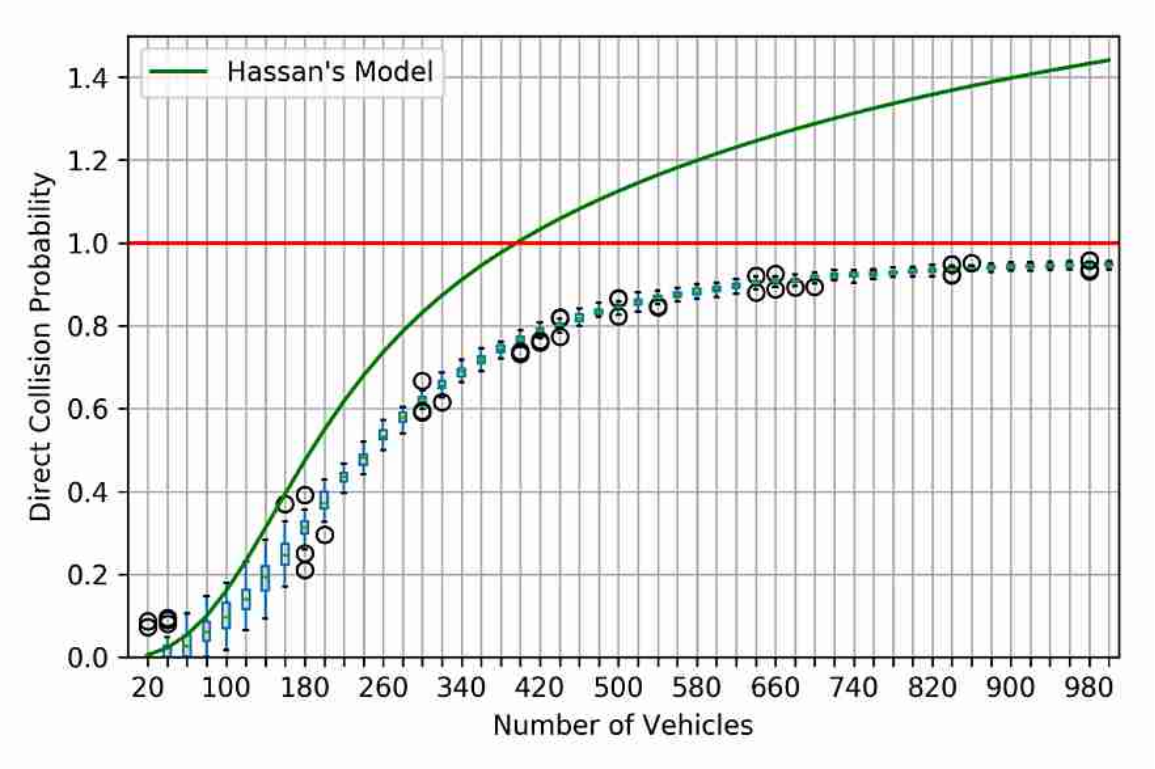

Fig. 3.6 Comparison between Veins and Hassan's model in direct collision probability

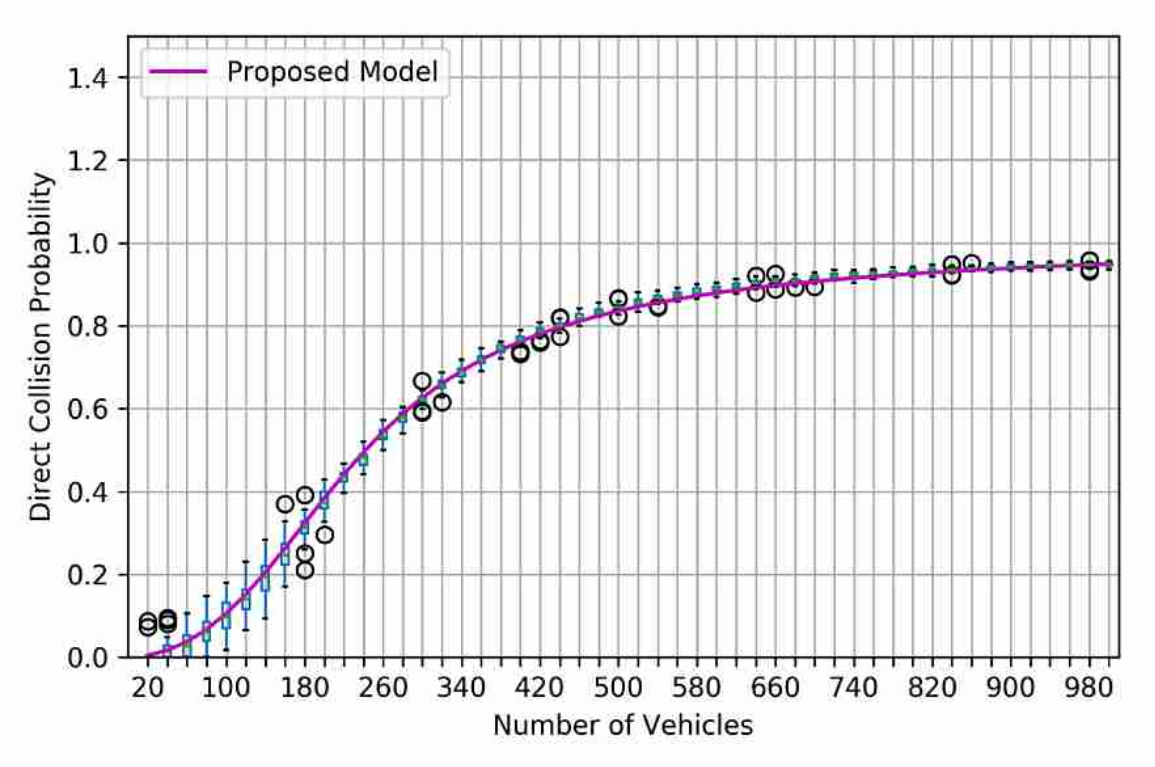

Fig. 3.7 Comparison between Veins and the proposed model in direct collision probability

Compared to Hassan's model, the *Collision Probabilistic Model* in the proposed module shows a much better performance in terms of direct collision probability. From a mathematical view, the Root Mean Square Error (RMSE) between the simulation result and analytical models is calculated. The RMSE represents the sample standard deviation of the differences between observed values and predicted values. Generally, a lower RMSE value indicates a better fit of the predicted values. The formula of RMSE is expressed as:

$$RMSE = \sqrt{\frac{\sum_{i=1}^{N}(f-o)^2}{N}} \tag{3.38}$$

where

$RMSE$ is the root mean square error;

f is the forecast value, i.e. the analytical models' results;

o is the observed value, i.e. the Veins' results;

N is the number of paired values.

The RMSE between the Veins' result and Hassan's model is 0.314, while the RMSE between the Veins' result and the *Collision Probabilistic Model* is just 0.008. It is obvious that the results of the *Collision Probabilistic Model* show a much better fit to the simulation data than that of Hassan's model.

After the validation of the direct collision probability part, the next step is to validate the hidden terminal collision part. However, the hidden terminal case should not be conducted separately, as direct collisions also take place within the hidden terminals. This indicates it will be troublesome to consider the hidden terminal collision as an independent part. Instead, it is better to validate the total collision probability. In order to keep the validation work simple and clear, part of the Veins' results in direct collision probability test is used in validating the total collision probability, but in a different way. Recall that in direct collision probability test there are 50 repetitions of each simulation, starting from 20 vehicles to 1000 vehicles, with every incremental step of 20 vehicles. Each repetition with the same vehicle number is independent. Thus, it can be assumed that every two repetitions of the same vehicle density simulation comprise two groups of vehicles, in which the vehicles in one of the groups are not aware of the existence of the other group's vehicle. In such a way, the hidden terminal problem is created artificially. If any two or more transmitted packets have time overlaps, a collision occurs, and the involved packets are considered as lost without discriminations of direct collisions or hidden terminal collisions.

For a better explanation, a figure of collision packets on timescale is presented. As shown in Fig. 3.8, the grey and blue rectangles represent the packets from two groups of vehicles respectively. There are two collisions in this figure. The first collision involves packets: #1, #4, #5, and the second collision involves packets: #7 and #3. According to the above statements, the second collision only includes hidden terminal collision, as they are from different groups,

without awareness of each other's existence. Yet, the first collision includes both a direct collision and a hidden terminal collision. Before #1 packet's transmission is finished, #4 and #5 coincidentally start transmission at the same time slot, thus all the three packets are lost in the same collision. However, it should not be said that packet #4 is lost only because of the hidden terminal or direct collision, as both are involved. This explains that it is not wise to consider the hidden terminal collision as an independent part.

Fig. 3.8 Concept of colliding packets on timescale

The total collision probability results of Veins simulation are shown in Fig. 3.9, based on the above collision concept and the simulation results of vehicle numbers in the range of [20, 500]. As stated earlier, every two repetitions of the simulations with same vehicle number comprise a total collision probability test, which means the number of vehicles will be double that of the relevant direct collision probability test. The x-axis represents the number of vehicles in the network, starting from 40 vehicles to 1000 vehicles, with incremental steps of 40 vehicles. The y-axis shows the total collision probability, in the range of [0, 1]. The total collision probability grows more rapidly than the direct collision probability in Fig. 3.5. This also indicates that the hidden terminal collision is the main contributor to the total collision probability. Besides, the number of vehicles in the system strongly influences the randomness of the result, as with fewer vehicles the total collision probability shows a more dispersed spread.

In the *Collision Probabilistic Model*, the same range of the number of vehicles as that in the Veins simulation network is used, from 40 to 1000 vehicles, with incremental steps of 40 vehicles. In each step, the vehicles are separated into two groups. The vehicles within the same group are able to hear from each other, while the vehicles from different groups cannot communicate with each other. The values of the packet length, the transmitting power and the packet sending frequency stay the same. Fig. 3.10 shows the comparison of the total collision probability between *Collision Probabilistic Model* and Veins' results. The results of *Collision Probabilistic Model* are coloured in magenta. The majority of the magenta curve is well-matched with the median values of the boxplot (Veins' result). The RMSE value for the total collision probability between the Veins' results and the probabilistic model is 0.01. Now, it can be stated that the validation work for the *Collision Probabilistic Model* in the proposed module is finished with a convincing result. The next chapter will give a brief overview of how to couple the proposed module with vehicle mobility simulators and relevant result analyses,

with the intention of providing a platform for generating realistic road-traffic impact analysis of vehicular communication networks.

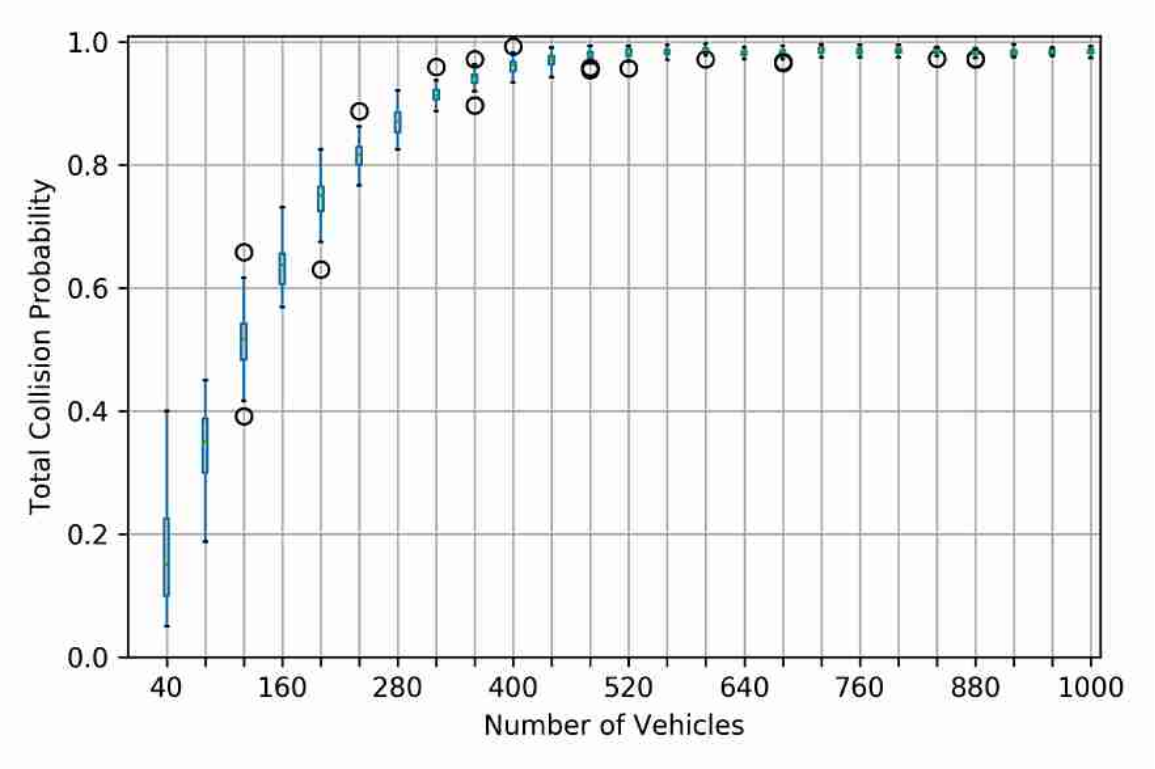

Fig. 3.9 Boxplot of the total collision probability in Veins

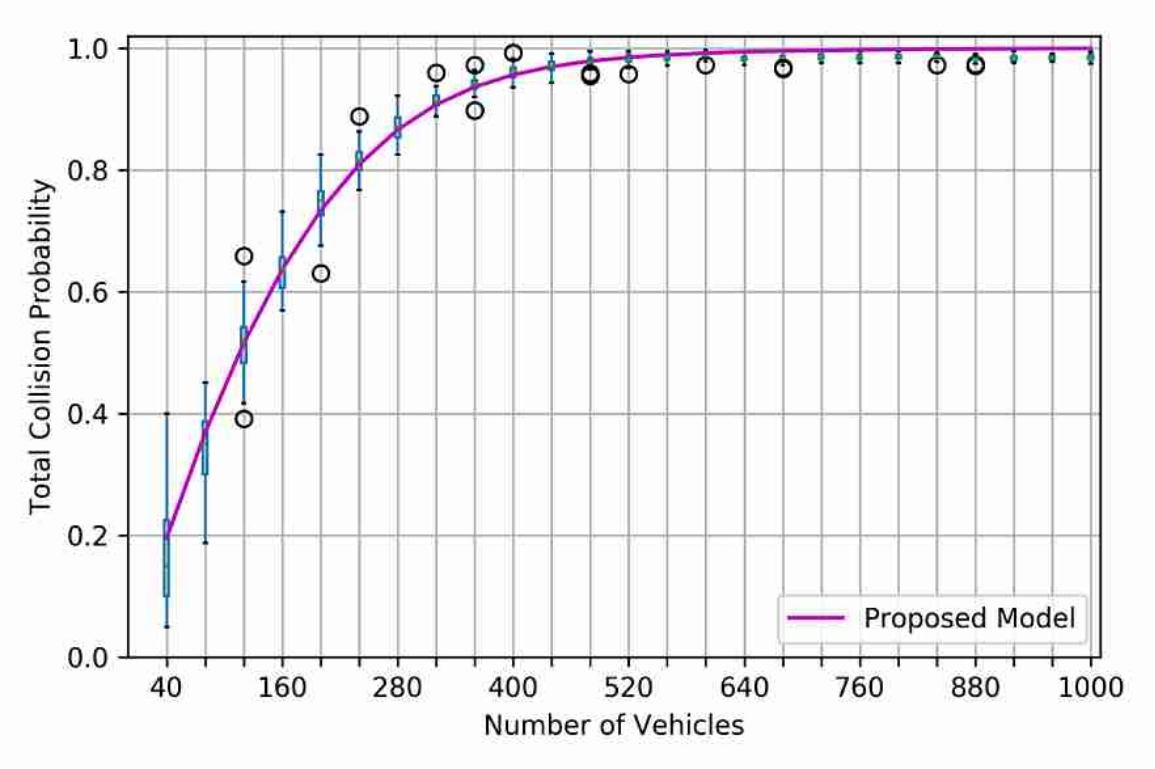

Fig. 3.10 Comparison between Veins and the proposed module in terms of total collision probability

4 Coupling with Road Traffic Simulation

A realistic road-traffic impact analysis of vehicular communication networks requires the co-operation of both the communication network and the road traffic network. Most studies tended to focus on only one part of them, either on the communication network with limited consideration of impacts from road traffic or on the road traffic network with an assumption of perfect communication network implementation. Only a few researches provide opportunities for coupling the communication network and the road traffic simulator, but with a limitation to small-scale networks because of the high demand for computational power. In such a context, the proposed module is designed to consider the impacts from both sides of realistic communication networks and realistic vehicle mobility, for a comprehensive view of evaluating vehicular communication networks. Additionally, since the proposed module is an analytical approach, it has the intrinsic characteristic of less required computational effort, hence, the potential of implementing it with large-scale networks. In this chapter, first, the process of coupling the proposed module with SUMO is outlined and then the analyses of the impacts of influencing factors on two performance metrics are demonstrated. After that, the coupling result of the proposed module with SUMO is compared with Veins' result.

4.1 Coupling process

For the coupling case, Luxembourg SUMO Traffic (LuST) scenario from (Codeca, Frank, Faye, & Engel, 2017) was chosen as the study scenario. The authors of LuST scenario aimed to provide a scenario able to meet the common requirements in terms of size, realism and duration for vehicular networking research. This scenario has a standard topology common in mid-size European cities, with real information concerning traffic demands and mobility patterns of 24 hours. In the scenario, a Region of Interest (ROI) area is picked, which is at the city centre, with a size of 2.5×1.5 km^2 roughly. Fig. 4.1 shows the LuST scenario with the ROI area. The red shaded areas in the figure represent the buildings, and the black curves are the roads. The green rectangle area denotes the ROI area. One second during the afternoon peak hour is chosen as the simulation time window, denoted as [61700, 61701] second in SUMO. In real time, this is at around 05:08 P.M. The simulation step length is set as 0.1 second, which is aligned with the recommendation of the packet sending frequency for vehicles in the communication protocol.

To explain the coupling process in a better way, the coupling flowchart is presented in Fig. 4.2. The first step of the coupling is to connect SUMO with the proposed module, with TraCI (Wegener, Axel, et al., 2008) used as the interface of SUMO. After a warming up session of 500 seconds, the coupling starts. As depicted in *Section 3.1 Module Structure*, the road traffic simulation provides the vehicle positions data. For each simulation time step, a current road network layout is built with the positions of vehicles and the building geometries within the ROI area. From the current road network layout, the number of neighbours and number

of hidden terminals for the tagged communicating pair can be obtained. Every two vehicles are checked if they can hear from each other. As long as the receiving power level between the two vehicles exceeds the threshold, the two vehicles comprise a communicating pair. The calculation of the receiving power level depends on the link type of transmission. If there are buildings blocking the LOS of a communicating pair, the transmission link type of the communicating pair is NLOS. Otherwise, the link type is LOS. With a LOS transmission, only the two-ray interference model is used. With an NLOS transmission, except two-ray interference model, an additional shadowing model – obstacle model is used. The small-scale fading model is excluded here because of its nondeterministic effect that can lead to difficulties in the comparison and validation work with Veins. For each communicating pair, the collision probabilistic model will calculate the total collision probability of the packets transmitted within them, with consideration of both direct collisions and hidden terminal collisions. After processing all the communicating pairs in the current time step, SUMO takes the control back and runs for another simulation time step. When the simulation time limitation is reached, the connection between SUMO and the proposed module closes.

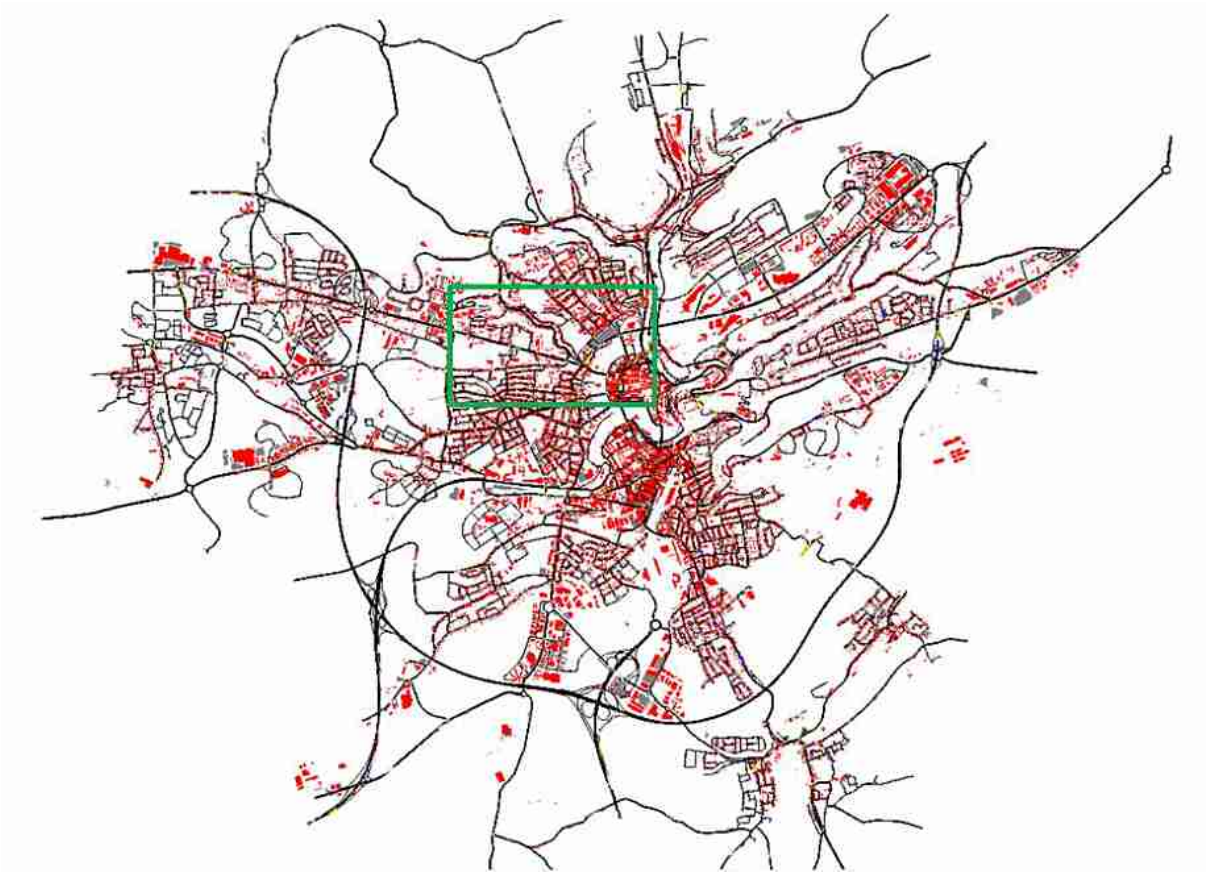

Fig. 4.1 LuST with the ROI area

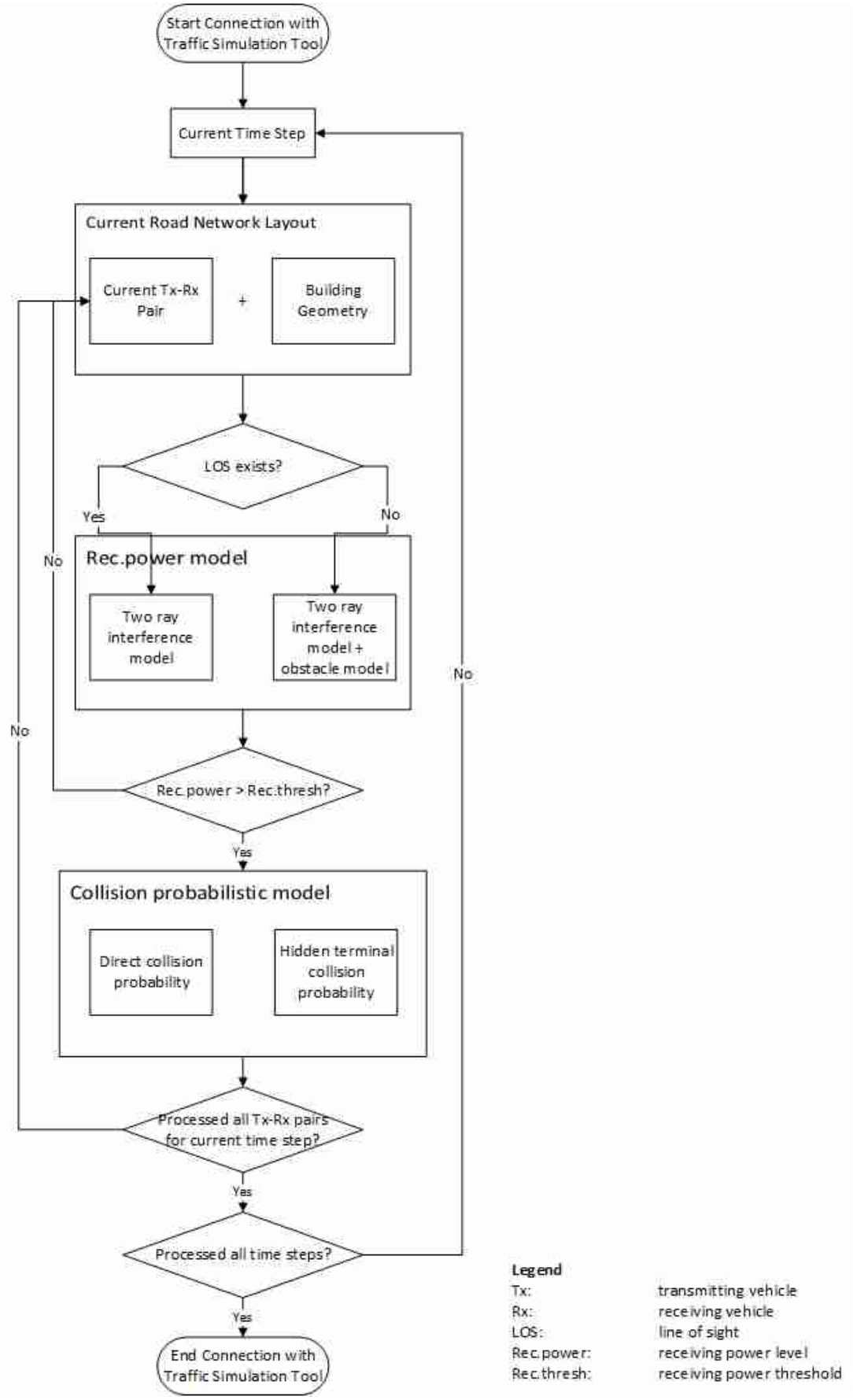

Fig. 4.2 Flowchart of coupling with a traffic simulation tool

The initial simulation running time of the coupling work was around 7 hours, which was too much for the practical use of generating road-traffic impact analysis. One of the potential bottlenecks that require high computational effort is the building geometry traversal process. As explained earlier, for each communicating pair, the building geometry and vehicles positions determine whether the link type of transmission is via LOS or NLOS. For NLOS transmission, obstacle model requires the number of exterior intersecting walls and the intersecting distance of the buildings as inputs. As the study scenario is an urban area, the number of buildings is rather large, which significantly increases the computational effort. In order to speed up this process, each building is denoted as a bounding box that contains its four boundary points, thus the left bottom, the left top, the right bottom and the right top points. The current communicating pair is also represented as a bounding box, which is formed by the (x, y) coordinates of the transmitter and the receiver. Each bounding box of buildings is given an R-tree index. R-trees are tree data structures used for spatial access methods, for indexing multi-dimensional information such as geographical coordinates, rectangles or polygons (Guttman, 1984). A rough checking of intersection between bounding boxes of buildings and the communicating pair is executed. This gives the R-tree indexes of all potential intersecting candidates of building bounding boxes. Then all candidate buildings are checked accurately if any of them intersects with the LOS of the transmitting and receiving vehicles.

Another bottleneck lies in obtaining the number of neighbours and hidden terminals for each communicating pair. The initial idea is that after getting all the communicating pairs, for every pair, the neighbours of both the receiver and the transmitter are checked, and the hidden terminals are the ones that are not in the transmitter's group of neighbours but in the receiver's group of neighbours. This means that the computational complexity is N^3, given that the number of vehicles is N. For speeding up this process, instead of checking the transmitter and the receiver of every communicating pair, the number of neighbours of every vehicle that involved in communicating pairs is calculated first. In such a way, the complexity reduces to N^2. The number of neighbours and number of hidden terminals are accessed through the saved data structure of the transmitter and the receiver.

Significantly, with these two solutions, the simulation running time reduces to roughly 10 minutes. It should be stated that other improving solutions also exist, such as parallel programming. Parallel programming and the design of efficient parallel programs are well established in high-performance computing for many years (Rauber & Rünger, 2013). Parallel programming is a type of computation in which many calculations or the executions of the processes are carried out simultaneously. A more detailed explanation will be presented in *Chapter 6.*

The available outputs for the coupling study include: current simulation time, the transmitting vehicle ID, the receiving vehicle ID, the receiving power level of the packet, the positions of the transmitter and receiver, the distance between them, the number and vehicle IDs of neighbours, the number and vehicle IDs of hidden terminals, and the total collision probability of the packet. Based on the outputs, the impact analyses of the influencing factors on two performance metrics will be presented in the following two sections. The two performance

metrics are the receiving power level and the total collision probability. *Section 4.2* focuses on the receiving power level. *Section 4.2* demonstrates investigation on the total collision probability.

4.2 Analysis of the receiving power level

The influencing factors of the receiving power level include the distance between the transmitter and the receiver, the intersecting wall distance, and the intersecting wall numbers. This section focuses on the impact of vehicles' distance on the receiving power level. As two-ray interference model is used as the path loss channel model in the proposed module, it is assumed that the relationship between the vehicles' distance and the receiving power level should be similar to the red curve in Fig. 4.3.

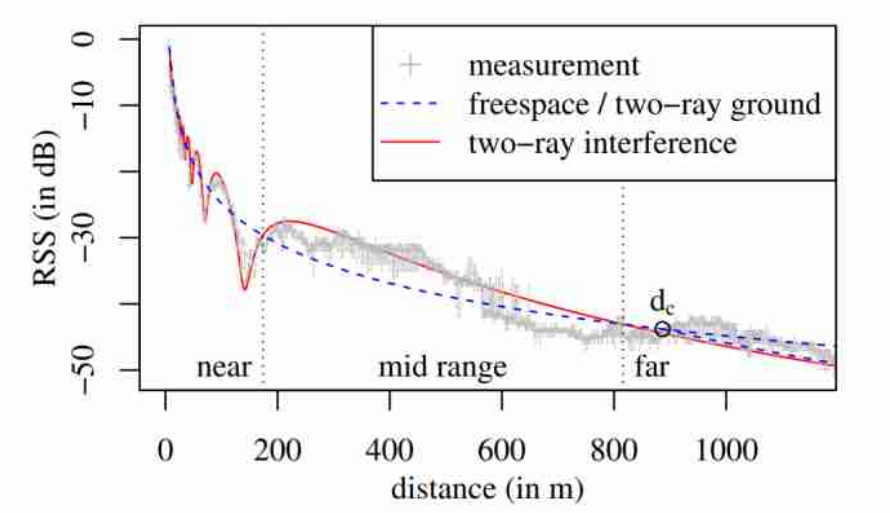

Fig. 4.3 Received Signal Strength vs. Distance between transmitter and receiver (Sommer, C., & Dressler, F., 2011)

The analysis result of the vehicles' distance vs. the receiving power level is shown in Fig. 4.4. The x-axis is the distance between the transmitter and the receiver, and the y-axis represents the receiving power level of the packet, with units in [dBm]. According to (IEEE standards, 2016), the receiving power level threshold is set as -89[dBm], denoted as the red horizontal line in Fig. 4.4. Comparing Fig 4.3 and Fig. 4.4, it can be said that the trends of the curves are similar, but the values vary to a certain extent, due to the fact that they are in different scenarios with different building geometry and vehicle mobility. It shows clearly that with a longer distance between the transmitter and the receiver, the receiving power level is lower. There are two scattered curves in Fig. 4.4, one is narrow with high receiving power levels, and the other one is broader with lower receiving power levels. They are comprised of transmissions via LOS and NLOS respectively. This indicates that the receiving power level is highly influenced by the intersecting buildings. Additionally, Fig. 4.4 shows that most of the packets transmitted via NLOS cannot be sensed by potential receivers, as a consequence of low receiving power levels.

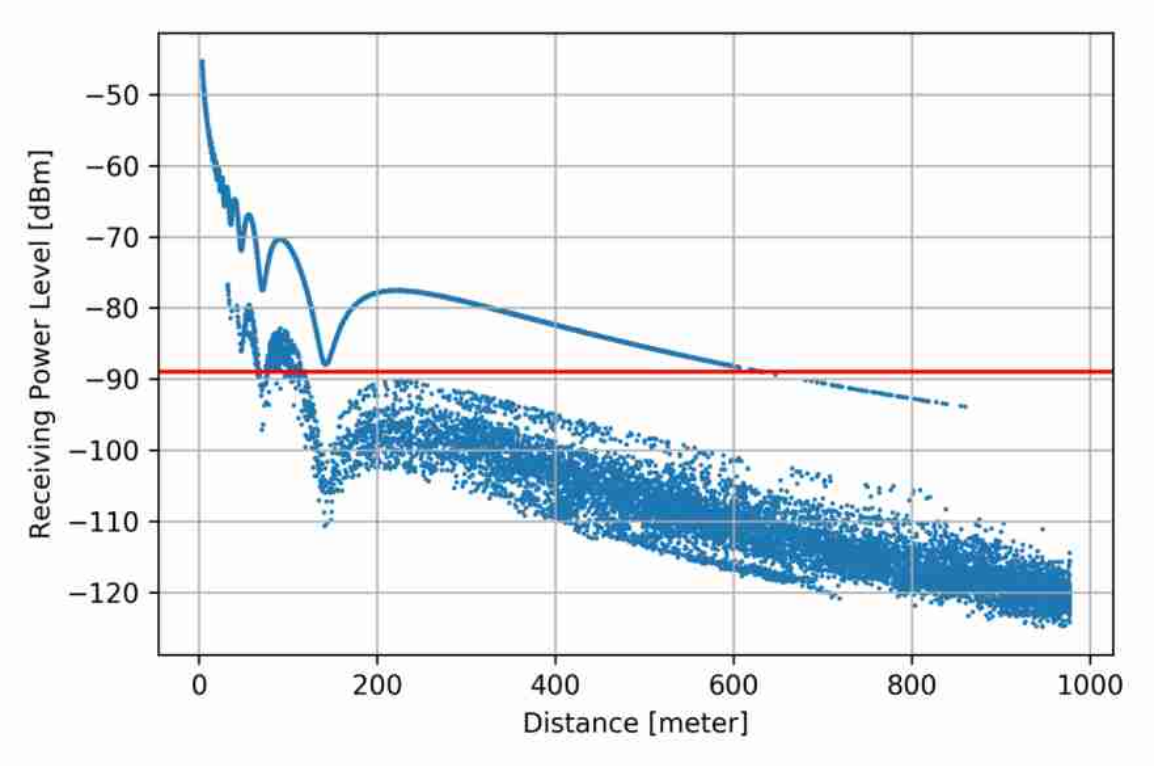

Fig. 4.4 Distance vs. Receiving Power Level of coupling result

With regard to the intersecting wall distance, a more detailed and categorized plot of vehicles' distance vs. the receiving power level is shown in Fig. 4.5. The data are categorized into eight groups, based on the wall distance, starting from zero (LOS transmission) to 600 meters, with incremental steps of 100 meter. This figure also proves that the scatter dots of thinner curve in Fig. 4.4 are transmitted via LOS. For most of the packets that are transmitted via LOS, they have higher receiving power levels than the threshold (the red horizontal line), thus with higher packet reception probabilities. With longer intersecting wall distance, the receiving power level of the packet is lower. Another factor, the intersecting wall number in obstacle model, shows similar influences on the receiving power level, as shown in Fig. 4.6. The maximum intersecting wall number in the result is 90. For sure with such a number of intersecting walls, the receiving power level of the packet will be lower than the threshold (the red horizontal line). Nevertheless, for a complete view of the result, the data is also coloured to different groups based on the intersecting wall number, and in this figure, there are six groups. The blue curve is denoted as the LOS transmitted packets again.

Both Fig. 4.5 and Fig. 4.6 show a clear relationship between the obstacles and the receiving power level of the packet, thus shadowing effects from obstacles decrease strongly the receiving power levels. One thing should be noticed is that vehicles and foliage are not considered as obstacles in calculating the receiving power levels. Though heavy trucks, foliage, overpasses etc. can make differences in calculating the receiving power levels, the information of these obstacles are not available and the level of difficulty in including these factors is much higher. Therefore, their impacts are excluded in this study.

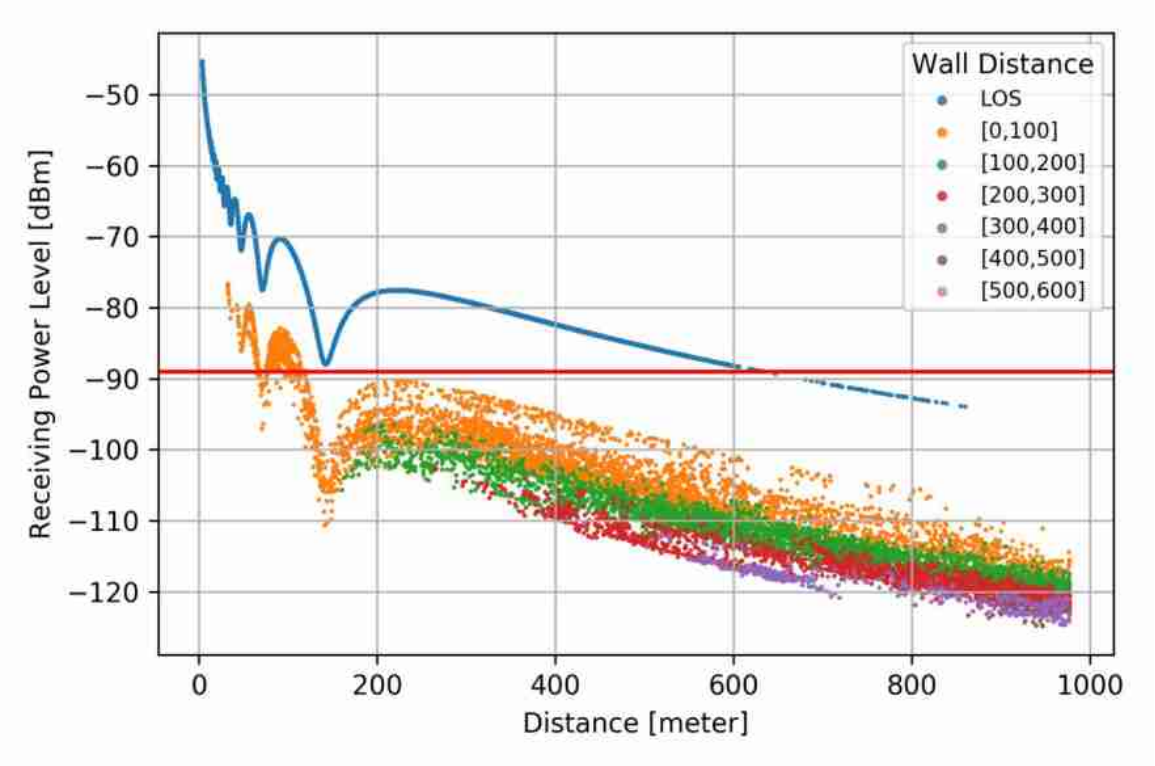

Fig. 4.5 Distance vs. Receiving Power Level of coupling result (categorized by Wall Distance)

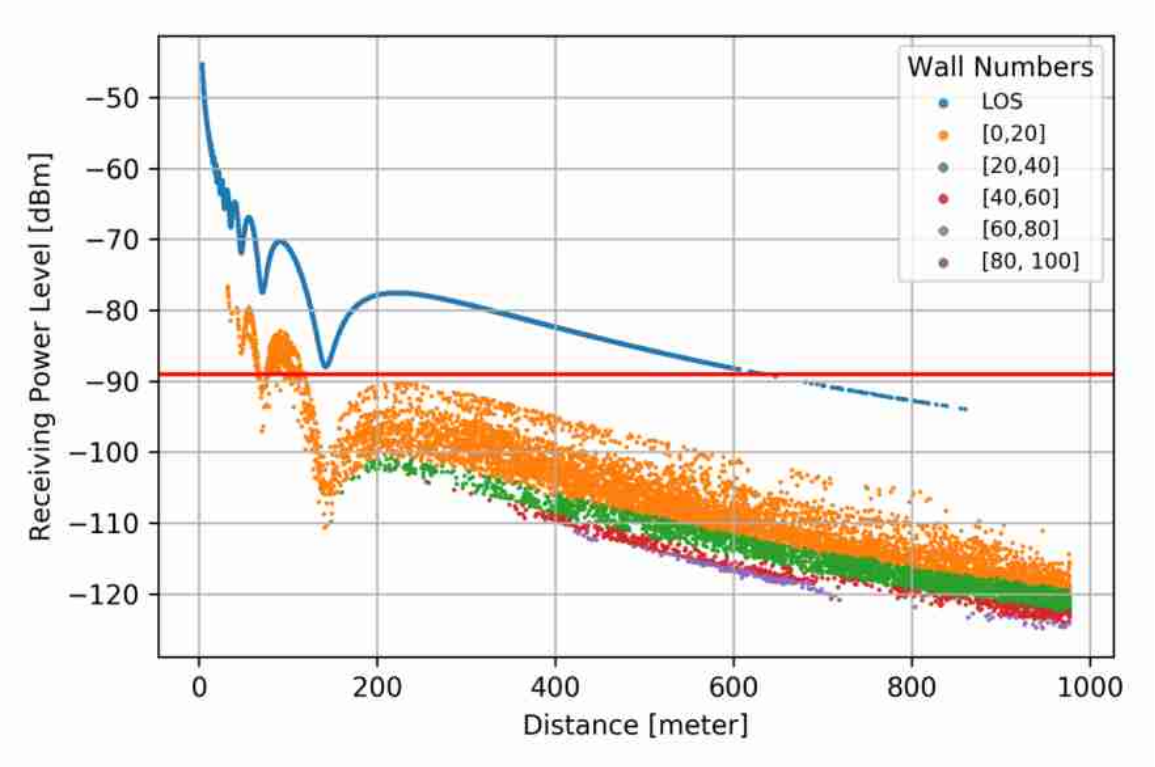

Fig. 4.6 Distance vs. Receiving Power Level of coupling result (categorized by Wall Numbers)

4.3 Analysis of the total collision probability

The total collision probability is considered as the focus of this study, because most of the analytical models cannot fulfil its reliability requirement and it is the simulators' bottleneck of required computational effort. This section gives detailed analyses of it. First, the influence of distance between the vehicles on the total collision probability is analysed in Fig. 4.7. The x-axis shows the distance between the transmitter and the receiver, and the y-axis represents the total collision probability. This figure includes all possible communicating pair packets, regardless of the constraint of receiving power levels. For packets with receiving power levels lower than the threshold, they are considered as lost packets and given a 1.0 value for the total collision probability. From this figure, it is observed that as the distance increases, the total collision probability shows an upward tendency. This can be explained as with a longer distance between the transmitter and receiver, there could be more obstructing buildings and more interference from other vehicles.

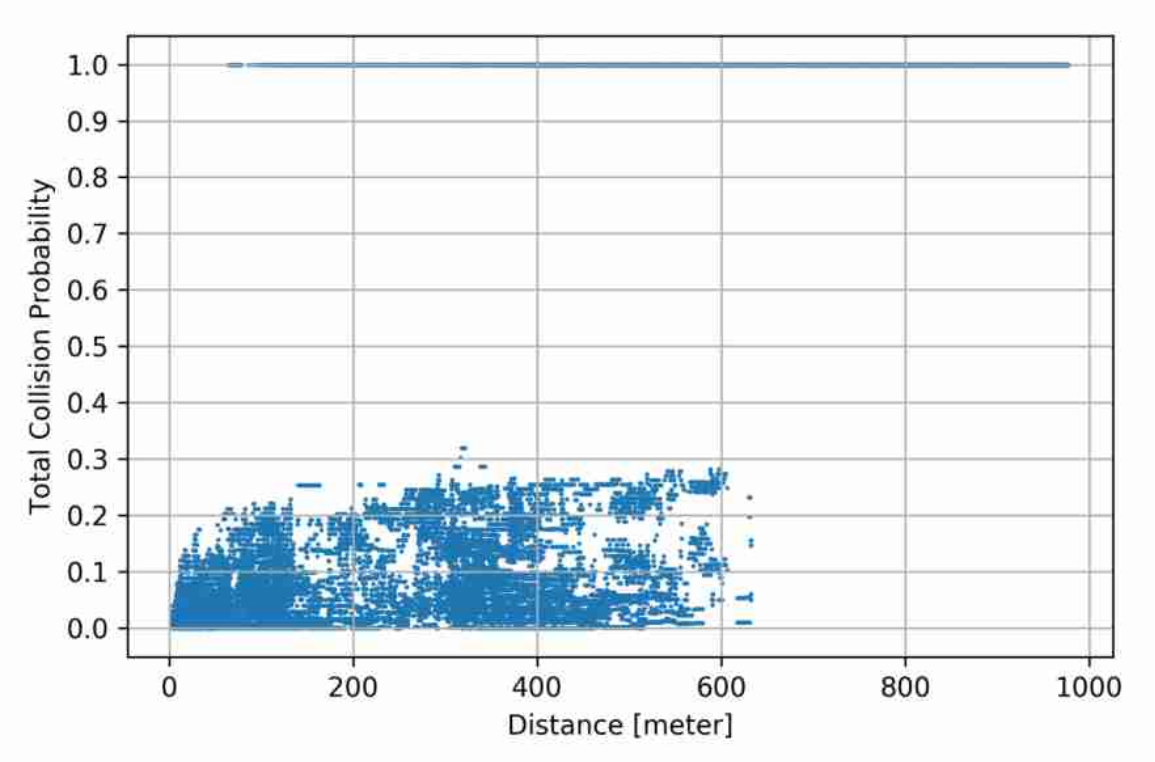

Fig. 4.7 Distance vs. Total Collision Probability of coupling result

Based on the collision probabilistic model, there are two kinds of direct influencing factors on the total collision probability. One is the number of neighbours, and the other one is the number of hidden terminals. Recall that the neighbours of the transmitter have a strong impact on direct collisions, while the hidden terminals bring forth hidden terminal collisions. Here, the lost packets with lower receiving power levels are not included. Only the packets with higher receiving power levels than the threshold are included in the following analyses.

The impacts of neighbours on the total collision probability are demonstrated in Fig. 4.8 and Fig. 4.9. In Fig. 4.8, the x-axis is the vehicles' distance, and the y-axis shows the total colli-

sion probability, in a range of [0, 1]. The data is classified into five groups, based on the number of neighbours, starting from [0, 10] to [40, 50], as the maximum number of neighbours in the result is 42. The total collision probability in this plot is distributed in the range of [0, 0.35]. Recall that the number of neighbours is determined in such a way: the neighbours are able to sense the packet sent by the transmitter, thus the receiving power levels at the neighbours are higher than the threshold. However, the coloured dots locate rather disorderly in this figure. The figure indicates that the classification of the number of neighbours does not help much in evaluating the impacts of it on the total collision probability. Therefore, another analysis that excludes the influence of distance is shown in Fig. 4.9.

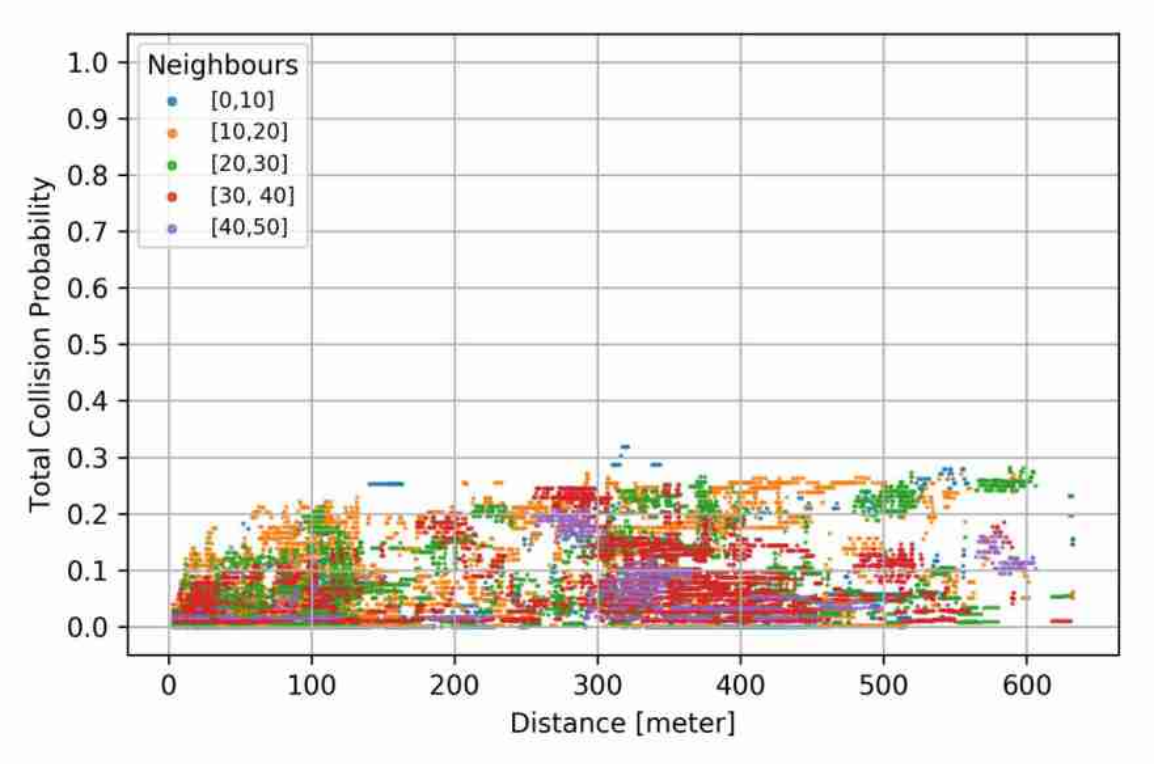

Fig. 4.8 Distance vs. Total Collision Probability of coupling result (categorized by Number of Neighbours)

Fig. 4.9 displays the relationship between the number of neighbours and the total collision probability, regardless of the influences of vehicles' distance. The x-axis is the number of neighbours and the y-axis represents the total collision probability. Same with Fig. 4.8, only packets that with higher receiving power levels than the threshold are presented in Fig. 4.9. It can be seen from Fig. 4.9 that the lower bound of the total collision probability shows a rising tendency with increasing number of neighbours. This indicates that there is a positive correlation between the number of neighbours and the total collision probability. The spread of the total collision probability shows a decreasing tendency with increasing number of neighbours. In addition, it also confirms that CSMA/CA plays an important role in controlling interferences from nearby vehicles. Otherwise, there will be a more evenly distributed total collision probability through the x-axis.

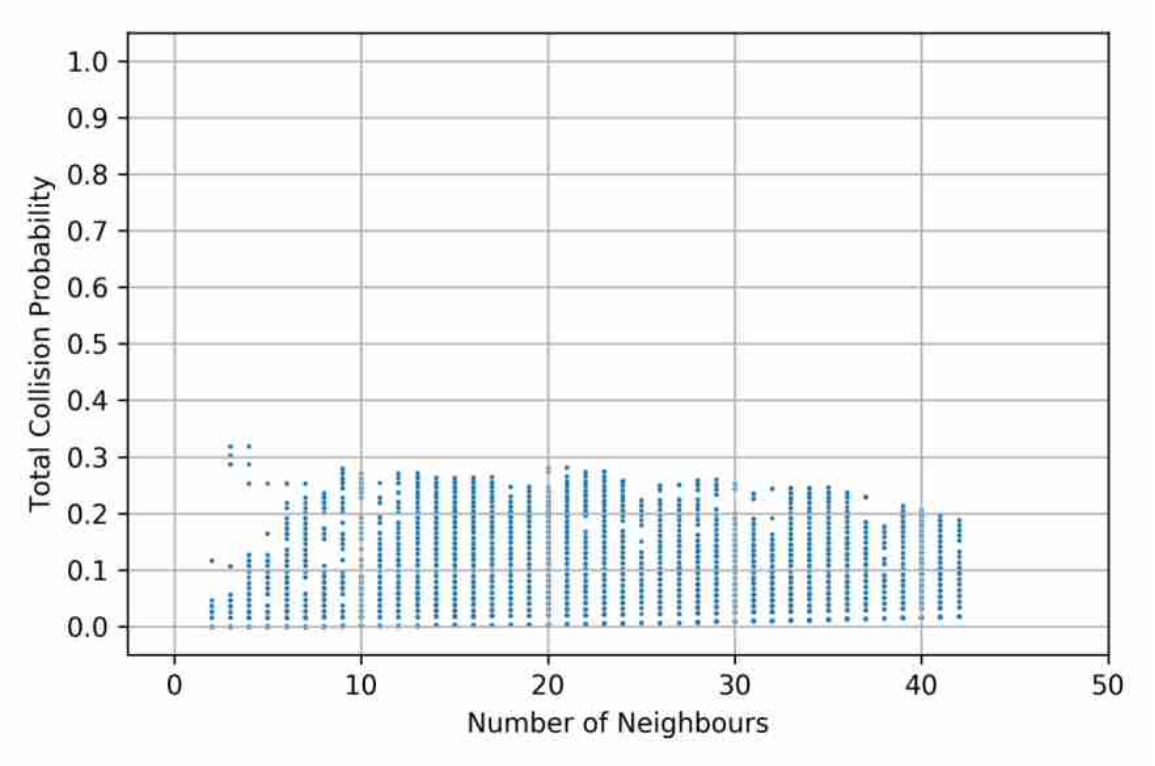

Fig. 4.9 Number of Neighbours vs. Total Collision Probability of coupling result

Fig. 4.10 and Fig. 4.11 describe the impacts of hidden terminals on the total collision probability. The maximum number of hidden terminals in the result is 35. The data is categorized into four groups based on the number of hidden terminals. The vehicles' distance and the total collision probability are the x and y-axis respectively. Again, only packets with higher receiving power levels than the threshold are taken into account. From this figure, it shows a clear hierarchical y-position of the coloured dots. This means that the total collision probability heavily depends on the number of hidden terminals. For receivers with less than ten hidden terminals, the total collision probability at them is distributed in the range of [0, 0.1], coloured in blue dots. The orange dots represent the total collision probability at receivers with hidden terminals of [10, 20]. The green and red dots represent the groups with hidden terminals of [20, 30] and [30, 40] respectively. Fig. 4.11 presents a plot excluding the distance influence, only involves the hidden terminals and the total collision probability. In this graph, the x-axis is the number of hidden terminals, and the y-axis shows the total collision probability. There is a significant rise in the total collision probability due to the growing number of hidden terminals. This supports the statement that the hidden terminals' existence is the main reason for high total collision probability.

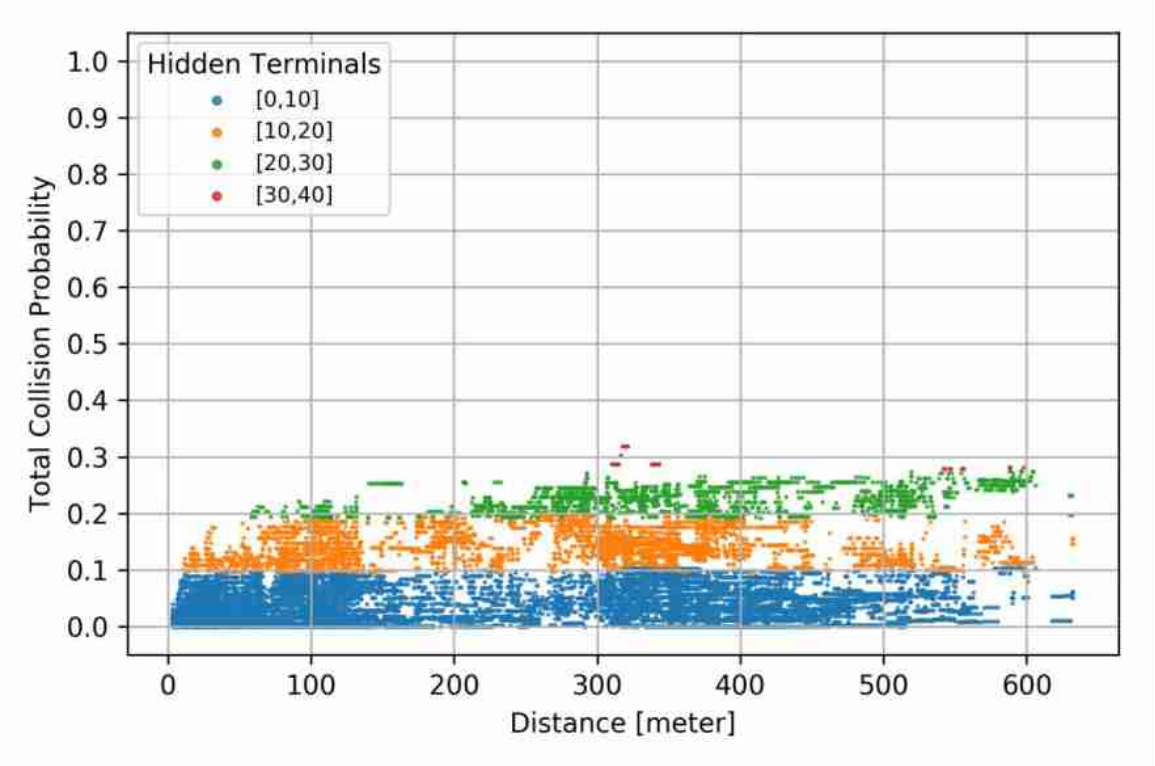

Fig. 4.10 Distance vs. Total Collision Probability of coupling result (categorized by Hidden Terminals)

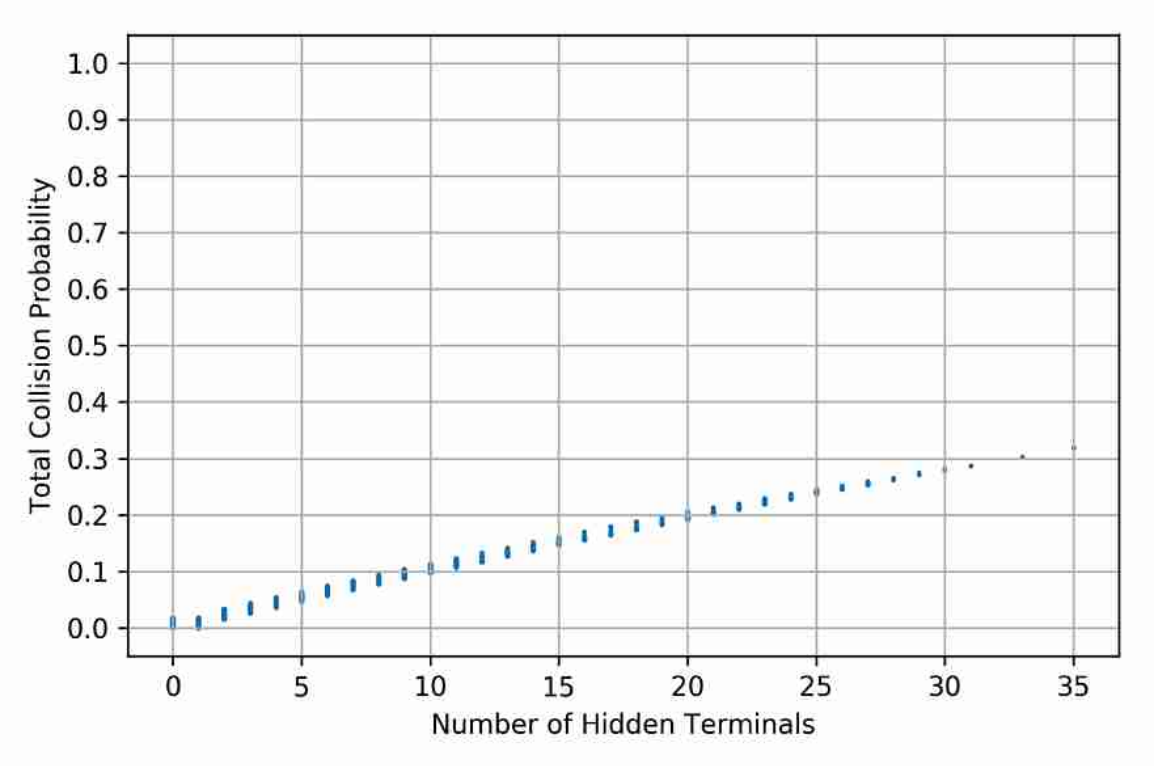

Fig. 4.11 Number of Hidden Terminals vs. Total Collision Probability of coupling result

4.4 Compare with Veins

A comparison of the coupling result between the proposed module and Veins is depicted in this section, with the intention of validating the proposed module that includes the realistic vehicle mobility impacts. The two aforementioned performance metrics are the focusing indicators of this comparison work. The base scenario LuST used here is the same as in *Section 4.1*.

Before explaining the comparison work, it should be stated that the impact of different types of antennas is ignored in the proposed module. Antennas are the actual interface of vehicles and wireless channels. As stated by (Eckhoff, Brummer, & Sommer, 2016), a slight change in antenna's angle can have considerable influences on the receiving power level and the transmission range. They also claimed that the packets reception of vehicles with realistic antenna patterns strongly depends on the attenuation caused by the angle of the antennas. Compared to the isotropic antennas, vehicles with realistic antenna patterns received considerably fewer packets from directions other than the front or the back of the vehicle (Eckhoff et al., 2016). Although the proposed module provides the option of including the antenna gains of vehicles, it cannot model the real antennas used in vehicular communication networks, which were shown to be anything but omnidirectional (Kwoczek et al., 2011). This is the intrinsic defect of analytical models. Therefore, for the concern of comparison, the influence of antenna patterns in both Veins and the proposed module are excluded.

For comparison of the receiving power level, it is necessary to check if the vehicle mobility in Veins and the proposed module are the same. The simulation time for the comparison of the receiving power level is one second, the same as in *Section 4.1*. This is done by adding default outputs of vehicle positions in Veins. It is expected that the vehicle mobility of Veins and the proposed module are not exactly the same. This is because Veins operates communication network in a discrete event simulation (OMNeT++), while the proposed module is based on time-driven simulation (SUMO). In other words, an event is recorded at the moment when a packet is transmitted in Veins, and this moment is unlikely to be the same as the exact time interval in SUMO. Thus, it is improbable to get the exact same receiving power level of each packet in the proposed module as in Veins, due to differences in event time and relevant vehicle positions. Fortunately, the differences of vehicle coordinates are still tolerable for comparison purpose. Fig. 4.12 shows the histograms of the receiving power level differences between Veins and the proposed module in ten-time steps, with 0.1-second intervals. The x-axis is the receiving power level difference, with units in [dBm]. The y-axis represents the number of transmitted packets. In the comparison work, only packets with higher receiving power levels than the threshold are considered. From this figure, it shows that there is no huge difference between the radio propagation calculation in Veins and the proposed module, as a majority of the packets show very limited difference in terms of the receiving power level. There are few packets with relatively high differences, which can be explicated that the fast-moving vehicles may lead to changes of the link type of transmission or the intersecting wall number and intersecting wall distance, thus, causing a higher difference between the receiving power levels.

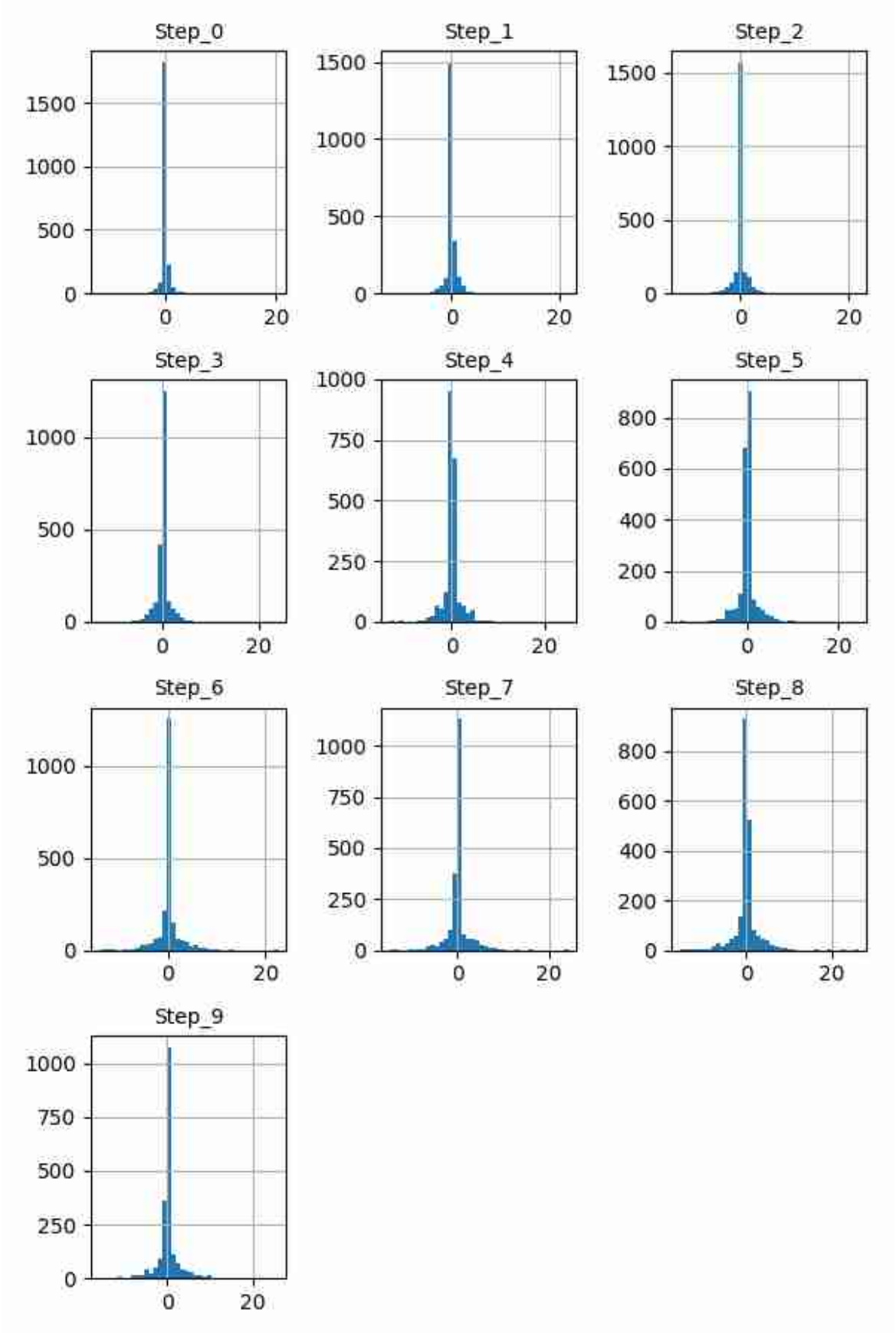

Fig. 4.12 Histograms of receiving power level differences between Veins and the proposed module

For comparison of the total collision probability, the base scenario is also LuST, but with different chosen time: 05:00, 06:00, 07:00, 09:00, 12:00 and 19:00. In every scenario, SUMO runs for ten seconds. The ROI area in this comparison is the same as in *Section 4.1* and *Section 4.2*. The numbers of vehicles within the ROI area are listed in Tab. 4.1. It is assumed that all vehicles within the ROI area are connected vehicles, with the same packet sending frequency, transmitting power and packet length, as in Tab. 3.1. Within these scenarios, the scenario with the maximum number of vehicles is in the afternoon peak hour, at 19:00, while the scenario with the minimum number of vehicles is in the early morning, at 05:00.

Real time	Number of connected vehicles within the ROI area
05:00	17
06:00	63
07:00	173
09:00	201
12:00	83
19:00	259

Tab. 4.1 Number of connected vehicles within the ROI area with different scenarios in SUMO

The comparison graphs between Veins and the proposed module are displayed in Fig. 4.13 and Fig. 4.14, with focus on the impacts of number of vehicles within the ROI area on the total collision probability. Fig. 4.13 excludes the influences of buildings as obstacles, while in Fig. 4.14, the buildings as obstacles are included in the analyses. The x-axis represents the number of vehicles in each scenario, and the y-axis denotes the total collision probability, starting from zero to one. Veins' results are presented in boxplot, and the proposed module data is coloured in magenta. It shows clearly that the total collision probability grows with increasing of the number of connected vehicles. This finding is in accordance with the previous result in *Section 3.3.4*. This figure can also be a reference for the impacts of penetration rate of the connected vehicles on the total collision probability. Besides, Fig. 4.14 with buildings as obstacles demonstrates lower total collision probability than Fig. 4.13 without buildings as obstacles. This could be explained that buildings as obstacles in general lower the receiving power levels of packets with NLOS links, reducing the number of neighbours and the number of hidden terminals, thus resulting in lower total collision probabilities.

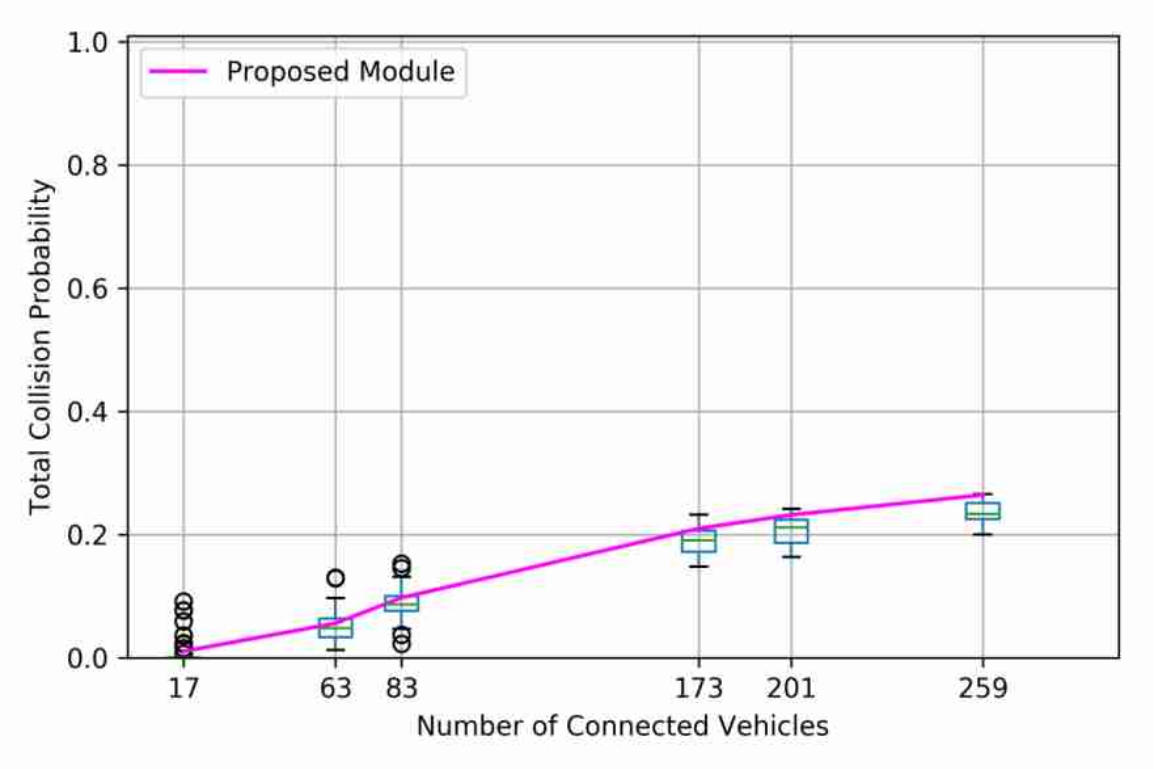

Fig. 4.13 Number of Connected Vehicles vs. Total Collision Probability of Veins (boxplot) and the proposed module, without buildings as obstacles

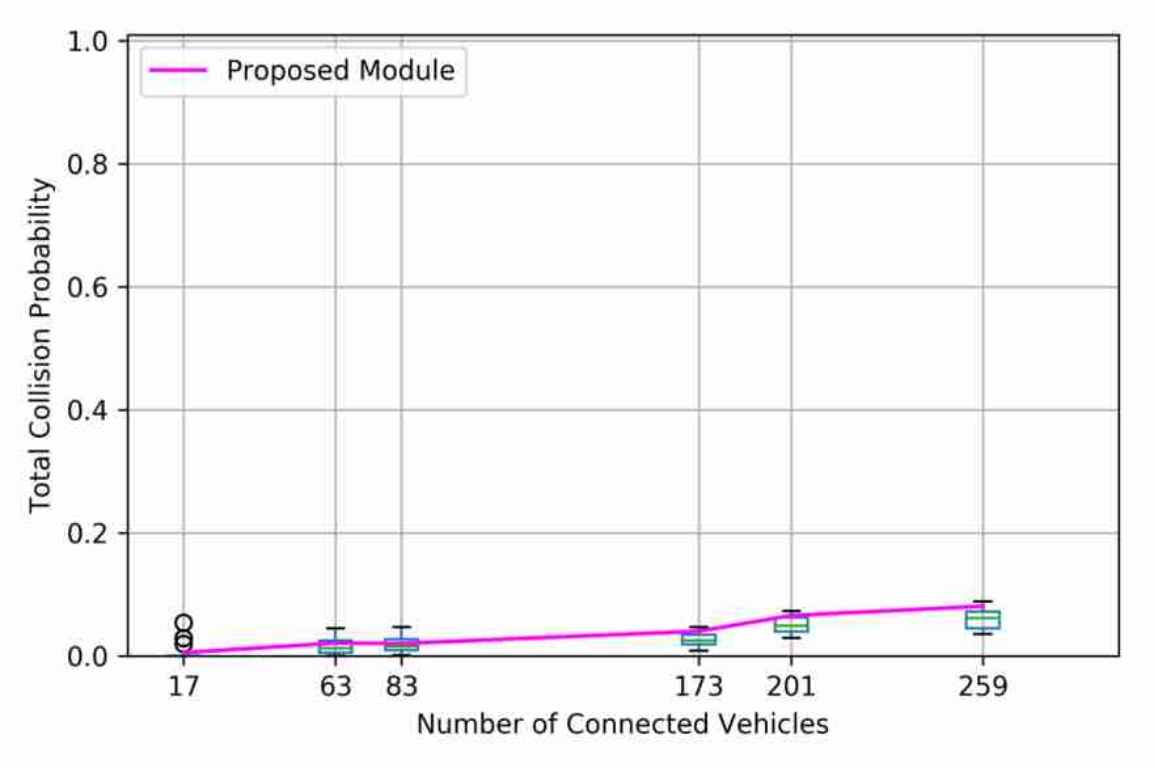

Fig. 4.14 Number of Connected Vehicles vs. Total Collision Probability of Veins (boxplot) and the proposed module, with buildings as obstacles

Significantly, the magenta curves in both figures fit well with the Veins data, which implies that when taking the vehicle mobility and building geometry into account, the proposed mod-

ule still shows a convincing result in the comparison and validation work with Veins, in terms of total collision probability. In addition, another interesting finding is that the proposed module slightly overestimates the total collision probability when compared to the Veins' result. This is because in Veins collisions do not always mean packets lost, instead, even when a collision occurs, the packets involved in the collision may still survive at some receivers, if they have higher SINR values able to be decoded by the receivers. While in the proposed module, a collision means that the involved packets are lost, indicating that the total collision probability calculated by the proposed module has to be a bit higher than the Veins' result.

In summary of this chapter, the performance of the proposed module in coupling with microscopic vehicle mobility simulators is well presented. Except the distance between the receiver and the transmitter, buildings as obstacles also have a significant impact on the receiving power level. The total collision probability strongly depends on the number of neighbours and hidden terminals. In the comparison work with Veins, the proposed module shows a satisfying result in terms of the receiving power level and the total collision probability. It can be said that the proposed module as an analytical approach that focuses on the performance assessments of vehicular communication networks is able to be an alternative to simulators in this field, with a high reliability.

5 Case Study of Cooperative Intelligent Transportation Systems

Over recent years, the emphasis in ITS has turned to Cooperative ITS (C-ITS) (also known as *connected vehicle technology* in the United States), in which vehicles are allowed to communicate with other vehicles and infrastructure. C-ITS offer the road users a more comfortable and safer task, providing more information on the surrounding road traffic conditions and environment. The technologies considered are not just limited to V2V, V2I and I2V, but could be anything V2X. With the help of wireless networks, they are expected to significantly improve traffic safety, efficiency and the comfort of driving. While in reality, the performance of C-ITS technologies highly depends on local conditions and vehicle mobility effects.

Consequently, a realistic C-ITS implementation requires the participation of adequate assessment of vehicular communication network performance with particular attention. In this chapter, a case study in C-ITS framework is presented, focusing on the implementation of the proposed module for evaluating the performance of V2I communication networks. Except V2V communication, the proposed module is also capable of evaluating V2I applications. Here, the public transport priority request on cooperative transport control scheme is taken as an example of V2I communication. In the rest of this chapter, a more detailed overview and new potentials of traffic signal systems with public transport priority are presented, followed by an explanation of the case study with relevant sensitivity analysis.

5.1 Traffic signal systems with public transport priority

Before discussing traffic signal systems with public transport priority, the reasons of choosing public transport priority application as the case study will be firstly explained. Public transport requires a particular consideration in transportation systems, because of its fundamental importance for operating high proportion of passenger traffic. However, the attractiveness of public transport is not as high as private vehicles, due to the low riding comfort and long travel time. The scheduled stops, limited start-up acceleration and braking deceleration lead to considerably lower travel speeds than private vehicles. Moreover, the varying dwelling times at stops result in varying arrival times at the traffic signals. Because of that, traditional green wave designed for private vehicles are not effective for public transport, especially after passing through several intersections (Verkehrswesen & Innerorts, 2003). Delays incurred by public transport vehicles at signalized intersections typically account for ten to 20 percent of travel time (Evans & Skiles, 1970), which means public transport priority at traffic signals can make a significant contribution in reducing travel time. Through tracking the real-time information of public transport via vehicular communication networks, C-ITS can improve the riding comfort and reduce the travel time of public transport by providing suitable green waves along intersections. Public transport vehicles with OBU devices continuously

transmit their speed, position, acceleration etc. to traffic signals, in this way they can be allocated on request an additional portion of green time at all intersections of a section.

Next, an overview of traffic signal system will be given. The traffic signal systems can be categorized into three control schemes: fixed-time control, traffic-actuated control and adaptive control. The fixed-time control uses a fixed plan with constant cycle time, and according to the current traffic situation, different plans can be selected. The traffic-actuated control (rule-based) takes advantage of loop detectors to detect the vehicle's presence, and based on the vehicle actuation logic it allocates the minimum or maximum phase timing interval. It has been widely used in Germany especially in context with public transport priority (Brilon & Wietholt, 2013). The adaptive control provides a fully real-time feedback of the traffic signal to dynamic variation of the traffic demand for each cycle at an intersection (Shaghaghi, Jabbarpour, Noor, Yeo, & Jung, 2017).

For fixed-time traffic signal programs, only long green periods of the green wave for public transport are recommended when considering public transport priority. Due to the low flexibility and strongly negative impacts on other road users, it is seldom used. For traffic-actuated and adaptive control program, the precondition is the spatial and temporal detection of individual public transport vehicles. The common way of capturing vehicles' information is by taking advantage of loop detectors and video based traffic monitoring cameras etc. (Shaghaghi et al., 2017). However, the ability of the latter two kinds of traffic signal systems to optimize public transport flows is limited by the detection capabilities of current detecting technologies (Mahendran, PI, Hebert, & Xie, 2014). The currently used technologies cannot distinguish the vehicle types, yet this distinction is of high importance when deploying public transport priority (Mahendran et al., 2014). C-ITS technologies can easily distinguish between different vehicle types, even providing more details about the vehicles, thus, offering unique opportunities to optimize public transport flows in urban environments.

5.2 Case study with sensitivity analysis

According to *Guidelines for Traffic Signals* (Verkehrswesen & Innerorts, 2003), if public transport requests a demand phase, the request signal has to be sent out as early as possible before the stop line is reached. Depending on speed and local conditions, the request point may be located between 250 and 500m before the stop line. Additional inquiry criteria are necessary if intersections or stops are closely spaced. Based on this principle, a case study of cooperative public transport priority control scheme is implemented with the proposed module.

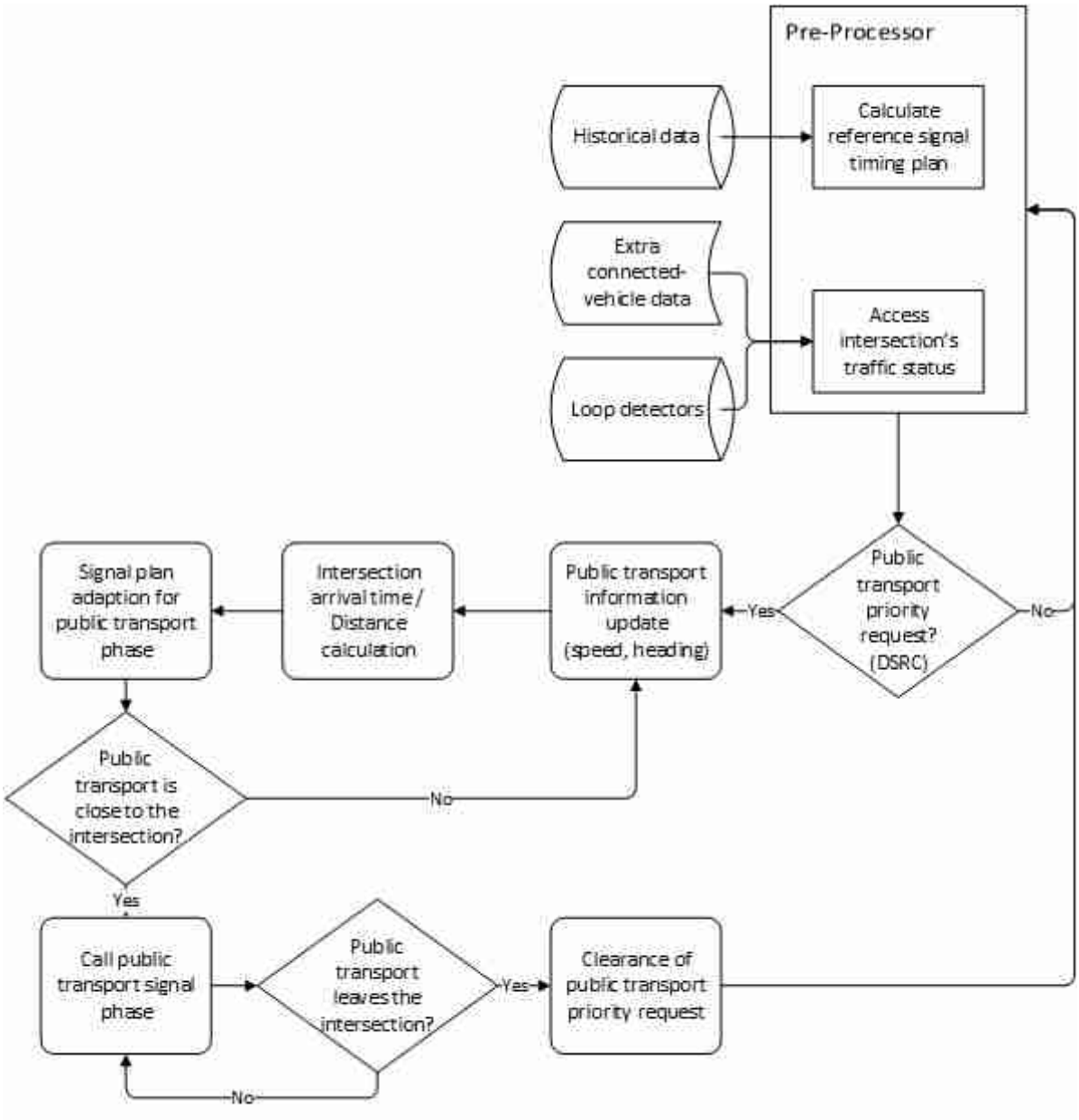

Fig. 5.1 Concept of cooperative public transport priority control scheme

The concept of the control scheme is presented with a flow chart, as shown in Fig. 5.1. First, the pre-processer includes two parts of work: one is the calculation of the reference signal-timing plan, based on historical data; the other one is for accessing intersection's traffic status, with the help of extra connected-vehicle data and loop detectors. After the pre-processing, it is determined whether there is a public transport priority request, which will be sent via DSRC. This is considered as the pre-request point, where a public transport priority request signal is sent. Once the control scheme receives a public transport priority request, the individual public transport vehicle information will be updated, including speed, heading, location, acceleration etc. By taking advantage of this information, the arrival time of individual public transport vehicle at the intersection or its distance from the intersection is calculated. Based on the arrival time prediction, the signal plan is prepared for adaption of public transport demand phases. Before the implementation of public transport demand phases, it

is essential to confirm that the individual public transport vehicle is close to the intersection. If it is still in the far-end of the intersection, the public transport information in the control scheme keeps updating. Once the individual public transport vehicle approaches the intersection within a certain distance (considered as the main-request point), the public transport demand phase is called. When the intersection receives a signal indicating that the individual public transport has passed through, the public transport priority request will be cleared. This is considered as the clear-request point. It should be noted that in the whole process, the public transport individual vehicle continuously sends its information with a fixed frequency, which ensures that the control scheme keeps tracking its status.

Based on this concept, the proposed module is implemented with V2I communication. The centre of the attention in this case study is not the algorithm of public transport priority control scheme, but the performance of C-ITS technology in such a scenario. The impacts of potential influencing factors on the V2I applications' performance are investigated. The same base scenario is used as in previous chapters, but the main difference is that the proposed module will not focus on each communicating pair of vehicles but on the communication of public transport vehicles to traffic signals. Three intersections in the ROI area are selected as the infrastructure side of V2I communication, and the position of the intersections are obtained from SUMO.

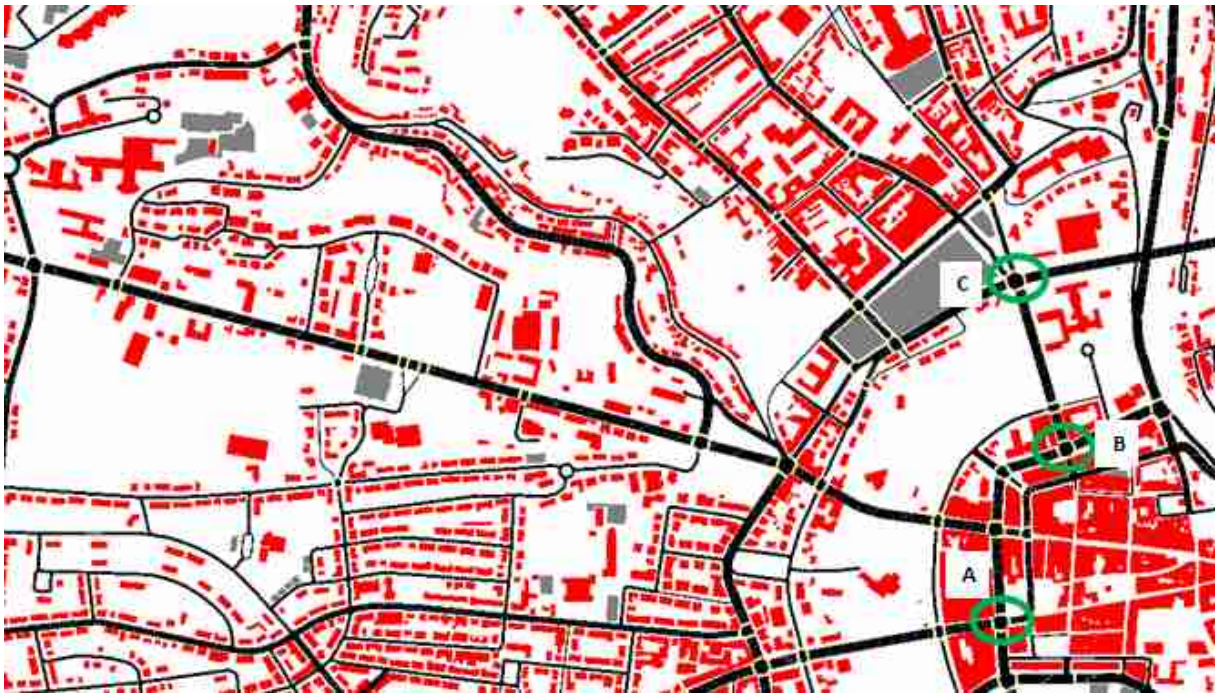

Fig. 5.2 ROI area with selected intersections

The three selected intersections are shown in Fig. 5.2, labelled as A, B and C. These intersections are located at the main bus routes of the scenario. The SUMO simulation runs for ten seconds as in real time, with a step length of 0.1second. The transmitting power level, packet length, receiving power level threshold and packet sending frequency stay the same as in previous chapters. Here, the results are analysed basing on the three intersections, as shown in Fig. 5.3, Fig. 5.4 and Fig. 5.5. It is assumed that all vehicles in the scenario are

equipped with DSRC devices and keep broadcasting their status information with the same fixed frequency.

The first plots in the three figures display the impact of the distance on the receiving power level of packets. The x-axes represent the distances between the public transport individual vehicle and the traffic signal. The y-axes are the receiving power levels, and the red horizontal lines are used for denoting the receiving power level threshold. Again, the receiving power level threshold determines whether the packets can be received by the traffic signals. The curves in the first plots are not as clear as in *Chapter 4*, which is because the public transport vehicles only occupy a small portion of the vehicles, while in *Chapter 4* all the vehicles in the scenario are included. The highest receiving power levels at each intersection are different. Among the three intersections, intersection C has the highest receiving power level, as it has the lowest building density.

The second, third and fourth plots in each figure demonstrate the influences on the total collision probability from the distance, number of hidden terminals and number of neighbours respectively. Due to the limited amount of public transport individual vehicles, these plots do not show clear and well-presented relationships between the factors and the performance metric. However, some correlations between these factors and the total collision probability are still observable. The second plots indicate that within 200m, the total collision probability stays in the range of [0, 0.2], which is still tolerable for traffic signal adaption applications. From the third plots, the total collision probability shows a firm upward tendency with increasing number of hidden terminals. The influence of neighbours on the total collision probability is not as significant as the number of neighbours, as shown in the fourth plots. Apart from that, intersection C shows a better result on the total collision probability than the other two intersections. The results of the real world tests conducted by (Stahlmann, Möller, Brauer, German, & Eckhoff, 2017) also confirms the findings of the total collision probability results in this case study.

By comparing the three figures, it is obvious that the differences between building geometry lead to the variance of these intersections' result analyses. With a lower building density, the receiving power level and the total collision probability of intersection C shows better results than those of intersection A and B. Hence, the performance of vehicular communication networks is strongly environmental-dependent, which means that even for the same scenario it is critical to generate individual analysis on different intersections. A granted perfect assumption on the performance of vehicular communication networks is unrealistic and meaningless.

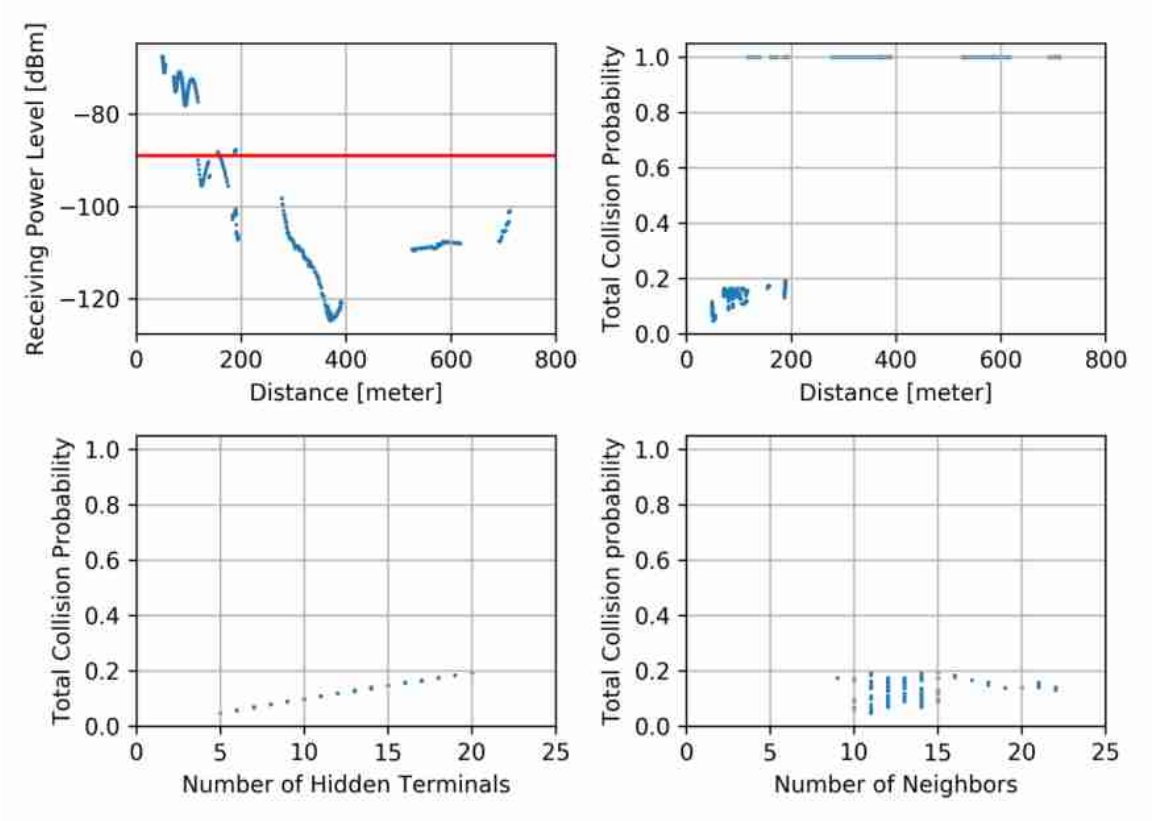

Fig. 5.3 Intersection A result analysis

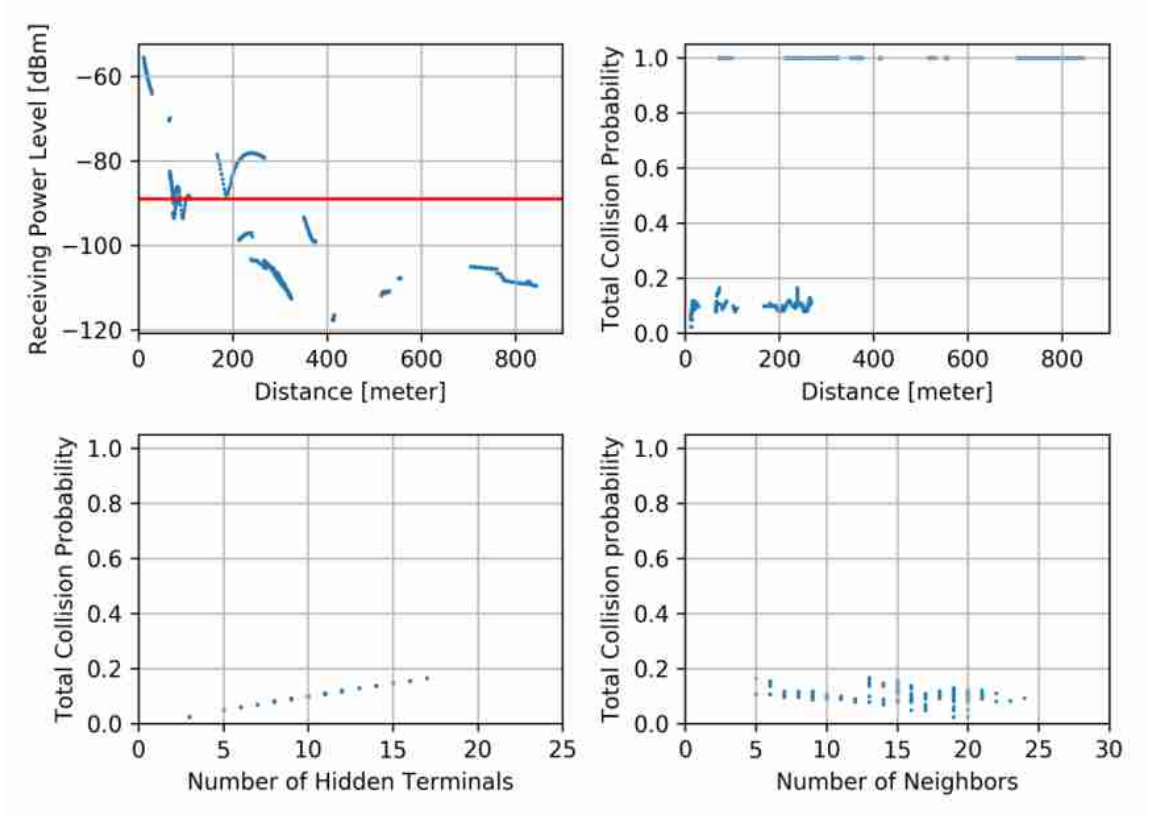

Fig. 5.4 Intersection B result analysis

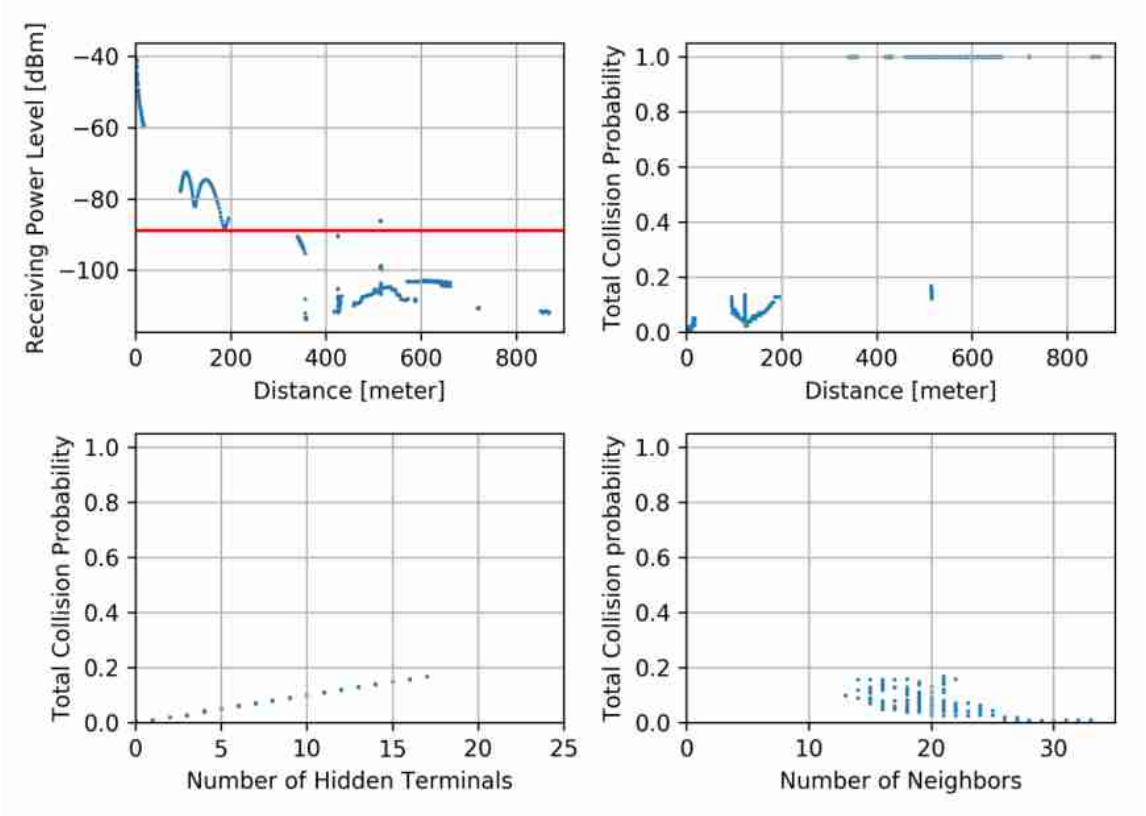

Fig. 5.5 Intersection C result analysis

Though the protocol recommends a maximum frequency of ten Hz for status message generation, this study also investigates in the influence of packet generation rate on the total collision probability, as shown in Fig. 5.6. For a better visualization, the three plots in Fig. 5.6 exclude the packets with lower receiving power levels than the threshold, which are considered as lost packets with 1.0 value for the total collision probability. The x-axes represent the packet generation frequency, with units in [Hz]. The y-axes are the total collision probability. From the three plots, it can be said that the packet generation rate has limited influences on the total collision probability. However, the results observed in these three figures show big difference to the ones observed by other studies: it is expected that a higher packet generation rate, thus a more intensive request for channel sources leads to an increase of total collision probability (Schmidt-Eisenlohr, 2010). This can be explained that with a limited number of connected vehicles, i.e. under unsaturated situations, packet generation rate will not significantly change the total collision probability, as the channel is still able to transmit such a number of packets.

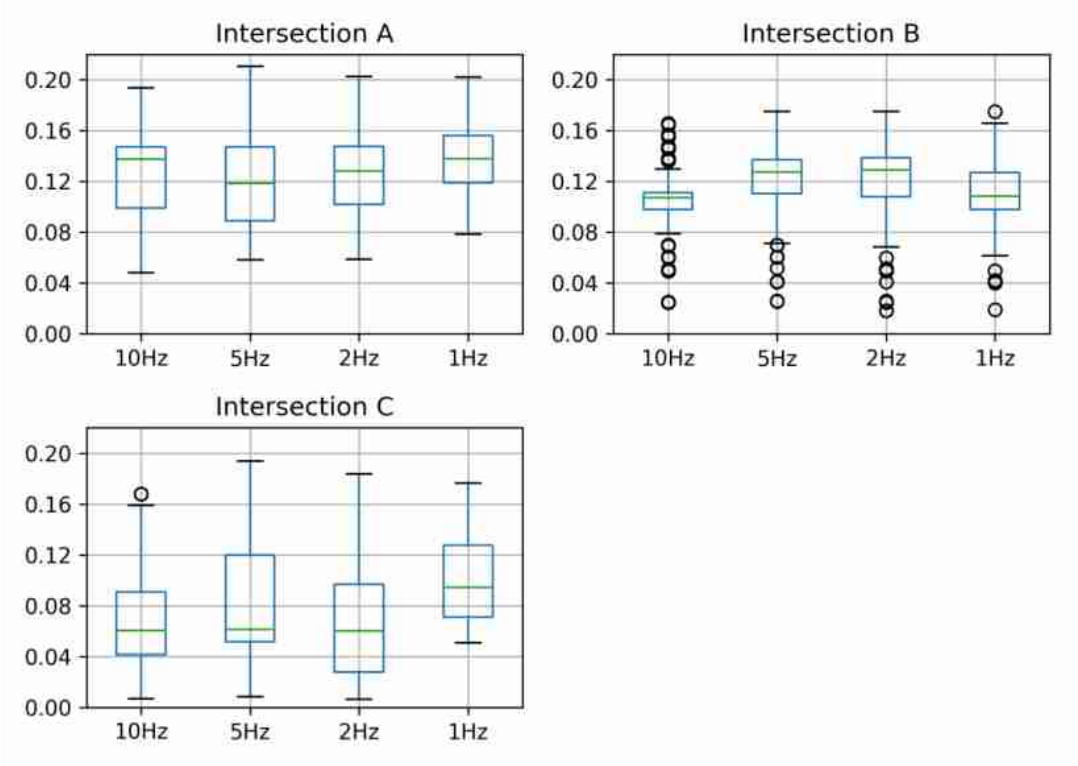

Fig. 5.6 Packet Generation Frequency vs. Total Collision Probability

Additionally, this case study gives some insights for developing an efficient cooperative public transport priority control scheme. When the public transport vehicle uses DSRC technology to send its priority request within 200 meters from the traffic signal, there is a much higher probability that the traffic signal can react with this request than that of farther distance, in terms of both the receiving power level and the packet reception probability. When the public transport is far away from the intersections (distance is longer than 200 m), infrastructure-based cellular-networks are recommended to use for status information updates, due to its wider coverage. Such an integration of DSRC-based and infrastructure-based wireless networks can give rise to extended wireless coverage, reduced employment cost and performance enhancement of C-ITS applications. Furthermore, by exclusively increasing the transmitting power level of the public transport vehicles, it is believed that the packet reception rate of public transport at the traffic signals can be enhanced.

6 Discussion

The performance assessment of vehicular communication networks is of high importance. It gives a first view on the feasibility of C-ITS applications and provides advices on measures of performance enhancement. Currently, the most commonly used methodology for evaluating the performance is by using simulators. Yet, from the side of traffic engineering, using an integration of communication network simulators with road-traffic simulation tools seems not as attractive as using analytical models, because of the required computational effort and the complexity. Moreover, the existing analytical models cannot provide a reliable solution to this challenge. In such a context, traffic engineers tend to obtain road traffic data directly from vehicle mobility simulators for generating road-traffic impact analysis of C-ITS applications. With unrealistic assumption of a perfect performance of vehicular communication networks, they define the communication range of the vehicles as a circular area with the transmitter as the centre of the circle and a default distance as the radius, in which packets are transmitted without delay or loss. While in reality, due to radio propagation factors and interferences, only in a tiny minority cases loss-free scenario could happen. Thus, this study focuses on evaluating the realistic performance of vehicular communication networks through analytical approaches. In this chapter, first, the loss-free scenario, simulators and the proposed module are compared in *Section 6.1*, in terms of plausibility, flexibility, complexity and scalability. *Section 6.2* presents a discussion about the contributions, limitations, and potentials of the proposed analytical approach.

6.1 Comparison between loss-free, simulators and proposed module

In this section, the proposed module is compared with Veins and loss-free scenario in four perspectives: plausibility, flexibility, efficiency, and scalability, as shown in Tab. 6.1. The loss-free scenario is defined as the scenario that in which the vehicular communication networks performs perfectly within a circular area (a transmitter as the centre of the circle, a default distance as the radius) and the road traffic data can be easily accessed through vehicle mobility simulators without any delay or influences of packet losses. The simulators represent the sequential simulators for analysing vehicular communication networks. The proposed module is an analytical approach that integrates the realistic vehicle mobility impacts and wireless channel characteristics, and it has been tested with Veins for validation.

Features	Loss-free	Simulators	Proposed Module
Plausibility	Low	High	High
Flexibility	High	Medium	High
Efficiency	High	Low	Medium
Scalability	High	Low	High

Tab. 6.1 Characteristics comparison between loss-free, communication network simulators and the proposed module

In respect of plausibility, the loss-free scenario is unrealistic because many investigations as well as this study have proven that vehicular communication networks can be anything but perfect, particularly in urban scenarios with the presence of a multitude of obstacles and interferences. Not only the packet reception probability but also the transmission ranges heavily depend on the surrounding environment, and none of them is deterministic, identical or consistent. For communication network simulators with consideration of realistic vehicle mobility and realistic wireless channel characteristics, they show a high plausibility in terms of performance evaluation. For example, Veins, a widely used framework, provides reasonable analysis for simulating vehicular communication networks. The proposed approach, on the basis of both a study of relevant literature and extension of an existing analytical model, shows a convincing result when compared with Veins, in terms of receiving power level, transmission range and total collision probability. Therefore, one can say that both Veins and the proposed module have a high plausibility.

Concerning flexibility, it is defined as the easiness of implementing with different vehicle mobility simulators and for different kinds of V2X communications. Due to its characteristic as analytical approaches and limited required inputs from vehicle mobility simulators, the core of the proposed module is a bunch of formulas, which results in easy implementation with different microscopic vehicle mobility simulators. In addition, except V2V communication, the proposed module also demonstrated its capabilities in analysing V2I communication, as shown in *Chapter 5.* It is believed that I2V communication analysis can also benefit from the proposed module, with slight adjustment. For the loss-free scenario, the road traffic data can always be directly accessed from various vehicle mobility simulators, with high flexibility while sacrificing plausibility. In general, communication network simulators show a lower flexibility, as most of the simulators are bound to one specific vehicle mobility simulator, and for different kinds of V2X communications, they are required to use different modules and inherent models.

From the perspective of efficiency, i.e. required computational resources, there is no additional computational effort from the loss-free scenario because it does not consider any realistic vehicular communication network performance. This certainly saves computational resources, however, at the cost of plausibility. While the simulators and the proposed module

require additional computational effort. In particular, the sequential simulators consume a large number of computational resources because they simulate the mechanism of the protocol and the wireless channel characteristic. Compared to simulators, the proposed module shows lower requirements of computation time and memory space, as it demonstrates the wireless communication network in a statistical way. Additionally, for V2I or I2V communication, the proposed module demands much less effort than that of V2V communication.

On the side of scalability, it is obvious that the loss-free scenario can be applied in any size of networks since it has no requirements of additional computational resources. However, for simulators such as Veins, they are constrained to small-scale networks, because of the lack of processing resources as sequential simulators. Therefore, a city-scale vehicular communication simulation network has not yet existed. The proposed module provides a new opportunity for this problem. It is believed that by means of proper improvements such as parallel programming, the proposed module will be able to solve city-scale vehicular communication networks, which will be discussed explicitly in the next part.

6.2 Contributions, limitations and potentials

By developing the proposed module and coupling it with a microscopic road-traffic simulation tool, new potentials for evaluating the C-ITS road-traffic impact analysis are offered. The influencing factors and their impacts on the communication network performance are analysed, emphasizing the receiving power level and the total collision probability. The obstacles and distances between the transmitters and the receivers decrease the receiving power levels of the packets, implying that under different surrounding environments, the performances of vehicular communication networks vary. The neighbours and hidden terminals, especially the latter ones, have significant impacts on the total collision probability of the packets. The analyses also illustrate that the total collision probability has a strong dependence on the connected-vehicles density. These findings raise the awareness of evaluating the performance of vehicular communication networks for generating road-traffic impact analysis of C-ITS applications.

For the purpose of further implementation, the proposed module has been validated with a well-developed and widely used vehicular communication network framework - Veins. By coupling with microscopic vehicle mobility simulator (SUMO), the validation work takes into account the realistic vehicle mobility impacts. It is found that with a larger number of connected vehicles (also considered as higher penetration rate of connected vehicles) there is a more intensive request for channel resources resulting in an increase of total collision probability. The validation result also shows that the proposed module can be an alternative approach for assessing the performance of inter-vehicular communication networks, not only under unsaturated but also saturated situations. This is a breakthrough for analytical models, as the existing analytical models are often criticized due to their unrealistic assumptions and conditioned applying scenarios.

Moreover, the proposed module is easy to implement not only in the field of V2V communication but also V2I communication, which indicates the high flexibility and extendibility of the proposed module. The case study of C-ITS shows the capabilities of the proposed module in V2I communication, and the concept design of the traffic signal control scheme offers a new opportunity of implementing public transport priority with the help of C-ITS technology. It also gives insights on the requirements and notifications when developing efficient C-ITS control scheme. The distance between the public transport individual vehicles and the intersection determines the reception of the public transport status packets at intersections to a certain degree. Other influencing factors include building density, the number of hidden terminals and neighbours. Although packet generation rate is believed to have an important influence on the total collision probability, this study has found that it has limited impacts in unsaturated situations. In order to ensure enough time of signal adaption preparation for public transport demand phase, it is recommended to integrate the DSRC and infrastructure-based wireless networks, with the benefit of extended area coverage. Besides, for an absolute public transport priority, the exclusive increase of the transmitting power level of public transport can be helpful.

There are also limitations of the proposed module. First, it is not capable of modelling the impacts of different antenna patterns on the receiving power level of the packet, which is a significant influencing factor in reality (Eckhoff et al., 2016). Second, only buildings are considered as the obstacles, even though in urban areas foliage, overpasses and heavy trucks can also block the LOS transmission. Third, the Quality of Service strategies and multi-channel operations such as alternating access are not included in the proposed module. Fourth, the computational effort of the proposed module is still a hindrance for promotion, because some well-developed simulators may even consume less computational effort than the proposed module. The bottleneck of computing time may lie in the processing of building geometry traversal.

Although the current version of the proposed module does not present strong advantages in terms of required computational effort, it shows more potential when using parallel simulation and implementing with city-scale networks. Currently, none of the existing simulators that focus on modelling real-time vehicular mobility and inter-vehicular communication is implemented as parallel or distributed networks (Ahmed, M. S., Hoque, M. A., & Pfeiffer, P., 2016), because most of them are implemented as sequential programs, for instance, Veins. Furthermore, scalability is the other important limitation of simulators. Due to the lack of processing resources, sequential simulations are constrained to small-scale urban environments (Ahmed, M. S., Hoque, M. A., & Pfeiffer, P., 2016). However, the proposed module can benefit from parallel programming and further operate city-scale networks, as it has the potential parallelism. By dividing the proposed module into smaller independent parts, like different communicating pairs of vehicles, the smaller parts or tasks can be solved at the same time because they can access the same memory of vehicle locations and building geometry concurrently, and the data dependency between each communicating pair is quite limited. If the parallel programming is achieved, the execution of the proposed module can be finished in a shorter wall-clock time. As a consequence of executing the proposed module efficiently,

parallel programming can scale with the network size, thus it can solve larger problems (Ortega-Arjona, 2010). This will provide a new vision of evaluating C-ITS applications with city-scale networks.

7 Conclusion

The main motivation of C-ITS is to improve traffic safety and efficiency. With such intention, the performance assessment of the used technology should not be ignored. It should be considered as a pre-requirement and an inherent part from the very start, as the performance assessment determines the feasibility of C-ITS applications. With such awareness, this study has developed an analytical approach for the performance evaluation, which is more reliable and comprehensive than some other analytical models. Compared to communication network simulators, the analytical approach is more efficient, flexible and scalable, and it can even be an alternative to some communication network simulators. The coupling of the analytical approach with the microscopic traffic simulation tool SUMO for both V2V and V2I communication has proved that the performance of vehicular communication networks is highly affected by the distances and obstacles between the transmitter and the potential receivers, as well as the interferences from others. The impacts of the multiple influencing factors on the two selected performance metrics (the receiving power level and the total collision probability) are also analysed explicitly in this study. The analyses have shown that it is not wise to consider the performance of vehicular communication networks as perfect in reality, especially in urban scenarios with dense buildings and high penetration rate of connected vehicles.

The developed analytical approach has offered a new possibility for a detailed performance analysis in vehicular communication networks and opened several future research directions. The parallel programming of the analytical approach will be beneficial to reduce the required computational resources and further implement in city-scale communication networks, which has not yet been realised with current simulators, analytical models or FOT. Another open research direction is that the development of more realistic wireless channel models, which should be validated with FOT. For instance, obstacles such as heavy trucks, overpasses and foliage should be taken into account. Besides, the future participation of pedestrians and cyclists in C-ITS applications is also interesting, which requires more attention from the side of realistic mobility. There is also a demand of analysing the realistic impacts of I2V communication on road traffic efficiency.

The integration of realistic road traffic mobility and realistic wireless network is the precondition for evaluating the impacts of C-ITS applications. With this conception in mind, this study contributes to the researches of C-ITS with new possibilities.

List of References

5G AMERICAS. (2016). V2X Cellular Solutions(white paper).

AHMED, M. S., HOQUE, M. A., & PFEIFFER, P. (ED.) 2016. Comparative study of connected vehicle simulators: IEEE.

ARANITI, G., CAMPOLO, C., CONDOLUCI, M., IERA, A., & MOLINARO, A. (2013). LTE for vehicular networking: A survey. IEEE Communications Magazine, 51(5), 148–157. https://doi.org/10.1109/MCOM.2013.6515060

BARCELO, J., FERRER, J. L., & MONTERO, L. (1989). AIMSUN: Advanced Interactive Microscopic Simulator for Urban Networks. Vol I: System Description, and, 2.

BARCELÓ, J. (2010). Fundamentals of traffic simulation: Springer.

BARR, R. (2004). Swans-scalable wireless ad hoc network simulator. User Guide.

BARR, R., HAAS, Z. J., & VAN RENESSE, R. (2005). JiST: An efficient approach to simulation using virtual machines. Software: Practice and Experience, 35(6), 539–576.

BIANCHI, G. (2000). Performance analysis of the IEEE 802.11 distributed coordination function. IEEE Journal on Selected Areas in Communications, 18(3), 535–547. https://doi.org/10.1109/49.840210

BOBAN, M. (2013). T-SET Final Research Report.

BOBAN, M., VINHOZA, T. T. V., FERREIRA, M., BARROS, J., & TONGUZ, O. K. (2011). Impact of Vehicles as Obstacles in Vehicular Ad Hoc Networks. IEEE Journal on Selected Areas in Communications, 29(1), 15–28. https://doi.org/10.1109/JSAC.2011.110103

BRILON, W., & WIETHOLT, T. (2013). Experiences with adaptive signal control in Germany. Transportation Research Record: Journal of the Transportation Research Board. (2356), 9–16.

CAMERON, G. D. B., & DUNCAN, G. I. D. (1996). PARAMICS—Parallel microscopic simulation of road traffic. The Journal of Supercomputing, 10(1), 25–53.

CASSIDY, W. G., JABER, N., RUPPERT, S. A., TOIMOOR, J., TEPE, K. E., & ABDEL-RAHEEM, E. (2012). Interference modelling and SNR threshold study for use in vehicular safety messaging simulation. In 2012 26th Biennial Symposium on Communications (QBSC): 28 - 29 May 2012, Kingston, Ontario, Canada (pp. 52–55). Piscataway, NJ, Piscataway, NJ: IEEE. https://doi.org/10.1109/QBSC.2012.6221350

CHEN, S., XU, H., LIU, D., HU, B., & WANG, H. (2014). A Vision of IoT: Applications, Challenges, and Opportunities With China Perspective. IEEE Internet of Things Journal, 1(4), 349–359. https://doi.org/10.1109/JIOT.2014.2337336

CODECA, L., FRANK, R., FAYE, S., & ENGEL, T. (2017). Luxembourg SUMO Traffic (LuST) Scenario: Traffic Demand Evaluation. IEEE Intelligent Transportation Systems Magazine, 9(2), 52–63. https://doi.org/10.1109/MITS.2017.2666585

DRESSLER, F., SOMMER, C., ECKHOFF, D., & TONGUZ, O. (2011). Toward Realistic Simulation of Intervehicle Communication. IEEE Vehicular Technology Magazine, 6(3), 43–51. https://doi.org/10.1109/MVT.2011.941898

ECKHOFF, D. (2016). Simulation of privacy-enhancing technologies in vehicular ad-hoc networks.

ECKHOFF, D., BRUMMER, A., & SOMMER, C. (2016). On the impact of antenna patterns on VANET simulation. In O. Altintas (Ed.), 2016 IEEE Vehicular Networking Conference (VNC): Date, 8-10 Dec. 2016 (pp. 1–4). Piscataway, NJ: IEEE. https://doi.org/10.1109/VNC.2016.7835925

ECKHOFF, D., & SOMMER, C. (2015). Simulative performance evaluation of vehicular networks. In W. Chen (Ed.), Woodhead publishing series in electronic and optical materials: number 72. Vehicular communications and networks: Architectures, protocols, operation and deployment / editor, Wai Chen (pp. 255–274). Amsterdam: Elsevier. https://doi.org/10.1016/B978-1-78242-211-2.00012-X

ECKHOFF, D., & SOMMER, C. (ED.) 2012. A multi-channel IEEE 1609.4 and 802.11 p EDCA model for the veins framework.

EDWARDS, C., HANKEY, J., KIEFER, R., GRIMM, D., & LEASK, N. (2011). Understanding Driver Perceptions of a Vehicle to Vehicle (V2V) Communication System Using a Test Track Demonstration. SAE International Journal of Passenger Cars - Mechanical Systems, 4(1), 444–461. https://doi.org/10.4271/2011-01-0577

EVANS, H. K., & SKILES, G. W. (1970). Improving public transit through bus preemption of traffic signals. Traffic Quarterly, 24(4).

FLORIAN, M. A., MAHUT, M., & TREMBLAY, N. (2006). A simulation-based dynamic traffic assignment model: Dynameq: Centre for Research on Transportation.

FONT, JUAN LUIS, ET AL. (ED.) 2010. ARCHITECTURE, DESIGN AND SOURCE CODE COMPARISON OF NS-2 AND NS-3 NETWORK SIMULATORS: SOCIETY FOR COMPUTER SIMULATION INTERNATIONAL.

GÖRMER, JANA, ET AL. (ED.) 2011. DECISION SUPPORT FOR DYNAMIC CITY TRAFFIC MANAGEMENT USING VEHICULAR COMMUNICATION.

GUTTMAN, A. (1984). R-TREES: A DYNAMIC INDEX STRUCTURE FOR SPATIAL SEARCHING (VOL. 2): ACM.

HAFEEZ, K. A., ZHAO, L., MA, B., & MARK, J. W. (2013). Performance Analysis and Enhancement of the DSRC for VANET's Safety Applications. IEEE Transactions on Vehicular Technology, 62(7), 3069–3083. https://doi.org/10.1109/TVT.2013.2251374

HAN, C., DIANATI, M., TAFAZOLLI, R., KERNCHEN, R., & SHEN, X. (2012). Analytical Study of the IEEE 802.11p MAC Sublayer in Vehicular Networks. IEEE Transactions on Intelligent Transportation Systems, 13(2), 873–886. https://doi.org/10.1109/TITS.2012.2183366

HASSAN, M. I., VU, H. L., & SAKURAI, T. (2011). Performance Analysis of the IEEE 802.11 MAC Protocol for DSRC Safety Applications. IEEE Transactions on Vehicular Technology, 60(8), 3882–3896. https://doi.org/10.1109/TVT.2011.2162755

IEEE STANDARDS (2016). IEEE Standard for Information technology--Telecommunications and information exchange between systems Local and metropolitan area networks--Specific requirements - Part 11: Wireless LAN Medium Access Control (MAC) and Physical Layer (PHY) Specifications. (IEEE standards, 802.11-2016). Piscataway, NJ, USA: IEEE.

IEEE STANDARDS ASSOCIATION. (2013). IEEE guide for Wireless Access in Vehicular Environments (WAVE) architecture. IEEE Std, 1609-0.

KRAJZEWICZ, D. (2009). Kombination von taktischen und strategischen Einflüssen in einer mikroskopischen Verkehrsflusssimulation: VDI-Verlag.

KRAJZEWICZ, DANIEL, ET AL. (ED.) 2002. SUMO (Simulation of Urban MObility)-an open-source traffic simulation.

KRAUß, S. (1998). Microscopic modeling of traffic flow. Investigation of collision free vehicle dynamics.

KWOCZEK, A., RAIDA, Z., LACIK, J., POKORNY, M., PUSKELY, J., & VAGNER, P. (2011). Influence of car panorama glass roofs on Car2Car communication (poster). In I. Staff (Ed.), 2011 3rd IEEE Vehicular Networking Conference (pp.246–251). [Place of publication not identified]: IEEE. https://doi.org/10.1109/VNC.2011.6117107

LIU, Y., XU, Y., LI, D., & WANG, W. (2014). Device-to-Device Communication in LTE-A Cellular Networks: Standardization, Architecture, and Challenge. In IEEE 79th Vehicular Technology Conference (VTC Spring), 2014: 18-21 May 2014, Seoul, Korea ; proceedings ; [including papers of the] Second International Workshop on Vehicular Traffic Management for Smart Cities (VTM 2014) (pp.1–5). Piscataway, NJ: IEEE. https://doi.org/10.1109/VTCSpring.2014.7022878

LOWNES, N. E., & MACHEMEHL, R. B. (ED.) 2006. VISSIM: A multi-parameter sensitivity analysis: Winter Simulation Conference.

MA, X., YIN, X., WILSON, M., & TRIVEDI, K. S. (2013). MAC and application-level broadcast reliability in vanets with channel fading. In 2013 International Conference on Computing, Networking and Communications: (ICNC) : January 28-31 2013, San Diego, USA (pp. 756–761). Piscataway, NJ: IEEE. https://doi.org/10.1109/ICCNC.2013.6504183

MACIEJEWSKI, M. (2010). A comparison of microscopic traffic flow simulation systems for an urban area. Transport Problems, 5(4), 27–38.

MAHENDRAN, A., PI, S. S., HEBERT, M., & XIE, X.-F. (2014). Bus Detection for Adaptive Traffic Signal Control. CMU-Penn TSET–A US DOT University Transportation Center, Tech. Rep.

MALONE, D., DUFFY, K., & LEITH, D. (2007). Modeling the 802.11 Distributed Coordination Function in Nonsaturated Heterogeneous Conditions. IEEE/ACM Transactions on Networking, 15(1), 159–172. https://doi.org/10.1109/TNET.2006.890136

MARTINEZ, F. J., TOH, C. K., CANO, J.-C., CALAFATE, C. T., & MANZONI, P. (2011). A survey and comparative study of simulators for vehicular ad hoc networks (VANETs). Wireless Communications and Mobile Computing, 11(7), 813–828. https://doi.org/10.1002/wcm.859

MATOLAK, D. W., SEN, I., & XIONG, W. (2006). Channel Modeling for V2V Communications. In 2006 3rd Annual International Conference on Mobile and Ubiquitous Systems--Workshops: San Jose, CA, 17-21 July 2006 (pp.1–7). Piscataway NJ: IEEE. https://doi.org/10.1109/MOBIQW.2006.361749

MIR, Z. H., & FILALI, F. (2014). LTE and IEEE 802.11p for vehicular networking: A performance evaluation. EURASIP Journal on Wireless Communications and Networking, 2014(1), 89. https://doi.org/10.1186/1687-1499-2014-89

MODELER, O. (2009). Opnet technologies inc.

NAKAGAMI, M. (1960). The m-Distribution—A General Formula of Intensity Distribution of Rapid Fading. In W. C. Hoffman (Ed.), Statistical methods in radio wave propagation: Proceedings of a symposium held June 18-20, 1958 (pp. 3–36). New York: Symposium Publications Division, Pergamon Press. https://doi.org/10.1016/B978-0-08-009306-2.50005-4

ORTEGA-ARJONA, J. L. (2010). Patterns for parallel software design: John Wiley & Sons.

P. GASPAR, Z. SZALAY, ET.AL. (2014). Highly Automated Vehicle Systems: BME-MOGI.

PAIKARI, E. (2014). Connected Vehicle Extension and Integration of Traffic and Discrete Event Simulation Systems--Applied to Evaluations Based on Dedicated Short Range Communication for Safety and Mobility Indices. University of Calgary.

PAPADIMITRATOS, P., LA FORTELLE, A., EVENSSEN, K., BRIGNOLO, R., & COSENZA, S. (2009). Vehicular communication systems: Enabling technologies, applications, and future outlook

on intelligent transportation. IEEE Communications Magazine, 47(11), 84–95. https://doi.org/10.1109/MCOM.2009.5307471

RAPPAPORT, T. S. (2002). Wireless communications: Principles and practice / Theodore S. Rappaport (2nd ed.). Prentice Hall communications engineering and emerging technologies series. Upper Saddle River, N.J., Great Britain: Prentice Hall PTR.

RAUBER, T., & RÜNGER, G. (2013). Parallel programming: For multicore and cluster systems: Springer Science & Business Media.

RONDINONE, M., MANEROS, J., KRAJZEWICZ, D., BAUZA, R., CATALDI, P., HRIZI, F. LIN, L. (2013). iTETRIS: A modular simulation platform for the large scale evaluation of cooperative ITS applications. Simulation Modelling Practice and Theory, 34, 99–125.

SANTA, J. AND GÓMEZ-SKARMETA, A.F. (ED.) 2008. Potential of cellular networks in vehicular communications.

SCHMIDT-EISENLOHR, F. (2010). Interference in vehicle-to-vehicle communication networks: Analysis, modeling, simulation and assessment. Zugl.: Karlsruher Inst. für Technologie, Diss., 2010. Karlsruhe: KIT Scientific Publ.

SCHÜNEMANN, B. (2011). V2X simulation runtime infrastructure VSimRTI: An assessment tool to design smart traffic management systems. Computer Networks, 55(14), 3189–3198.

SEPULCRE, M., & GOZALVEZ, J. (2011). On the importance of application requirements in cooperative vehicular communications. In WONS 2011: 2011 Eighth International Conference on Wireless On-Demand Network Systems and Services (pp. 124–131). [Piscataway, N.J.]: IEEE. https://doi.org/10.1109/WONS.2011.5720180

SHAGHAGHI, E., JABBARPOUR, M. R., NOOR, R. M., YEO, H., & JUNG, J. J. (2017). Adaptive green traffic signal controlling using vehicular communication. Frontiers of Information Technology & Electronic Engineering, 18(3), 373–393.

SLUIJSMANS, D. (2011). Performance Evaluation of Data Dissemination Protocols for an Infrastructure-to-Vehicle Cooperative Traffic Light Application. University of Twente.

SOMMER, C., ECKHOFF, D., GERMAN, R., & DRESSLER, F. (2011). A computationally inexpensive empirical model of IEEE 802.11p radio shadowing in urban environments. In WONS 2011: 2011 Eighth International Conference on Wireless On-Demand Network Systems and Services (pp.84–90). [Piscataway, N.J.]: IEEE. https://doi.org/10.1109/WONS.2011.5720204

SOMMER, C., GERMAN, R., & DRESSLER, F. (2011). Bidirectionally Coupled Network and Road Traffic Simulation for Improved IVC Analysis. IEEE Transactions on Mobile Computing, 10(1), 3–15. https://doi.org/10.1109/TMC.2010.133

SOMMER, C., JOERER, S., & DRESSLER, F. (2012). On the applicability of Two-Ray path loss models for vehicular network simulation. In Vehicular Networking Conference (VNC), 2012 IEEE (pp. 64–69). Piscataway, NJ: IEEE. https://doi.org/10.1109/VNC.2012.6407446

SOMMER, C., & DRESSLER, F. (ED.) 2011. Using the right two-ray model? A measurement based evaluation of PHY models in VANETs.

STAHLMANN, R., MÖLLER, M., BRAUER, A., GERMAN, R., & ECKHOFF, D. (2017). Exploring GLOSA systems in the field: Technical evaluation and results. Computer Communications. Advance online publication. https://doi.org/10.1016/j.comcom.2017.12.006

SUTHAPUTCHAKUN, C., SUN, Z., & DIANATI, M. (2012). Applications of vehicular communications for reducing fuel consumption and CO2 emission: The state of the art and research challenges. IEEE Communications Magazine, 50(12), 108–115. https://doi.org/10.1109/MCOM.2012.6384459

TSUGAWA, S. (2005). ISSUES AND RECENT TRENDS IN VEHICLE SAFETY COMMUNICATION SYSTEMS. IATSS Research, 29(1), 7–15. https://doi.org/10.1016/S0386-1112(14)60113-8

UZCATEGUI, R., & ACOSTA-MARUM, G. (2009). Wave: A tutorial. IEEE Communications Magazine, 47(5), 126–133. https://doi.org/10.1109/MCOM.2009.4939288

VARGA, A. (ED.) 2001. Discrete event simulation system.

VERKEHRSWESEN, F. F. S.-U., & INNERORTS, A. V. (2003). Guidelines for traffic signals: RiLSA; English version. Köln: FGSV Verl.

WANG, Z., & HASSAN, M. (ED.) 2009. The throughput-reliability tradeoff in 802.11-based vehicular safety communications: IEEE.

WEGENER, AXEL, ET AL. (ED.) 2008. TraCI: An interface for coupling road traffic and network simulators: ACM.

WIEDEMANN, R., & REITER, U. (1992). Microscopic traffic simulation: The simulation system MISSION, background and actual state. Project ICARUS (V1052) Final Report, 2, 1–53.

WORLD HEALTH ORGANIZATION. (2015). Global status report on road safety 2015: World Health Organization.

YAO, Y., RAO, L., LIU, X., & ZHOU, X. (2013). Delay analysis and study of IEEE 802.11p based DSRC safety communication in a highway environment. In Proceedings: [conference] ; 14-19 April 2013, Turin, Italy ; [including workshops] (pp.1591–1599). Piscataway, NJ: IEEE. https://doi.org/10.1109/INFCOM.2013.6566955

List of Abbreviations

AC	Access Category
AIFS	Arbitration Inter Frame Space
AIFSNs	Arbitration Inter Frame Space Numbers
BER	Bit Error Rate
CCH	Control Channel
C-ITS	Cooperative Intelligent Transportation Systems
CSMA/CA	Carrier Sense Multiple Access/Collision Avoidance
C-V2X	Cellular V2X
CW	Contention Window
DCF	Distributed Coordination Function
DIFS	Distributed Inter Frame Space
DSRC	Dedicated Short-Range Communication
D2D	Device-to-Device
EDCA	Enhanced Distributed Channel Access
EDCAF	Enhanced Distributed Channel Access Function
eMBMS	Evolved Multimedia Broadcast Multicast Service
eNB	Evolved Node B
ETSI	European Telecommunications Standards Institute
FOT	Field Operational Tests
ICS	ITS Control Stations
IEEE	Institute of Electrical and Electronics Engineers
IFS	Inter Frame Space
ITS	Intelligent Transportation Systems

I2V	Infrastructure-to-vehicle
LOS	Line of Sight
LTE	Long Term Evolution
LTE-A	Advanced LTE
LuST	Luxembourg SUMO Traffic
MAC	Medium Access Control
MBMS	Multimedia Broadcast Multicast Service
NLOS	Non-Line of Sight
OBU	On Board Unit
OFDM	Orthogonal Frequency Division Multiplexing
PHY	Physical
ProSe	Proximity Services
PRP	Packet Reception Probability
QCI	QoS Class Identifier
QoS	Quality of Service
ROI	Region of Interest
RSU	Road Side Unit
SCH	Service Channel
SIFS	Short Inter Frame Space
SIM^{TD}	Sichere Intelligente Mobilität Testfeld Deutschland
SINR	Signal to Interference plus Noise Ratio
SUMO	Simulation of Urban Mobility
UE	User Equipment
UMTS	Universal Mobile Telecommunications System
VANETs	Vehicular Ad-hoc Networks

V2I	Vehicle-to-Infrastructure
V2V	Vehicle-to-Vehicle
V2X	Vehicle-to-everything
WAN	Wide Area Network
WAVE	Wireless Access in Vehicular Environment
3GPP	3rd Generation Partnership Project
5G	5th Generation

Glossary

Ad-hoc network	A local area network, especially one with wireless or temporary plug-in connections, in which some of the network devices are part of the network only for the duration of a communications session, while in some close proximity to the rest of the network
Antenna	A specialized transducer that converts radio frequency fields into alternating current or vice-versa
Antenna gain	A measure of the antenna's ability to direct or focus radio energy over a region of space
Back off time	The random length of time that a station waits before sending a packet on the local area network
Bandwidth	The carrying data capacity of a network
Beacon	Transmitted by an access point ten times per second, and advertises the existence of the access point on a particular channel or channels
CAMA/CA	A protocol for carrier transmission in 802.11 networks, acts to prevent collisions before they happen
Channel	The network path for wireless transmissions, with certain frequency and bandwidth
dBm	The decibel milliwatt, is used in radio communications as a measure of signal strength
DSRC	A wireless communication technology designed to allow automobiles in the intelligent transportation system to communicate with other automobiles or infrastructure technology
IEEE 802.11p	The standard developed by the IEEE for vehicular wireless networks
ITS	An application of sensing, analysis, control and communications technologies to ground transportation for improving safety, mobility and efficiency
I2V	Wireless communication that allows data from infrastructure can be delivered to the vehicle
Line of sight (LOS)	The level of obstruction on the path between two points

Wireless	Describes telecommunications in which electromagnetic waves carry the signal over part or all of the communication path
OFDM	A modulation technique used by standards with multiple carrier frequencies, for obtaining higher throughput and overcoming interference in discrete frequencies
Omni-directional	Typically refers to a primarily circular antenna radiation pattern
Packet	A basic message unit for communication across a network
QoS	Enables network to prioritize certain communication traffic types above others, so that critical or latency sensitive things gain preferred access to the network over lower prioritized or delay tolerated things.
Receiving power level threshold	A measurement of the weakest signal a receiver can receive and still correctly translate it into data
Transmission range	The distance between a transmitter and a receiver over which wireless transmissions can be successful
Transmitting power	The power level of radio transmission
V2I	Wireless communication that allows vehicles to share information with the components that support the transport system
V2V	Wireless transmission of data between motor vehicles

List of Symbols

A	$[second]$	Channel access delay
B	$[second]$	Total back off duration
D	$[second]$	Total delay time
d	$[m]$	Distance between transmitter and receiver
d_m	$[m]$	Internal distance that LOS intersects
$E[A]$	$[second]$	Mean of channel access delay
$E[B]$	$[second]$	Mean of a total back off duration
$E[S]$	$\left[\frac{second}{packet}\right]$	Average service time per packet
$E[T]$	$[second]$	Transmission time delay
$E[T_{res}]$	$[second]$	Mean of the residual lifetime of an ongoing transmission
$E[U]$	$[second]$	Mean of the back off counter value
$E[Y]$	$[second]$	Mean of the interruption time per slot
$erfc$		Complementary error function
$F_{Y\|X\leq T}(y)$		Probability distribution function of the remaining transmission time
$f_{Y\|X\leq T}(y)$		Probability density function of the remaining transmission time
G_t	$[dB]$	Antenna gain of the transmitter
G_r	$[dB]$	Antenna gain of the receiver
K	$[packet]$	Number of packets transmitted involved in one collision (modified version)
K_g	$[packet]$	Expectation number of packets generated during T period
K_{hid}	$[packet]$	Number of packets involved in one collision (hidden terminals)

K_{tr}	$[packet]$	Number of packets involved in one collision (direct collision)
L_i	$[dB]$	Attenuation component
L_{nkg}	$[dB]$	Attenuation from Nakagami-m fading model
L_{obs}	$[dB]$	Attenuation from obstacle model
L_{tri}	$[dB]$	Attenuation from two-ray interference model
N	$[veh]$	Number of vehicles within transmission range of tagged transmitter
$Nakagami(m, \frac{P_r{}'}{m})$		Nakagami-m distribution function
n	$[wall]$	Number of exterior walls that LOS intersects
N_h	$[veh]$	Number of hidden terminals
$Noise$	$[mW]$	Background noise
P_A		Probability of n packets from all vehicles generated during T period
P_B		Probability of no packet is generated during T period
$\overline{P_B}$		Probability of at least one packet is generated during T period
$\mathrm{P_b}$		Sensed channel busy probability (extended version)
p_b		Sensed channel busy probability (Hassan version)
p_c		Total collision probability
p_{dc}		Direct collision probability
$P(H_1)$		Probability of event H1
$P(H_2)$		Probability of event H2
P_r	$[dBm]$	Receiving power level
$P_r{}'$	$[dBm]$	Receiving power level of deterministic model calculation
P_t	$[dBm]$	Transmitting power level

Q	$[second]$	Queuing delay time
S	$[second]$	Service time, sum of channel access delay and complete transmission time of a packet
T	$[second]$	Complete transmission time of a packet, including one DIFS period
t_{data}	$[second]$	Data transmission time of one packet
t_{DIFS}	$[second]$	Duration of a DIFS period
U	$[second]$	Back off counter value
W_m	$[slot]$	Average number of back off slots before a transmission
Y	$[second]$	Interruption period per slot
β	$\left[\frac{dB}{wall}\right]$	Attenuation factor of intersecting exterior wall number
γ	$\left[\frac{dB}{m}\right]$	Attenuation factor of intersecting internal distance
ρ		Queue utilization
σ	$[second]$	A back off slot duration
τ		Probability of a vehicle attempts to transmit in an arbitrary slot, given there is one packet in the queue
λ	$\left[\frac{packet}{second}\right]$	Packet generation rate
$\Gamma_{\perp}$		Reflection coefficient
φ		Phase difference between LOS and ground
$\sum_{i \neq j} P_j$	$[mW]$	Sum of interference from other vehicles

List of Figures

List of Tables

Declaration concerning the Master's Thesis

I hereby confirm that the presented thesis work has been done independently and using only the sources and resources as are listed. This thesis has not previously been submitted elsewhere for purposes of assessment.

Singapore, Jan 15th, 2018

Meng Xie

Meng Xie